Stony Brook University

Synthesis of Next Generation Taxanes and Tumor-Targeting Taxane-Based Drug Conjugates using Linolenic Acid as Tumor-Targeting Module

A Thesis Presented

by

Melvin Parasram

to

The Graduate School

in Partial Fulfillment of the

Requirements

for the Degree of

Master of Science

in

Chemistry

Stony Brook University

May 2011

Stony Brook University

The Graduate School

Melvin Parasram

We, the thesis committee for the above candidate for the

Master of Science degree, hereby recommend

acceptance of this thesis.

Distinguished Professor Iwao Ojima
Advisor
Department of Chemistry

Assistant Professor Isaac Carrico
Chair
Department of Chemistry

Professor Dale G. Drueckhammer
Third Member
Department of Chemistry

This thesis is accepted by the Graduate School

Lawrence Martin
Dean of the Graduate School

Abstract of the Thesis

Synthesis of Next Generation Taxanes and Tumor-Targeting Taxane-Based Drug Conjugates using Linolenic Acid as Tumor-Targeting Module

by

Melvin Parasram

Master of Science

in

Chemistry

Stony Brook University

2011

Cancer is the second major cause of death in the United States and is the leading cause of death of patients below the age of 85. Traditional chemotherapeutics, such as paclitaxel (Taxol ®) and docetaxel (Taxotere ®) have had a significant impact in the field of chemotherapy because of their unique mechanism of action of inducing apoptosis by stabilizing microtubules during mitotic cell division. However, studies have indicated that these drugs are not active in multi-drug resistant (MDR) cancer cells. MDR arises from the overexpression of ATP-binding cassette proteins which enable the cancer cell to remove cytotoxic agents from the cell via ATP dependent efflux pumps, resulting in the loss of efficacy of the drug. In addition to the problem of MDR, traditional chemotherapeutics have little or no specificity, which leads to systemic toxicity, causing severe and harmful side effects. Therefore, it is important to develop next

generation taxoids with increased potency and activity in MDR expressing cancers, as well as to incorporate these cytotoxic agents to tumor-targeting delivery systems to ensure selective cytotoxicity and reduce systemic toxicity. In general, these delivery systems include a tumor-targeting module (TTM) and a cytotoxic agent.

Highly potent next generation taxanes, SB-T-1214, SB-T-121602, and SB-T-121302, were synthesized via Ojima-Holton coupling protocol using enantiopure β-lactam and modified 10-Deacetyl-Baccatin III (10-DAB). The β-lactam required for the Ojima-Holton coupling protocol was afforded via two synthetic routes; Staudinger [2+2] cycloaddition followed by enzymatic resolution protocol and by the chiral ester enolate-imine cyclocondensation. In addition, tumor-targeting drug conjugates were synthesized using linolenic acid (LNA) as the tumor-targeting module. LNA is an essential fatty acid which plays a crucial role in many metabolic processes. Polyunsaturated fatty acids, such as LNA, are greedily taken up by tumor cells as biochemical precursors, making them effective tumor-targeting agents. Several LNA drug conjugates were synthesized, including LNA-SB-T-1214 and LNA-SB-T-121602 as well as a tumor targeting drug conjugate that incorporates a methyl-branched disulfide linker.

Dedicated to my late Grandmother, Niswari Parasram,

My Parents, Tularam and Parbattie Parasram

And My Brother, Marvin Parasram

TABLE OF CONTENTS

Chapter I

Synthesis of Next Generation Taxanes Anticancer Agents

Chapter II

Tumor-Targeting Taxane-Based Drug Conjugates using Linolenic Acid as Tumor-Targeting Module

LIST OF FIGURES

Figure **Page**

Chapter I

Chapter II

LIST OF SCHEMES

Scheme **Page**

Chapter I

Chapter II

LIST OF ABBREVIATIONS

Å- angstrom

ABC- ATP-binding cassette

Abl- Abelson proto-oncogene

Ac- acetyl

AcOH- acetic acid

Arg- Arginine

Anal- analysis

Atm- atmosphere

ATP- adenosine triphosphate

Bcr- breakpoint cluster region

Bd- broad doublet

Bn- benzyl

Boc- *tert*-butoxycarbonyl

b.p.- boiling point

br- broad

Bs- broad singlet

Bz- benzoyl

C- carbon

CAN- cerium(IV) ammonium nitrate

CCNSC- Cancer Chemotherapy National Service Center

CFM- confocal fluorescence microscopy

CML- chronic myelogenous leukemia

d- doublet

DAB- Deacetyl baccatin

DCC- *N*,*N*'-dicyclohexylcarbodiimide

dd- doublet of doublet

DCM- dichloromethane

DHA- docosahexaenoic acid

DIC- *N*,*N*-diisopropylcarbodiimide

DMAP- 4-*N*,*N*'-dimethylaminopyridine

DMF- *N*,*N*'-dimethylformamide

ee- enantiomeric excess

EGFR- epidermal growth factor receptor

EPA- eicosapentaenoic acid

Eq- equivalent

Et ethyl

et al.- and others

EtOAc- ethyl acetate

EtOH- ethanol

FA- folic acid

FIA- flow injection analysis

FDA- Food and Drug Administration

g- gram

GC- gas chromatography

GDP- guanosine 5'-diphosphate

GIST- gastrointestinal stromal tumors

Gly- Glycine

gp60- glycoprotein 60

GSH- glutathione

GTP- guanosine 5'-triphosphate

H - hour

HEX- hexanes

HOSu- *N*-hydroxysuccinimide

HPLC- high performance liquid chromatography

HSA- human serum albumin

Hz- hertz

IC_{50}- concentration for 50 % inhibition

iPr- isopropyl

IR- infrared spectroscopy

J- coupling constant

Kg- kilogram

L- liter

L.A.- Lewis Acid

LC- liquid chromatography

LDA- lithium diisopropylamide

LiHMDS- lithium 1,1,1,3,3,3-hexamethyldisilazide

LNA- linolenic acid

m- multiplet

M- molar or molarity

mAb- monoclonal antibody

MAPs- microtubule associated proteins

MDR- multi-drug resistance

MDS- methyldisulfanyl

Me- methyl

MeOH- methanol

Mg- milligram

MHz- megahertz

Min- minute

mL- milliliter

mM- millimolar

mmol- millimole

mol mole

m.p. melting point

MRP- Multidrug Resistance-Associated Proteins

MS-mass spectrometry

n-BuLi- n-butyllithium

NCI- National Cancer Institute

nM- nanomolar

NMR- nuclear magnetic resonance

PBS- phosphate buffered saline

Pgp- P-glycoprotein

Ph- phenyl

PLAP- pig liver acetone powder

pM- picomolar

PMP- *p*-methoxyphenyl

Ppm- parts per million

PUFA- Polyunsaturated fatty acids

Py- pyridine

q- quartet

RME- receptor-mediated endocytosis

r.t.- room temperature

s -singlet

SAR- structure-activity relationship

SET- Single Electron Transfer

SCID- Severe Combined Immunodeficiency

SPARC- secreted protein acidic and rich in cysteine

t -triplet

$t_{1/2}$- half time

t-Bu- tert-butyl

TAP- tumor activated prodrug

TBDMS- *tert*-butyldimethylsilyl

TEA- triethylamine

Tert- tertiary

TES- triethylsilyl

THF- tetrahydrofuran

TIPS- triisopropylsilyl

TLC- thin layer chromatography

TMS- trimethylsilyl

TTM- tumor-targeting module

U.S.- United States

UV- ultraviolet-visible

WCA- Whitesells Chiral Auxilliary

Wt- weight

[α]- specific optical rotation

β-LSM- *β*-Lactam Synthon Method

δ -chemical shift

µg- microgram

µL -microliter

µM -micromolar

µm- micrometer

µmol- micromole

ω-3- omega-3

ACKNOWLEDGEMENTS

First and foremost, I would like to express my deepest gratitude to my research advisor Distinguished Professor Iwao Ojima for giving me the opportunity to work and learn in his laboratory. I would also like to thank him for his guidance, support, and mentorship. I would also like to give a special thank you to Mrs. Patricia Marinaccio "the Ojima Group Mom" for her support and always having a smile on. I would also like to thank Mrs. Yoko Ojima and Dr. Iwao Ojima for their gracious hospitality.

I would also like to give a special thanks to Edison S. Zuniga for being my mentor throughout my research career. I thank him for his unrivaled guidance, patience, support and encouragement. I would also like to thank Joshua D. Seitz and William Burger for their helpful discussions. I wish to thank the rest of the members of the Ojima group, Dr. Stephen J. Chaterpaul, Dr. Joseph J. Kaloko, Gary Teng, Chi-Feng Lin, Chih-Wei Chien, Alexandra Athan, Dr. Olivier Marrec, Tao Wang, Lucy Li, Bora Park, Yang Zang, Dr. Manisha Das, Lucy Li, Christina Susanto, Togla Sevinc, Samsad Pavel, Divya Awasthi, and Dr. Kunal Kumar for their help. I would also like to especially thank the M.S. students in the Ojima group, Wen Chen and Winnie Situ for just going through this graduate program with me.

I would like to thank the brilliant chemistry department faculty members, who gave me a great foundation in chemistry, Dr. Robert Kerber, Dr. Nancy Goroff, Dr. Frank Fowler, Dr. Joseph Lauher, Dr. Jiangyong Jia, Dr. Philip Johnson, Dr. Zachary Katsamanis, Dr. Fernando. Raineri, Dr. Susan Oatis, Dr. Stephen Koch, Dr. Iwao Ojima, Dr. Nicole Sampson, Dr. Dale Drueckhammer, and the late Dr. Michelle Millar. I would like thank Dr. Isaac Carrico and Dr. Dale Drueckhammer for serving as my chair and third member on my M.S. committee.

I would also like to thank entire staff of the chemistry department's main office Ms. Carol Brekke, Ms. Charmaine Yapchin, and Ms. Katherine Hughes for your informative email, registration advice, and notification of deadlines. I would also like to thank the building managers, Mr. Alvin Silverstein and Mr. Michael Teta to maintaining the chemistry building and I would also like to thank the custodial staff for cleaning the 7^{th} floor.

Finally, I would like to thank my family and friends. I wish to thank the honorable brothers of the Zeta Chapter of Sigma Beta Rho Fraternity, Inc., for supporting me and providing me with a social outlet. I also wish to thank Sheriza Hussain for being there for me and encouraging me during all of the tough times. I want to express my deepest gratitude to my parents, Parbattie and Tularam Parasram, my brother, Marvin Parasram, and my cousin Vanessa Nowrang for their financial support, encouragement, support, and just being there for me when I needed you, Words cannot fathom how thankful I am to have all of you in my life.

Chapter I

Synthesis of Next Generation Taxoid Anticancer Agents

Table of Contents

§1.1. Introduction: Cancer and Cancer Therapy

§1.1.1 Cancer

Cancer is a leading cause of death worldwide and is likely to increase in frequency. In the United States, cancer is the second major cause of death and is the leading cause of death of patients below the age of 85.[1] This lethal disease takes nearly half a million lives in the United States each year.[2] Cancer is classified as a group of diseases in which cells uncontrollably divide past their normal growth limits. These cancerous cells impede and destroy neighboring tissues and organs, and in some cases, they also metathesize, spreading to other locations in the body via lymph or blood. Normal cells become cancerous due to mutations in their genetic material. Long term exposure to carcinogens, such as tobacco smoke, radiation, and chemical agents, are responsible for mutations that give rise to cancer. These mutated cells become insensitive to anti-growth signals, such as tumor-suppressor genes, resulting in the formation of a tumor. One means in which cancer can be prevented is by modifying lifestyle behaviors; eating healthy, staying fit, and abstaining from smoking. However, in some instances cancer cannot be prevented, thus, early detection and determining the best treatment option can sometimes increase patient survival.

§1.1.2 Treatment Options

There are several treatment options employed to treat cancer including surgery, radiation therapy, immunotherapy, and chemotherapy. The choice of therapy depends on location, stage,

and grade of the tumor. At times, these treatment options may not provide a cure for the cancer, but can alleviate symptoms and improve the quality of life for patients.

Surgery uses invasive techniques to remove tumors. This is a useful treatment option if the cancer has not metathesized. It is important that surgeons remove all traces of cancer cells to prevent recurrence of a tumor, thus, this process may require the removal of tissues/organs that neighbor the tumor.

Radiation therapy is the use of high-energy X-rays to destroy cancer cells. It is usually used to treat solid tumors and leukemia. Radiation therapy can be administered externally via external beam radiotherapy or internally via brachytherapy. This treatment only affects the area being treated; as a result, normal cells may be destroyed during treatment.

Immunotherapy is a relatively new field in the treatment of cancer. It is the process of increasing the patient's immune system to fight cancer through various therapeutic strategies. Some strategies involve the use of vaccines, bone marrow transplantation, and the use of interferons and other cytokines to induce an immune response.

Chemotherapy uses chemical agents or anticancer agents to kill cancer cells. Chemotherapeutics function on the premise that chemical agents are able to differentiate cancer cells from normal cells and destroy them. However, chemical agents cannot differentiate between cancer cells and normal cells and as a result, these agents kill both normal and cancer cells. This lack of specificity leads to systemic toxicity, resulting in several undesired and severe side effects such as hair loss, depression of the immune system, and damage to the liver, kidney and bone marrow.

§1.2. Paclitaxel

§1.2.1 Discovery and Development

In 1958, the National Cancer Institute (NCI) established the Cancer Chemotherapy National Service Center (CCNSC) as a public headquarters for the screening of potential anticancer compounds.[3] In 1960, they initiated a program to screen various plant species for anticancer activity.[4] Dr. Monroe E. Wall and Dr. Mansukh C. Wani of the Research Triangle institute, North Carolina, screened the bark of *Taxus brevifolia* (Pacific Yew) and found that the extract displayed antitumor activity in the Walker 256 carcinosarcoma, P1534 leukemia, and P388 leukemia assays.[5] Wall and Wani later determined that the active ingredient was paclitaxel (Taxol®) (**Figure 1**).

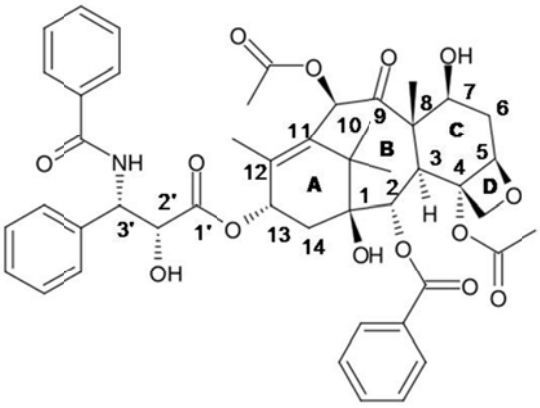

Figure 1: Structure of paclitaxel (Taxol ®).

The structure of paclitaxel is quite complex. It is a diterpene that contains a tetracyclic core and an *N*-benzoylphenylisoserine side chain at the C-13 position. This structure contains a total of 11 chiral centers and contains a nitrogen group and various oxygen functionalities.

After the discovery of the active structure, initial tests showed effective activity in various human solid tumor xenograph studies in nude mice.[6] Dr. Susan B. Horwitz and

coworkers discovered that paclitaxel had a unique mechanism of action of stabilizing microtubules. This stabilization inhibits microtubule depolymerization, causing the arrest of cellular division in the G2/M phase leading to early mitotic exit.[7] These discoveries lead to research via clinical trials in 1982. Clinical reports showed that paclitaxel was effective in refractory ovarian cancer and breast cancer.[8] Paclitaxel was later licensed to Bristol-Myers Squibb, where it was trademarked under Taxol ®. Presently, paclitaxel is the most widely used anticancer agent and is used in the treatment of ovarian cancer, breast cancer, and lung cancer, as well as Kaposi's sarcoma.

§1.2.2 Mechanism of Action

After the discovery of paclitaxel's potent cytotoxic activity, it was assumed that it possessed the same mechanism of action as typical spindle poisons such as colchicines or vinca alkaloids. These compounds act by inhibiting microtubule polymerization. Microtubules are essential components in cell structure and cell division. Inhibiting the formation of microtubules disrupts cell division and other normal functions, which induces apoptosis. In 1979, Horwitz and co-workers discovered that paclitaxel possessed a unique mechanism of action; instead of inhibiting microtubule polymerization, it actually promotes and stabilizes the formation of microtubules.[7] This stabilization prevents the dynamic depolymerization of microtubules causing the cell to be locked in between metaphase and anaphase of mitotic cell division. This anomaly eventually induces apoptosis.

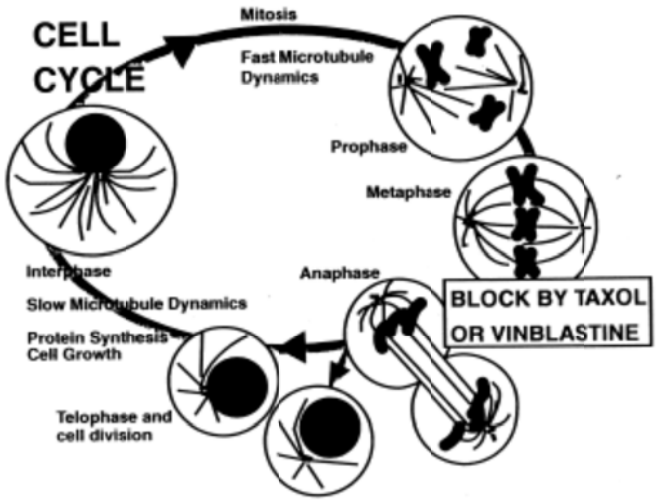

Figure 2: The function of anticancer agents on cell cycle.[9]

Microtubules are polymers of α- and β-tubulin dimers. Paclitaxel binds to the β-tubulin protein and upon polymerization, it stabilizes the structure. Normally, microtubules polymerize in the presence of guanosine 5[1]-triphospate (GTP), magnesium ions, and microtubule-associated proteins (MAPS). Paclitaxel was found to increase the rate and nucleation of the formation of microtubules in either the presence or absence of the microtubule polymerization promoting elements.[10] The resulting microtubule formed with paclitaxel is structurally different; it contains 12 protofilaments with a diameter of 22 nm instead of the normal structure which contains 13 protofilaments with a diameter of 23 nm. Microtubule polymerization and paclitaxel mechanism of action is shown in **Figure 3**.

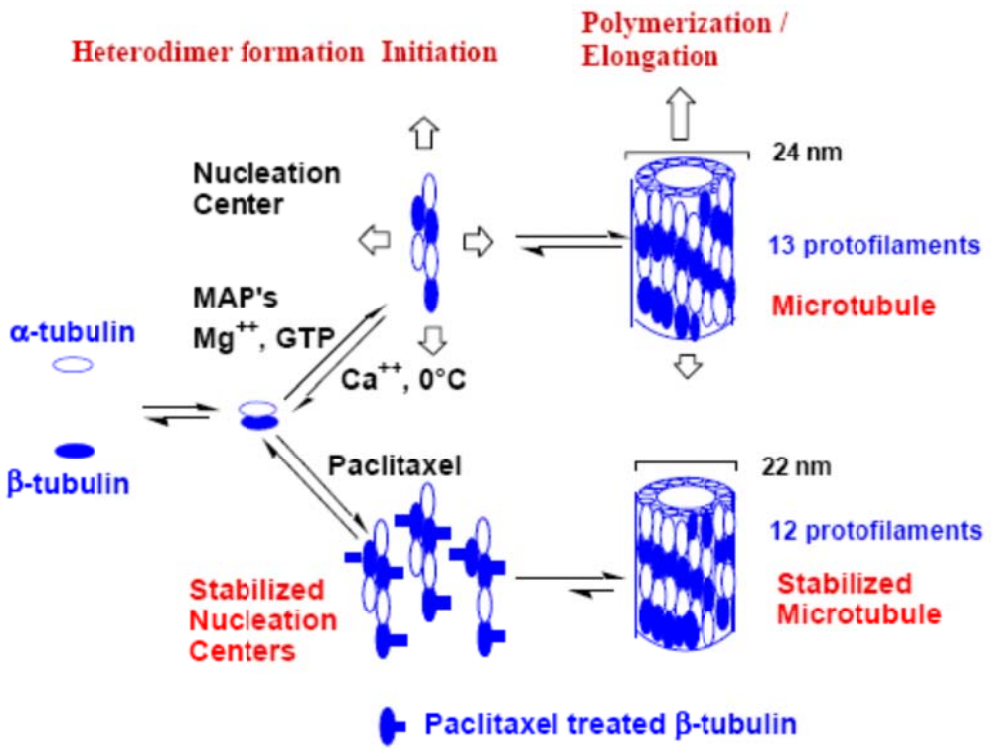

Figure 3: Representation of normal microtubule polymerization (upper) and Taxol®-promoted microtubule polymerization (lower).[11]

§1.2.3 Synthesis

Paclitaxel received worldwide attention as a promising anticancer agent. However, large scale clinical trials were hampered and structure activity relationships were not practical due to limited supply of the drug.[12] For nearly 20 years after its discovery, the major source of paclitaxel was isolated from the bark of *Taxus brevifolia* (Pacific Yew). The isolation process was extremely difficult and low yielding; 12 kg of bark afforded 0.5 g of paclitaxel (0.004 %).[5] In addition, the pacific yew is killed in the isolation process. Continued isolation of paclitaxel could have potentially led to several consequences, such as ecological problems and a decrease in the population of pacific yew. As a result, many researchers have found alternate methods to get paclitaxel to overcome these problems, such as the total synthesis of the natural product. The

total synthesis of paclitaxel has been accomplished by several research groups, Dr. Holton, Dr. Nicolaou, Dr. Danishefsky. Dr. Wender, Dr. Kuwajima, Dr. Mukaiyama, and Dr. Takahashi. However, none of these total synthesis method are feasible for a large scale production of paclitaxel.

Fortunately, Dr. Potier's group in France isolated 10-deacetyl baccatin III (10-DAB) from the leaves of *Taxus baccata* (European Yew).[13] Isolation from leaves gives high yields and the leaves are a renewable source. This compound is structurally similar to paclitaxel (**Figure 4**), however, 10-DAB(III) does not contain the functionalization at the C-10 position nor the C-13 side chain.

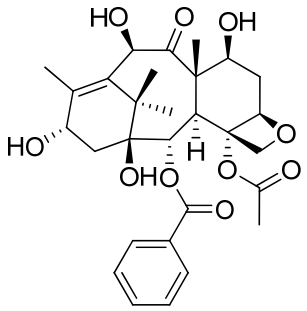

Figure 4: Structure of 10-Deacetyl-Baccatin III (10-DAB)

10-DAB can be used as a Taxol precursor in the semi-synthesis of paclitaxel, ensuring a large and long term supply of paclitaxel. Using 10-DAB in a semi-synthetic scheme, it becomes apparent that the attachment of a two chiral centered C-13 side chain needed. Ojima et al. has shown that the C-13 side-chain can be coupled to the baccatin scaffold using an enantiopure β-lactam in the presence of a strong base (**Scheme 1**).[14,15] This novel procedure for the preparation of taxoids using β-lactams is known as the β-lactam Synthon Method (β-LSM) or the Ojima-Holton coupling protocol. This procedure affords taxanes in high yields and it is a practical and efficient semi-synthetic method for large scale production of paclitaxel and paclitaxel analogs.

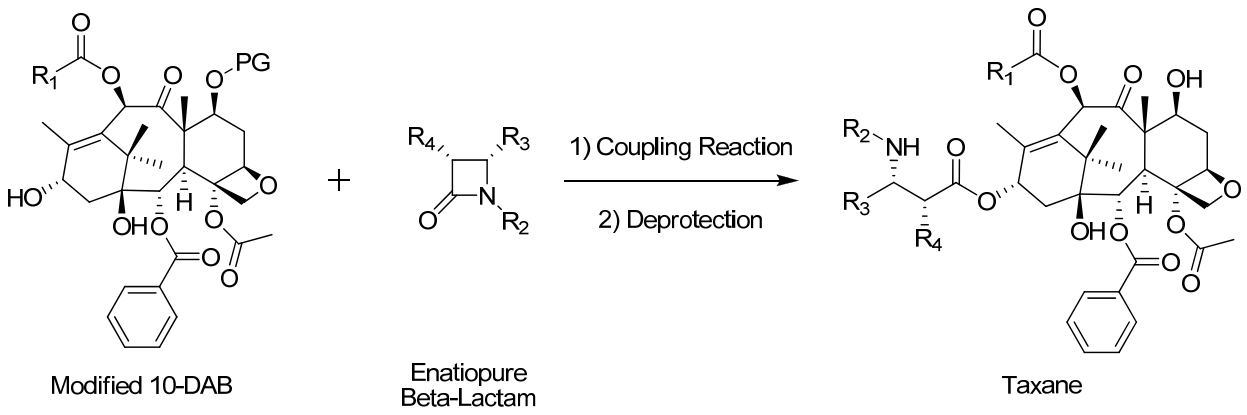

Scheme 1: General scheme for the Ojima-Holton Coupling Protocol.[14, 15]

§1.2.4 Multi-Drug Resistance (MDR)

Although paclitaxel possesses potent anticancer activity, studies have shown that this drug produces drug resistance in cancer cell lines and is not active in multi-drug resistance (MDR) cancer cell lines.[16] Multi-drug resistance is the condition of enabling a cell to become resistant to chemotherapeutic agents. MDR arises from, but is not limited to, the overexpression of specific tubulin isotypes[17] and the overexpression of ATP-binding cassette (ABC) transporters.[18] P-glycoprotein (Pgp) and multidrug resistance-associated proteins (MRP) are two molecular pumps from the ABC family that have been associated with MDR. Overexpression of these proteins allows for the efflux of chemotherapeutic agents through an ATP-dependent pump, which results in the loss of efficacy of the drug (**Figure 5)**.

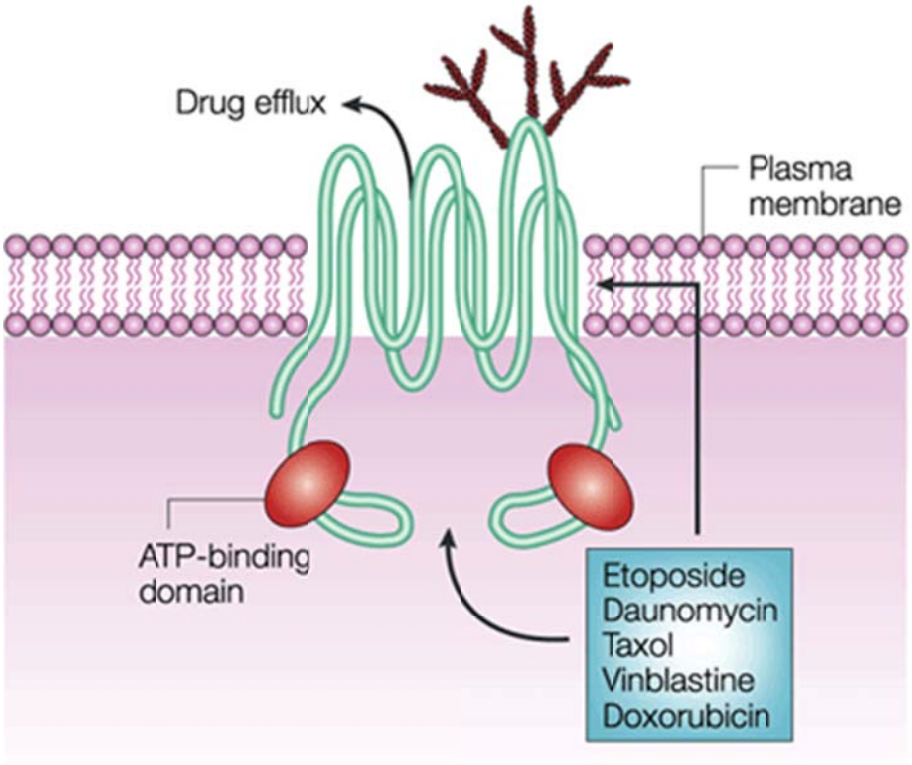

Figure 5: Efflux of Chemotherapeutics by pgp.

§1.2.5 Structure-Activity Relationship of Paclitaxel (SAR)

After practical synthetic methods were established, the large scale production of paclitaxel was achievable. Due to the nature of MDR in cancer cells and the availability of paclitaxel, numerous chemical modifications on the baccatin skeleton and the C-13 side chain have led to extensive SAR studies. These paclitaxel analogs can be more potent than the parent compound and can possibly reverse the effects of MDR in cancer cells. A summary of SAR studies of paclitaxel is shown in **Figure 6**.

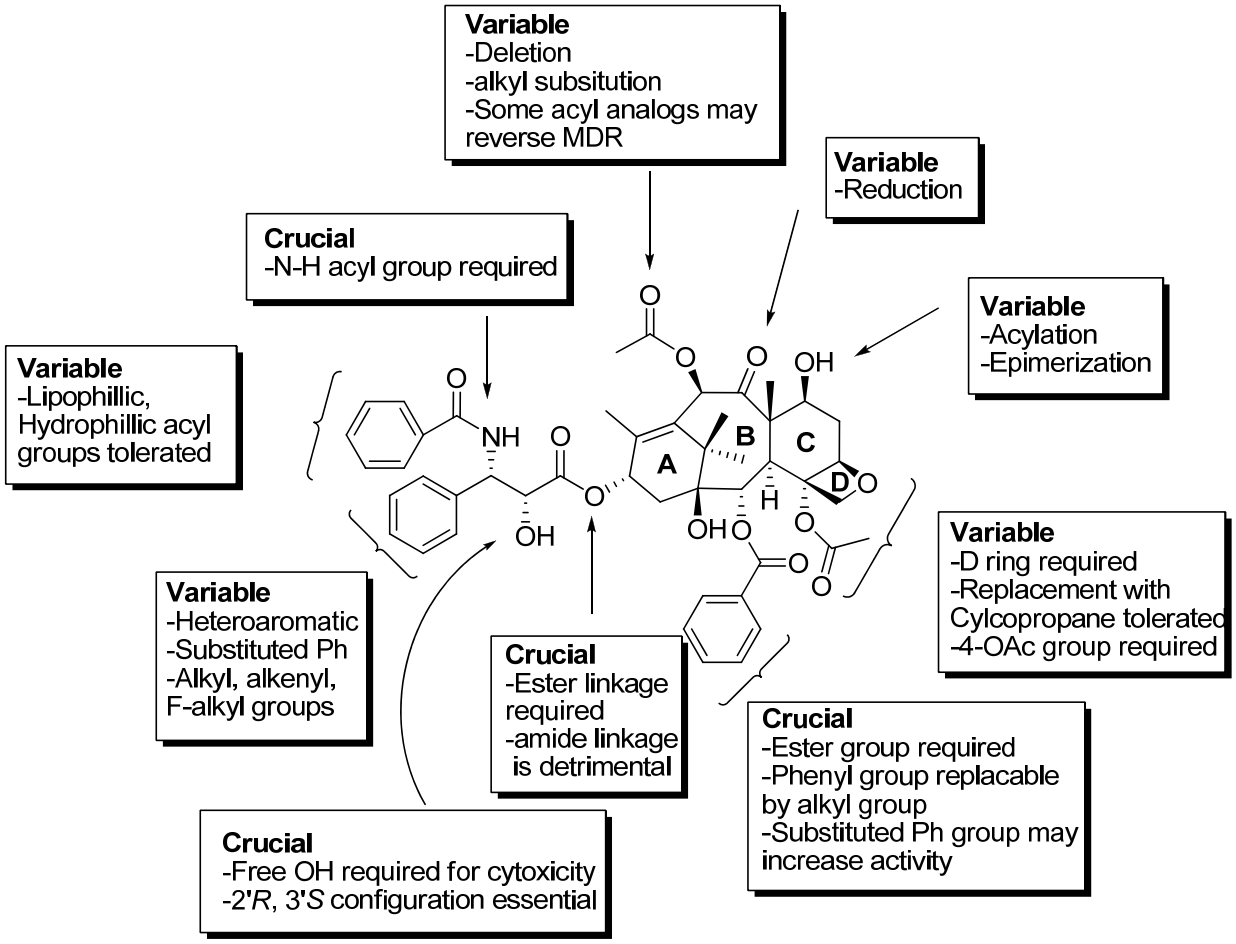

Figure 6: Summary of SAR studies of Paclitaxel.[19-28]

The C-13 side chain is an essential component in the activity of paclitaxel. The ester functionality on the C-13 side chain is required and replacement with an amide bond would lead to loss of activity.[20] The chirality at the C2' and C3' position, *S* and *R* respectively, are required for full activity. The isomer of paclitaxel (2'*R*, 3'*S*) is significantly less active; however, epimerization of one of the two stereocenters results in analogs with comparable activity.[21] The free C-2' hydroxyl group is essential for activity. The hydroxyl group participates in a hydrogen bond with either the Arg 396 or Gly 370 protein of β-tublin and thus required for tight binding to tublin.[22] The free hydroxyl group can be esterified to mask its activity and later hydrolyzed to activate the drug; this method is the rationale for "pro-drug" approaches. The C3' and the C3'N-

acyl substituents can be varied. The N-acyl group is required for activity and substitution of tertiary and aromatic groups have shown to improve efficiency. Tert-butyl group has been chosen at the C3'N position due to its favorable pharmacokinetic properties, as shown in the difference between paclitaxel and docetaxel.[23] Ojima et al. showed that the C 3'-phenyl group was not essential for the activity of novel analogues, and that a substitution of the 3'-phenyl with an isobutenyl moiety increased the activity of these analogues.[24]

The A, B, C, and D rings are required for optimal cytotoxicity. The northern face of the baccatin scaffold can be varied. The C-10 position has been shown to be recognized by the Pgp efflux pump, and modifications at this position can improve efficacy against MDR cancer cells.[25] Reduction at the C-9 position can be tolerated, but only slightly improves activity and does not prove to be very advantageous. The hydroxyl group at the C-7 position is optimal for activity, however, acylation or epimerization do not significantly alter its activity. The southern face of the baccatin scaffold is less flexible and can be slightly varied. Studies have shown that the removal of the benzoyl group and/or epimerization at the C-2 position results in a significant decrease in activity.[26,27] It was also found that introducing substituted phenyl groups at the *para* position was detrimental to activity due to disruptions of hydrophobic interactions, however, *meta* substitution generates analogs with superior activity.[28,29] The C-4 position can be substituted with small acyl groups, but large bulky groups results in the loss of binding.

With a great deal of information known on the structure of paclitaxel through extensive SAR studies and the establishment of efficient semi-synthetic methods, researchers can synthesize taxol analogs with increased potency and MDR reversing capabilities.

§1.3.0 β-Lactam

§1.3.1 Introduction

β-lactams are four-membered ring heterocyclic compound containing three carbon atoms and one nitrogen atom. The β-lactam ring is the central structure in several antibiotics families including penicillins, cephalosporins, carbapenemes, and monobactams. β-lactam antibiotics inhibit the synthesis of peptidoglycan, which is essential to maintain the integrity of bacterial cell walls.[30] The first synthesis of a β-lactam was accomplished by Hermann Staudinger in 1907 by the reaction of the Schiff base of aniline and benzaldehyde with diphenylketene in a [2+2] cycloaddition.[31] β-lactams are also very useful in synthesis because of their strain ring system, which can open upon nucleophilic attack. In 1991, Ojima et al. demonstrated that β-lactams can be used in the semi-synthesis of paclitaxel and newer generation taxoids (**Scheme 1**).[14]

A high enantioselective β-lactam can be afforded via two major synthetic routes; chiral ester enolate-imine cyclocondensation and Staudinger [2+2] cycloaddition followed by enzymatic resolution.[32] These methods have been well established in the Ojima lab for the synthesis of novel β-lactams.

§1.3.2.0 Synthesis of β-lactam via Staudinger [2+2] Cycloaddition followed by Enzymatic Resolution

The Staudinger reaction is a [2+2] cycloaddition between a Schiff base and a ketene to form a β-lactam. This method is economical due to the readily available Schiff bases and ketenes. The mechanism for the Staudinger [2+2] cycloaddition is shown in **Scheme 2**.

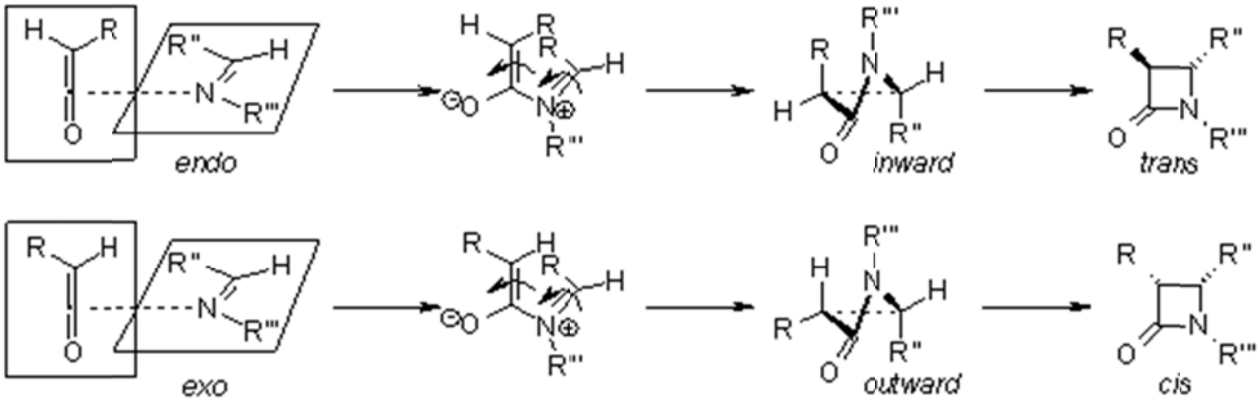

Scheme 2: The Staudinger [2+2] cycloaddition mechanism

to form the *trans* (upper) and *cis* (lower) β-lactam.

The imine adds to the ketene as a nucleophile in either an *endo* or *exo* fashion, which forms a zwitterionic intermediate. This intermediate undergoes electrocyclic conrotatory ring closure to yield the β-lactam. In general, (*E*)-imines lead preferentially to *cis*-β-lactams, while (*Z*)-imines lead to *trans*- β-lactams. However, Ab initio calculations have shown that the substituent groups on the ketene can modulate the imine approach.[33] If the substituent group is electron donating, the imine will add *exo* and con-rotatory ring closure will occur in an outward fashion to give *cis*-β-lactam, whereas, an electron withdrawing group will favor an *endo* approach and con-rotatory ring closure will occur in an inward fashion to give *trans*-β-lactam.

One method to obtain enantiopure β-lactam is through an enzymatic resolution of racemic β-lactam. It has been reported that several *Pseudomonas lipases* can be used as the enzyme in the enzymatic resolution of β-lactams.[34] The lipase preferentially cleaves the acetate group of the (-) enantiomer leaving the (+) enantiomer intact (**Scheme 3**).

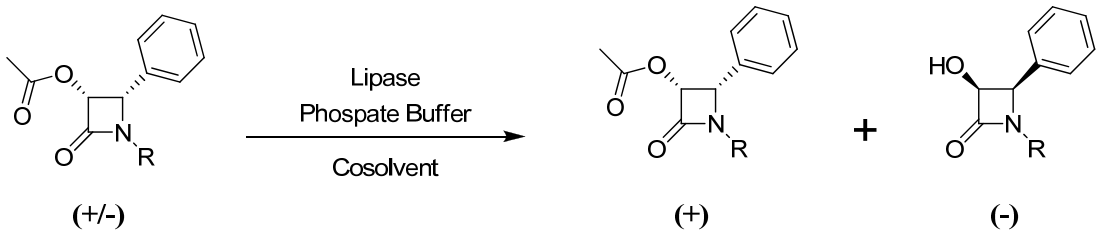

Scheme 3: Enzymatic resolution of racemic β-lactam.[34]

In the Ojima lab, *p*-anisidine is used as the nitrogen source for the formation of the imine. After Staudinger [2+2] cycloaddition and subsequent enzymatic resolution, the β-lactam produced will contain p-methoxyphenyl (PMP) group attached to the nitrogen. The PMP group can be removed with ceric ammonium nitrate (CAN) affording a free amine, which can be further modified with various substituents to give novel β-lactams. Varying the nitrogen substituent on the β-lactams can yield novel taxoids with different C'3 groups via Ojima-Holton coupling protocol. The reaction mechanism for the CAN deprotection of PMP is shown in **Scheme 4**.

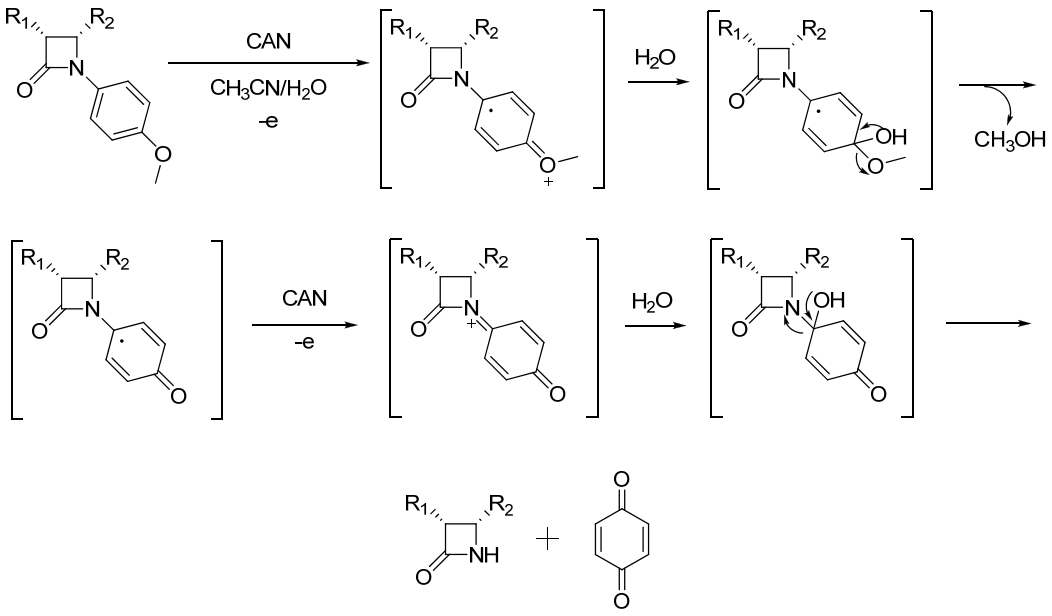

Scheme 4: Mechanism of the removal of PMP using CAN.

The mechanism for the removal of the PMP group involves two Single Electron Transfers (SET). The PMP group donates a single electron to cerium (IV) forming a radical cation intermediate that is susceptible to a nucleophilic attack by water. Donation of a second electron to another CAN molecule results in a quinone like radical which is then cleaved by the addition of a second water molecule producing the free amine, quinone and methanol as the primary products.

§1.3.2.1 Results and Discussion

The synthesis of the β-lactam began with the formation of the heterocyclic ring core *via* the Staudinger reaction between an imine and a ketene. The imine, **I-1**, was produced by the condensation reaction of 3-methyl-2-butenal in the presence of *p*-anisidine and a drying reagent. The imine, **I-1**, was used in the subsequent Staudinger [2+2] cycloaddition reaction without

purification. Compound **I-1** was reacted with acetoxyketene, generated *in situ* from acetoxyacetyl chloride and triethylamine in low temperature, that afforded a racemic mixture of *cis*- β-lactam, **I-2**, in low yields (**Scheme 5**).

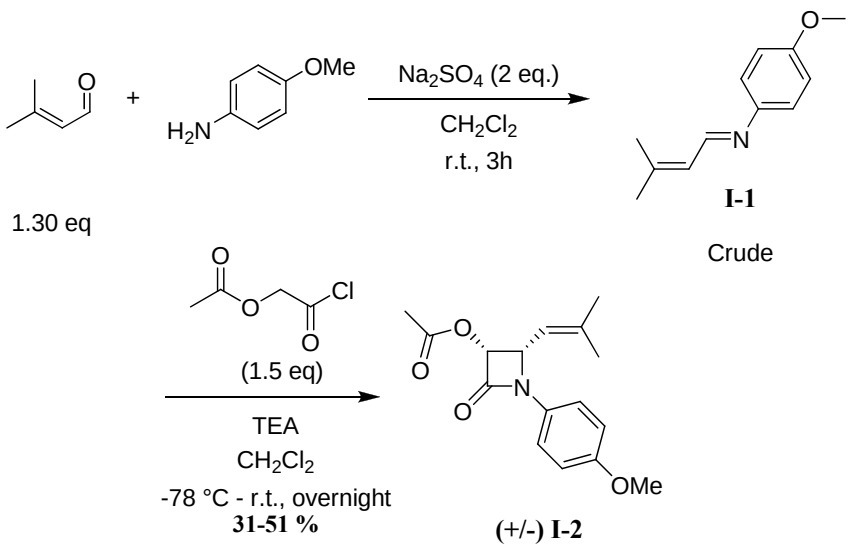

Scheme 5: Imine formation (upper) and Staudinger [2+2] cycloaddition reaction (lower)

The Staudinger [2+2] cycloaddition reaction was problematic. The formation of *trans*- β-lactam was observed, which attributed to the low yield. Since the ketene generated *in situ* from acetoxyacetyl chloride contained an acetoxy electron withdrawing group, the *trans*-β-lactam was the favored product. To prevent *trans* formation, the reaction temperature must be maintained at -78 ^{o}C to yield the desired but less stable *cis* conformer. The formation of *trans*-β-lactam during this reaction was due to the incorrect maintenance of a constant low reaction temperature and/or the addition speed of acetoxyacetyl chloride was rapid. Lowering and correctly maintaining the temperature, decreasing addition speed, or simultaneously cooling the acetoxyacetyl chloride during addition to the imine can reduce the formation of the undesired *trans*-β-lactam.

High percent enantiomeric excess (% ee) β-lactam was required for the Ojima-Holton coupling protocol. High % ee *cis*-β-lactam, **(+) 1-2,** was achieved in low yields *via* enzymatic resolution using PS-Amano lipase (**Scheme 6**). The hydrolyzed enantiomer was not quantified and was given to graduate student Wen Chen for her studies on β-lactam.

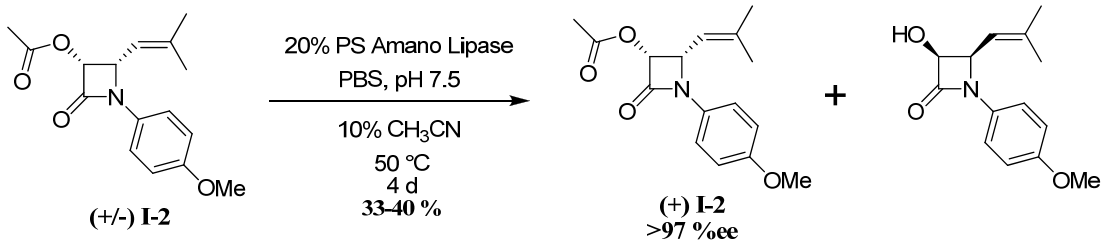

Scheme 6: Enzymatic Resolution of racemic β-lactam, **(+/-) I-2**

The activity of the lipase can be unpredictable and the lipase can be sensitive to changes in temperature and pH. The low yield may have resulted in the enzyme overreacting and hydrolyzing the acetate group of the (+) enantiomer. A possible reason for this over activity is that the reaction temperature may have been above the optimal temperature of this enzyme, 50 ^{o}C, which may have caused the enzyme to hydrolyze the (+), enantiomer. The reaction temperature must be maintained religiously in order to prevent the hydrolysis of the desired compound. A small scale hydrolysis of **(+) 1-2** to produce **(+) 1-3** was done to test the enantiomeric excess by HPLC using a chiral OD-H column. Results indicated that **I-2** had a >97 % ee.

The high optical purity of **(+) I-2** allowed for further modification. Compound **(+) I-2** was hydrolyzed to yield **(+) I-3**. The resulting alcohol was protected with TIPS, which afforded **(+) I-4** in high yields. Compound **(+) 1-4**, underwent CAN deprotection for the removal of the para-methoxyphenyl group that yield a free amine in compound **(+) I-5**, which a *t*-Boc moiety

was introduced in the subsequent reaction by Boc anhydride to give the β-lactam, **(+) I-6**, in high yields (**Scheme 7**).

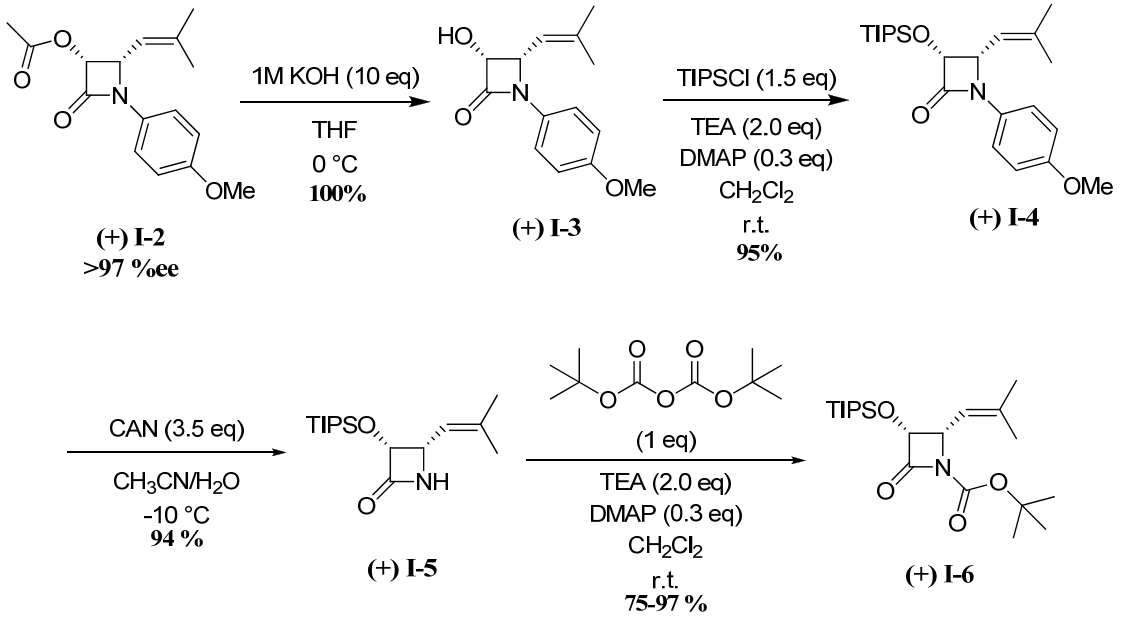

Scheme 7: Synthesis of β-lactam, **(+) I-6**.

§1.3.3.0 Synthesis of β-lactam via Chiral Ester Enolate-Imine Cyclocondensation

Another approach for the formation of a β-lactam is via chiral ester enolate-imine cyclocondensation. The chiral ester component is derived from Whitesell's chiral auxiliary (WCA). Chiral auxiliaries are widely used in chemical synthesis to introduce chirality in otherwise racemic compounds. The WCA can be synthesized by following the protocol developed by Whitesell; CuI-catalyzed ring opening with phenylmagnesium bromide to afford racemic *trans*-2-phenyl-cyclohexanol, the resulting alcohol is then acylated using acetic anhydride in the presence of DMAP, then subsequent enzymatic resolution using pig liver acetone powder (PLAP) to afford (-)-*trans*-2-phenyl-cyclohexanol, **(-) WCA** (**Scheme 8**).[35]

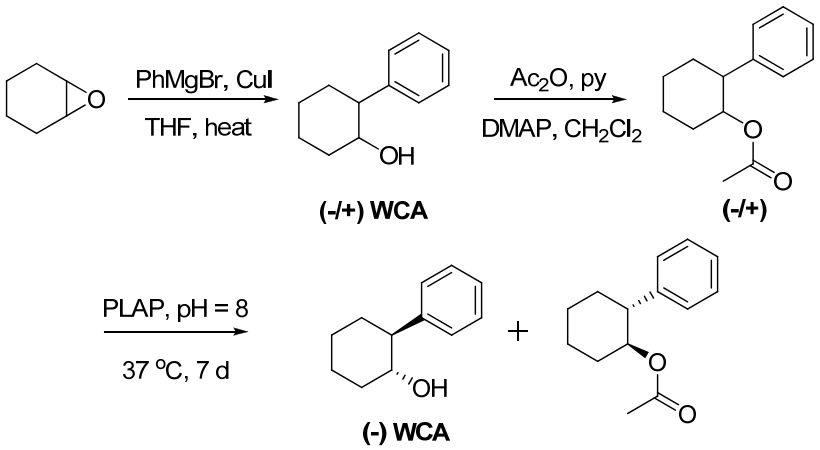

Scheme 8: Synthesis of Whitesell's Chiral Auxiliary, **(-) WCA**.[35]

Ojima *et. al.* has utilized WCA in the synthesis towards novel β-lactams via chiral ester enolate-imine cyclocondensation.[36] In the past, this method was the primary route toward the synthesis of novel β-lactams in the Ojima group (**Scheme 9**).

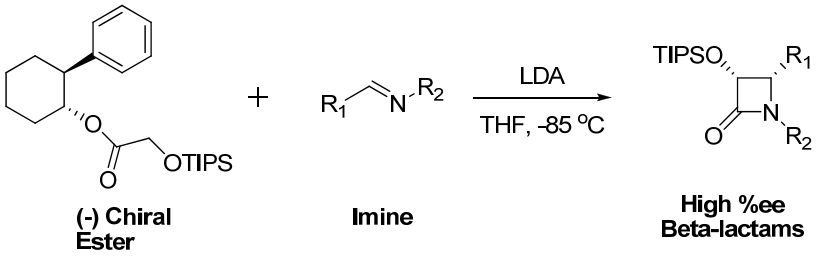

Scheme 9: Synthesis of β-lactams via Chiral Ester Enolate-Imine Cyclocondensation.[36]

The reaction mechanism of the chiral ester enolate-imine cyclocondensation is shown in **Scheme 10**.[37] At low temperatures, the chiral ester is isomerized to the (*E*)-enolate and adds to the least hindered side of the *trans*-imine, forming the β-amino ester intermediate. This intermediate undergoes cyclization upon warming to room temperature to afford the *cis*- β-lactam and regenerates the (-) WCA. The formation of the *cis*- β-lactam with high optical purity is due to the 6-member-ring transition state.

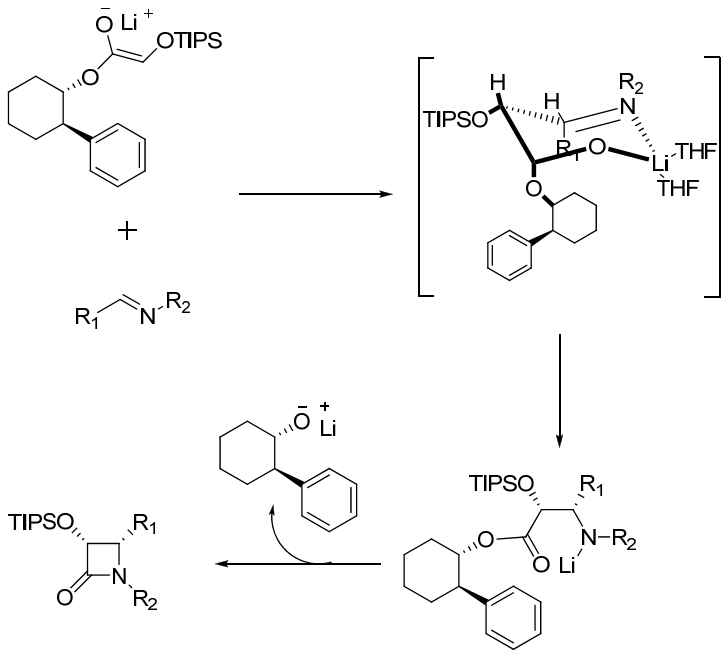

Scheme 10: Mechanism of the Chiral Ester Enolate-Imine Cyclocondensation.[37]

In recent years, the chiral ester route has been replaced by the economical Staudinger [2+2] cycloaddition followed by enzymatic resolution; which is outlined in the previous section. While both of these synthetic routes are fairly successful, both methods suffer from a lengthy and unpredictable enzymatic resolution. The enzymatic resolution reaction is an unattractive process because it is very tedious to monitor, large scale production requires large glassware for the phosphate buffer, may take up to a week to complete, and can give low yields. As a result, chiral ester enolate-imine cyclocondensation developed by Ojima *et al*. was revisited and was applied a new methodology presented by Sharpless *et al*.[38] This new methodology provides an asymmetric synthetic route towards the synthesis of high enantiopure **(-) WCA**, eliminating the use of an enzymatic resolution (**Scheme 11**).

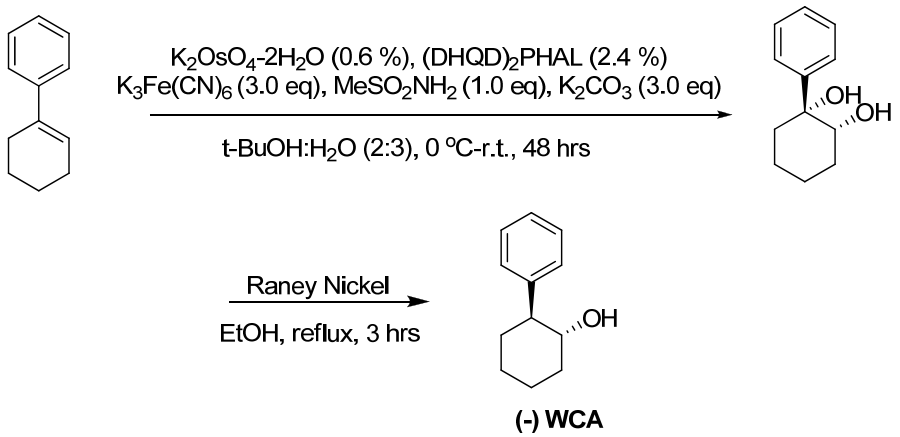

Scheme 11: Asymmetric synthesis of **(-) WCA** by Sharpless *et al.*[37]

Using the protocol presented by Sharpless *et. al.*, cyclohexenylbenzene proceeds through a Sharpless asymmetric dihydroxylation to the alkene to yield an asymmetric *cis*-diol. Subsequently, the diol undergoes benzylic reductive dehydroxylation in the presence of Raney Nickel to yield **(-) WCA** in moderate yields and excellent enantiopurity.

The Sharpless asymmetric dihydroxylation reaction occurs in the presence of osmium tetra oxide and a suitable ligand. The reaction mechanism of Sharpless asymmetric dihydroxylation to an alkene is displayed in **Figure 7**.[39] The first step is the formation of the active catalytic species, osmium tetroxide-ligand complex (2). A [3+2] cycloaddition occurs between the alkene (3) and the osmium tetroxide-ligand complex to give a heterocyclic 5 member ring intermediate (4). This intermediate undergoes basic hydrolysis to liberate the asymmetric diol (5) and reduced osmate (6). Lastly, potassium ferricyanide oxidizes the osmate which regenerates the active catalysis to continue the cycle.

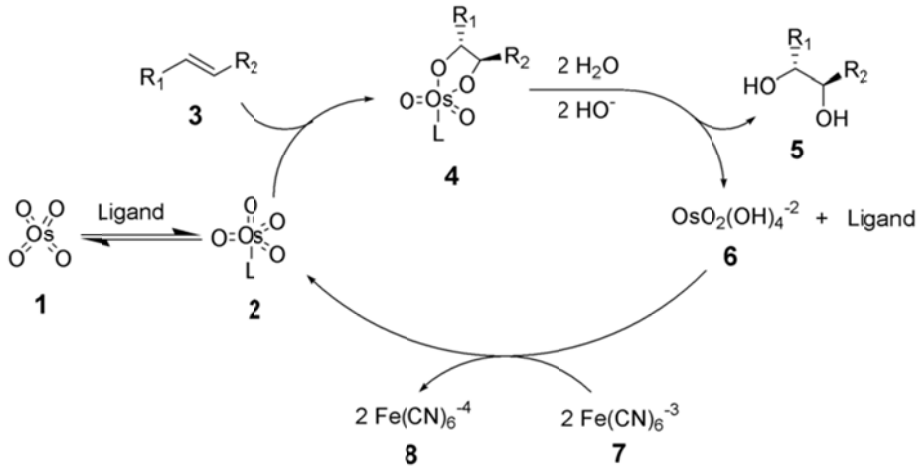

Figure 7: Mechanism of Sharpless asymmetric dihydroxylation.[39]

The *cis*-diol generated in the Sharpless asymmetric dihydroxylation reaction can be racemic because the osmium can deliver the hydroxyl from both the "top" face as well as the "bottom" face of the alkene. In order to selectively generate a single enantiomer, Sharpless developed a phthalazine class of chiral ligands, $(DHQD)_2$-PHAL and $(DHQ)_2$-PHAL, to selectively direct the delivery of the hydroxyl groups to the alkene. When $(DHQD)_2$-PHAL was used, "top" face attack occurred exclusively giving the (R)-adduct, whereas when $(DHQ)_2$-PHAL was used, "bottom" face attack occurred exclusively giving the (S)-product.

By incorporating Sharpless's methodology of the asymmetric synthesis of **(-) WCA** to the already established chiral ester enolate-imine cyclocondensation method developed by Ojima *et al*, one can possibly synthesize large amounts of chiral β-lactams with high optical purity in a timely and high yielding fashion.

§1.3.3.1 Results and Discussion

The synthesis of the β-lactam began with the synthesis of Whitesell's chiral auxiliary, **(-) WCA** (**I-8**). Cyclohexenylbenzene underwent Sharpless asymmetric dihydroxylation to afford the asymmetric *cis*-diol (**I-7**) in quantitative yield in the presence of osmium tetroxide, potassium ferricyanide, and the ligand $(DHQD)_2$-PHAL. The *cis*-diol was used crudely in the subsequent benzylic reductive dehydroxylation to give enantiopure Whitesell's chiral auxiliary, **(-) WCA** (**I-8**), in 50 % yield after recrystallization in pentane (**Scheme 12**).

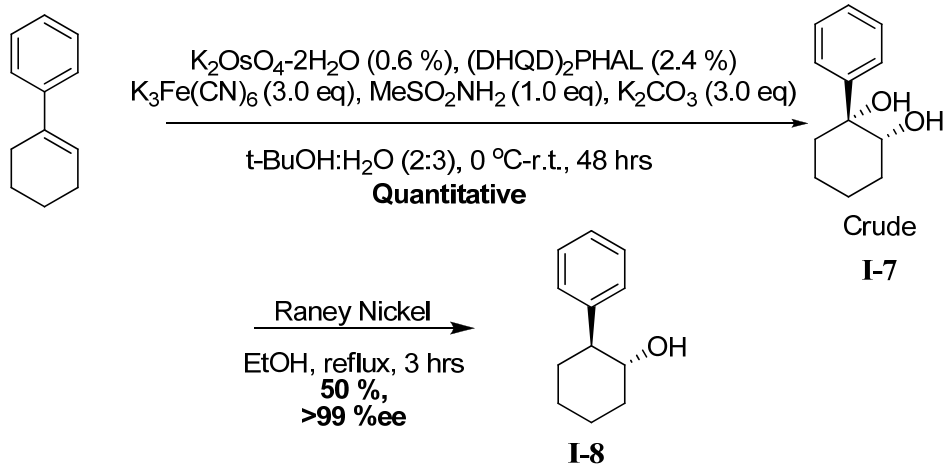

Scheme 12: Synthesis of enantiopure Whitesell's chiral auxiliary, **I-8**.

After enantiopure I-8 was obtained, the synthesis of the chiral ester can be accomplished via coupling of an acyl chloride moiety. The synthesis of the acyl chloride moiety is shown in **scheme 13**. Commercially available methyl glycolate was protected with TIPSCl in the presence of imidazole and DMF to give **I-9**. Compound **I-9** underwent hydrolysis by aqueous lithium hydroxide that afforded **I-10** in high yield. Aqueous lithium hydroxide was previously shown to selectively hydrolyze esters while not effecting large silyl-ether substituents, such as TBDMS or

TIPS.[40] The free carboxylic acid was transformed into an acyl chloride, **I-11**, in the presence of oxylal chloride and a catalytic amount of DMF.

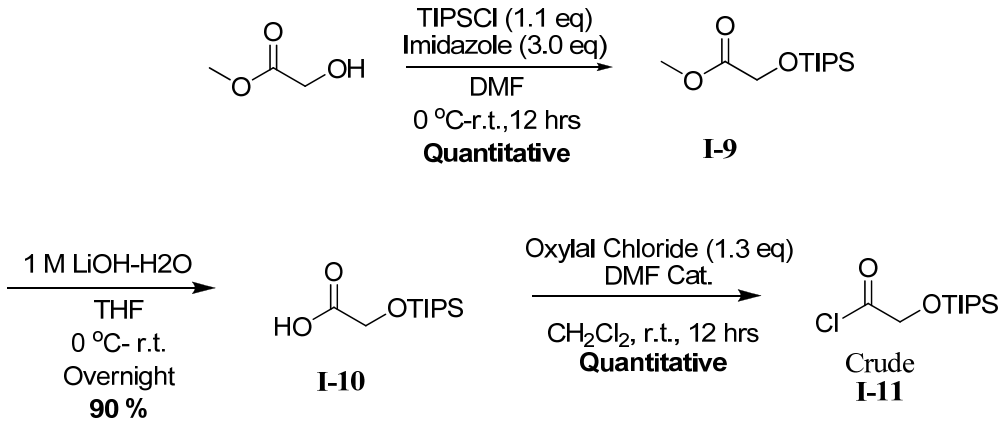

Scheme 13: Synthesis of the acyl chloride for chiral ester formation**.**

The synthesis of the chiral ester and subsequent cyclocondensation to form the β-lactam is shown in **scheme 14**. After the acyl chloride intermediate was synthesized **(I-11**), it was coupled to **I-8** in the presence of DMAP and pyridine that afforded the chiral ester, **I-12**, in high yield. The acyl chloride was used in the coupling reaction without purification. During the course of this reaction, HCl was generated which was trapped as a pyridine salt. With the Chiral ester in hand, the cyclocondensation reaction was done with the crude imine in freshly prepared LDA solution. The imine was slowly added over the course of 2 hours to the LDA-chiral ester solution via a syringe pump. Reaction was mixed overnight at -85 ^{o}C. LiHMDS was added to the solution upon completion. Purification of the crude product mixture was tedious and afforded the β-lactam in low yields after several recrystallizations. The %ee of the β-lactam was determined to be 98 % by HPLC.

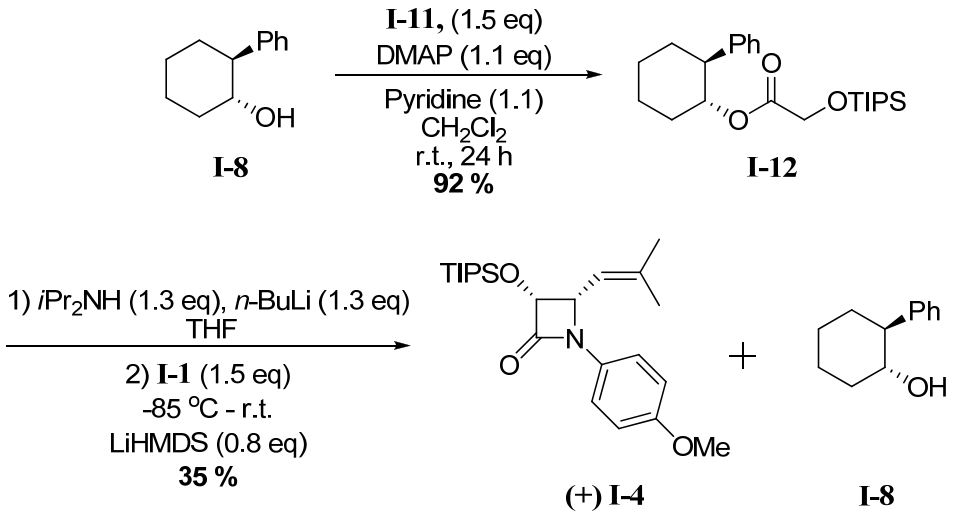

Scheme 14: Synthesis of Chiral ester and cyclocondensation with imine.

The high optical purity allowed for further modification by the same methods shown in **scheme 7**; **(+) I-4** underwent CAN deprotection and subsequent boc protection that afforded the desired β-lactam in good yields.

§1.4.0 Next Generation Taxanes

Paclitaxel and Docetaxel, have had an immense impact in the field of chemotherapy because of their ability to induce apoptosis by stabilizing microtubules, causing the arrest of cellular division in the G2/M phase leading to early mitotic exit.[5] As stated in earlier sections, recent reports have shown that treatment with these potent chemotherapeutic drugs has led to multi-drug resistance (MDR) in cancer cells.[16] Thus, it is extremely important to synthesize new generation taxoids with increased potency and activity in MDR expressing cancers.

MDR enables the cancer cell to remove cytotoxic agents out of the cell via ATP dependent efflux pumps, which results in the loss of efficacy of the drug.[18] P-glycoprotein (Pgp)

and multidrug resistance-associated proteins (MRP) are two molecular pumps from the ABC family that have been associated with MDR. According to extensive SAR studies on paclitaxel, the C-10 position shows a very high affinity for Pgp pump and C-2, C-4, C-1', and C-3'N acyl position shows good affinity for Pgp pump (**Figure 8**).[25] Modifying these positions with other functional groups may cause the drug to be unrecognizable to efflux pumps, thus increasing its potency and reversing the effects of MDR in cancer cells.

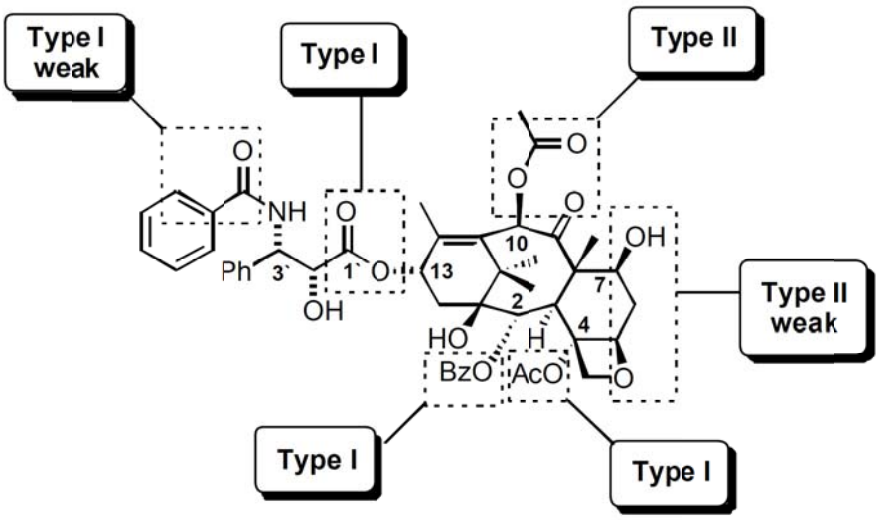

Figure 8: Paclitaxel recognition elements for Pgp. Type II shows stronger affinity for Pgp.[25]

Ojima *et. al*. have found that the C-3'-phenyl group was not an essential component in the activity of taxanes and that modification of the C-10 position with certain acyl groups as well as replacement of the phenyl group with an isobutenyl group at the C-3' position made taxene analogs with 2-3 orders of magnitude more potent than paclitaxel in MDR expressing cancer cell lines.[24] These highly potent taxanes were named 2nd generation taxanes. Of these second generation taxanes, SB-T-1214 has not only shown improved potency against MDR cell lines, but also shows increased activity in ovarian cell lines, 1A9PTX10 and 1A9PTX22, which contain point mutations in β-tubulin.[41] Another 2nd generation taxane, SB-T-1216, has shown to

induce cell death in a different mechanism than paclitaxel. Cell death induced by SB-T-1216 took place without the accumulation of cells in the G2/M phase but with a decreased number of G1 cells and the accumulation of hypodiploid cells, whereas, paclitaxel induced cell death is associated with accumulation of cells in the G2/M phase.[42] Second generation taxane, SB-1213 has also shown to enhance and alter polymerization of microtubules when compared to paclitaxel. These alterations caused by SB-T-1213 include the formation of unusual microtubule with attached extra protofilaments or open sheets; these differences may explain the heightened potency and efficacy of SB-T-1213.[43]

Kingston, et al. have reported that modifications at the meta position of the C-2 benzoate of paclitaxel has shown increased cytotoxicity in MDR cancer cell lines.[18] With this information at hand, Ojima *et. al.* have further modified the C-2 position of the baccatin core of 2nd generation taxanes. Modifications at the C-2 position include an electron rich substituent on the benzoyl group. These taxanes are also 2-3 orders of magnitude more potent than the parent compound and also show no difference in the IC_{50} values in both cancer cell lines and MDR expressing cancer cell lines, whereas 2nd generation taxanes show an decreased IC_{50} value in MDR cancer cell lines relative to non-MDR expressing cancer cell lines.[41] These taxanes that show no difference in potency in MDR and non-MDR cancer cell lines are called 3rd generation taxanes.[41] Structures of 2nd and 3rd generation taxanes are shown in **Figure 9**.

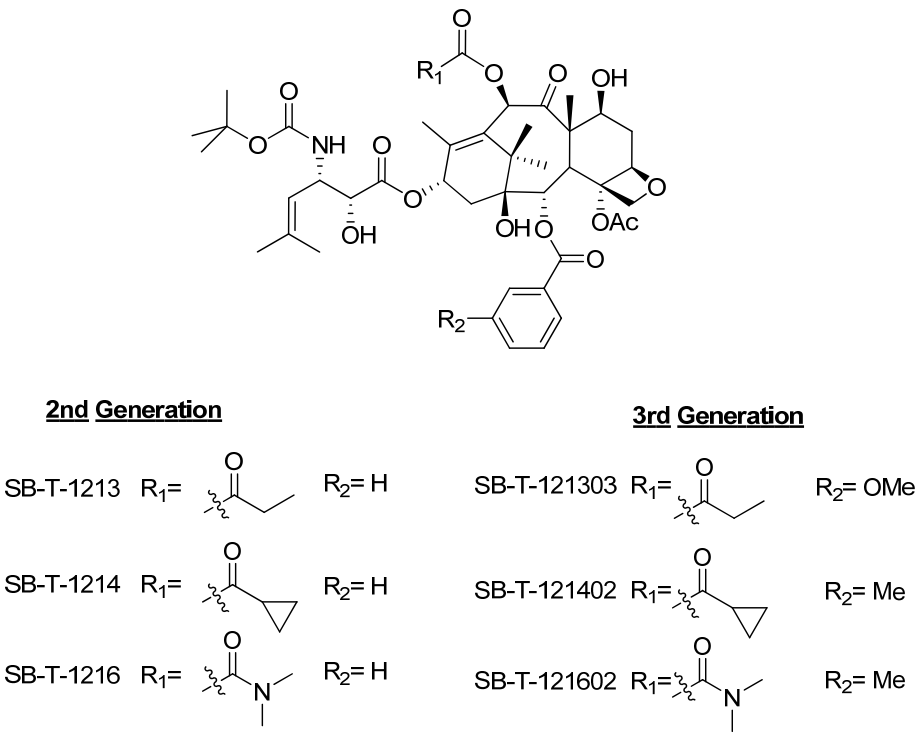

Figure 9: 2nd and 3rd generation taxanes.

The synthesis of next generation taxanes is of key interest in the Ojima lab. Chemical modifications on the 10-deacetyl baccatin III skeleton and subsequent attachment of the C-13 side chain *via* Ojima-Holton protocol using an enantiopure β-lactam are done to synthesize several different next generation taxanes.

§1.4.1 Synthesis of SB-T-1214

Modification of the baccatin core for the synthesis of SB-T-1214 began with the selective protection of the C-7 position on the natural product **10-DAB** using triethylsilyl chloride (TESCl) and imidazole in dimethylforamide (DMF). Selective protection at the C-7 position can occur because that is the most reactive hydroxyl group on the baccatin core. The desired 7-TES-DAB, **II-1**, was afforded in high yields. Compound **II-1** was then acylated at the C-10 position

in the presence of cyclopropanecarboxylic acid chloride and LiHMDS to yield modified 10-DAB (**II-2**) in moderate isolated yield. Modification at the C-10 position can be difficult; disubstituted product at the C-10 and C-13 positions can be obtained if the reaction time is lengthened. Slow dropwise addition of LiHMDS was done and it was carefully monitored to prevent disubstitution. The low yield is due to initial signs of disubstitution that occurred; the reaction was quenched to prevent further disubstitution, as a result a significant amount of **II-1** and **II-2** were both isolated and collected. Disubsitiution should be avoided because the C-13 position must be free for the Ojima-Holton coupling protocol and deacylation of the C-13 position can be difficult. It has been experimentally observed that large scale C-10 acylation gives high yields without diacylated side product. The collected **II-1** was re-subjected to the acylation reaction. **Scheme 15** shows the C-10 modification towards SB-T-1214. Several modified baccatins can be afforded using this protocol with necessary acyl chlorides.

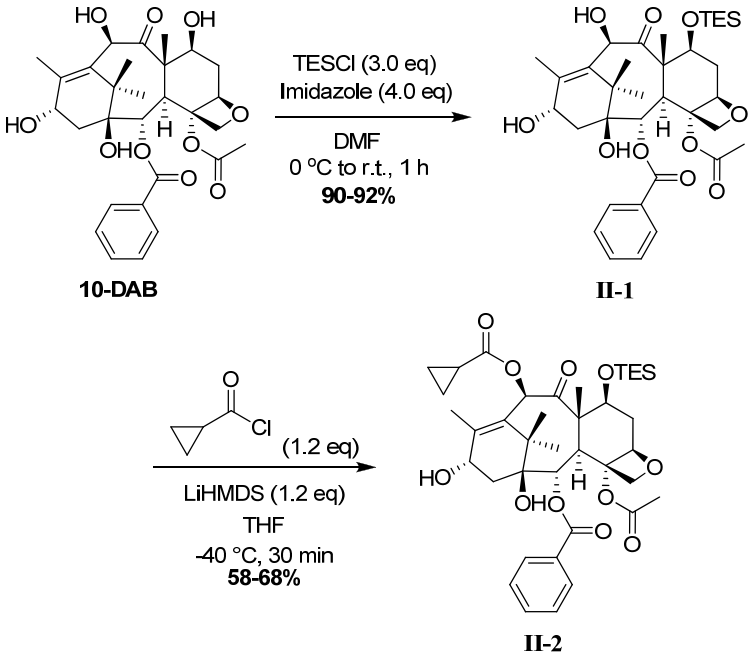

Scheme 15: 7-Tes protection of 10-DAB and subsequent C-10 modification towards SB-T-1214.

Compound **II-2** was then subjected to the Ojima-Holton coupling with high optical purity β-Lactam (>97% ee), which produced protected SB-T-1214 (**II-3**) in good yields. The β-Lactam used in the coupling was prepared via chiral ester enolate-imine cyclocondensation or Staudinger [2+2] cycloaddition followed by enzymatic resolution protocols. Subsequent deprotection in the presence of fluorine afforded SB-T-1214 (**II-4**) in high yields as shown in **scheme 16**.

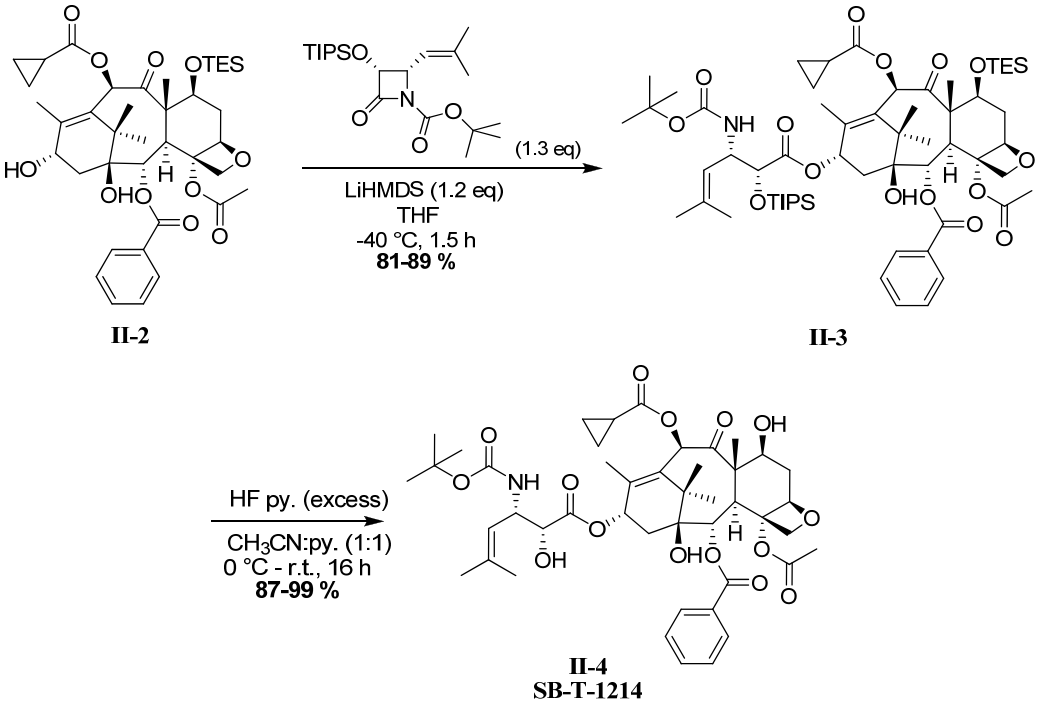

Scheme 16: Synthesis of SB-T-1214 via Ojima-Holton Coupling protocol.

§1.4.2 Synthesis of 3rd generation taxanes

As mention before, potent 3rd generation taxanes contain a meta substituent on the C-2 benzoyl group as well as modifications at the C-10 position on the baccatin core. Modification of C-2 position on DAB is shown in **scheme 17**.

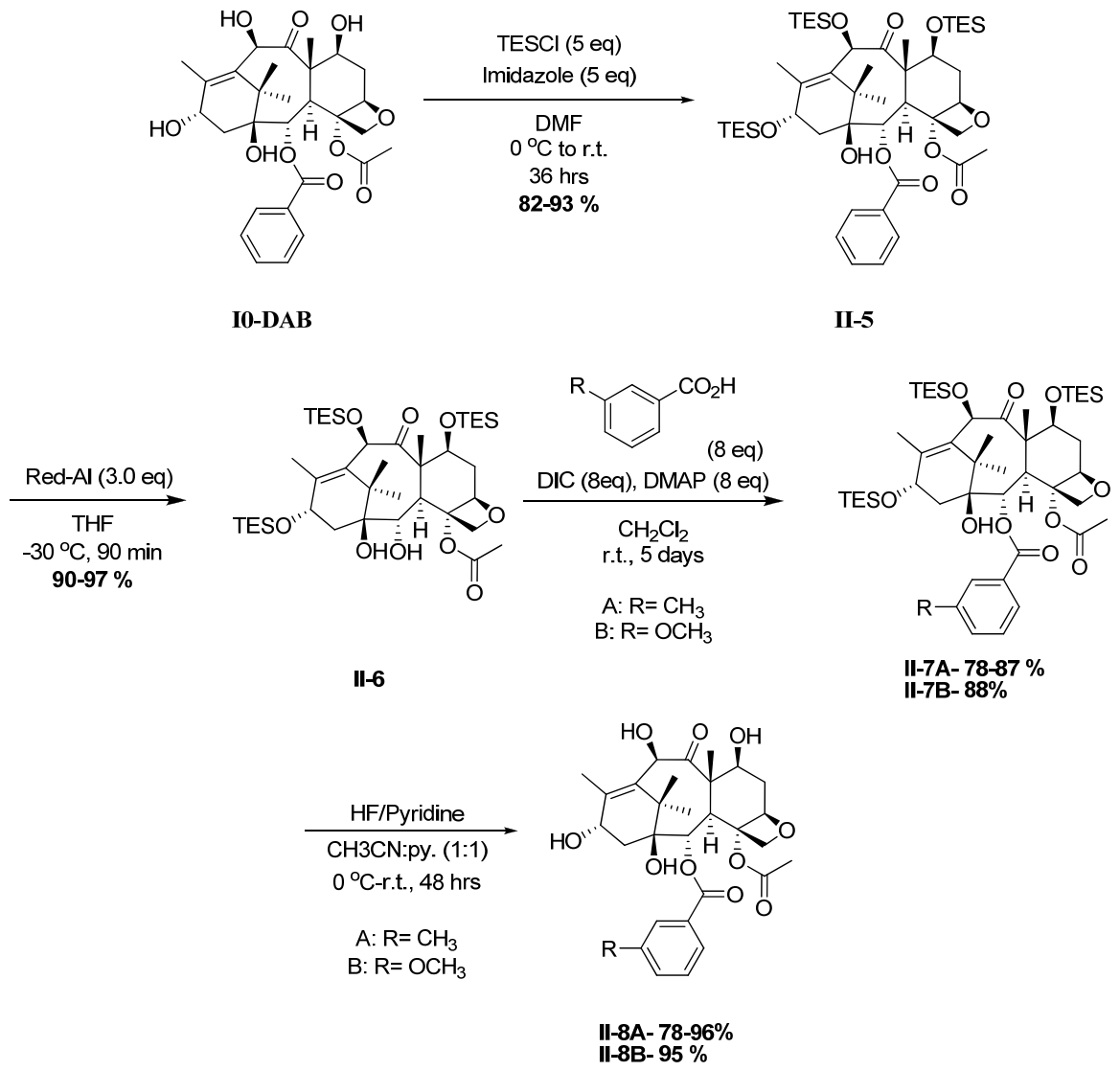

Scheme 17: Synthesis of C-2 modified DAB.

The synthesis towards 3rd generation taxanes began with the global protection of the baccatin core. The C-7, C-10, C-13 positions of the baccatin were protected with triethylsilyl chloride in Imidazole that afforded tri-TES-baccatin, **II-5**, in high yields. Subsequent reductive cleavage of the C-2 benzoate group was done using Red-Al, sodium bis(2-methoxyethoxy)aluminumhydride, which gave tri-TES-2-debenzyol-DAB, **II-6**, in excellent yields. Compound **II-6** was reacted with excess m-toluic acid (A) or 3-methoxy-benzoic acid (B)

in the presence of large amounts of 4-dimethylaminopyridine (DMAP) and N,N'-diisopropylcarbodiimide (DIC) in a concentrated dichloromethane solution for 5 days, which afforded tri-TES-2-m-methyl-benzyol-DAB, **II-7A**, and tri-TES-2-m-methoxy-benzyol-DAB, **II-7B**, in moderate to high yields respectively. In the coupling reaction, the substrate contains a free hydroxyl group at the C-1 position and with such excess coupling agents; it can be assumed that coupling can happen at the C-1 position in addition to coupling at the C-2 position. However, acylation at the C-1 position was not observed due to the fact that this hydroxyl group is buried in the DAB structure. Compounds **II-7B** and **II-7A** underwent subsequent deprotection in HF/pyridine to remove all the TES protecting groups from the baccatin skeleton that gave C-2 modified DABs, **II-8A** and **II-8B** in moderate to high yields.

Once the C-2 modified DAB was obtained, further modification at the C-10 position can be achieved using the same protocol shown in the modification of **10-DAB** for the synthesis of SB-T-1214 (**Scheme 15**). Compound **II-8A** underwent further C-10 modification shown in **Scheme 18**.

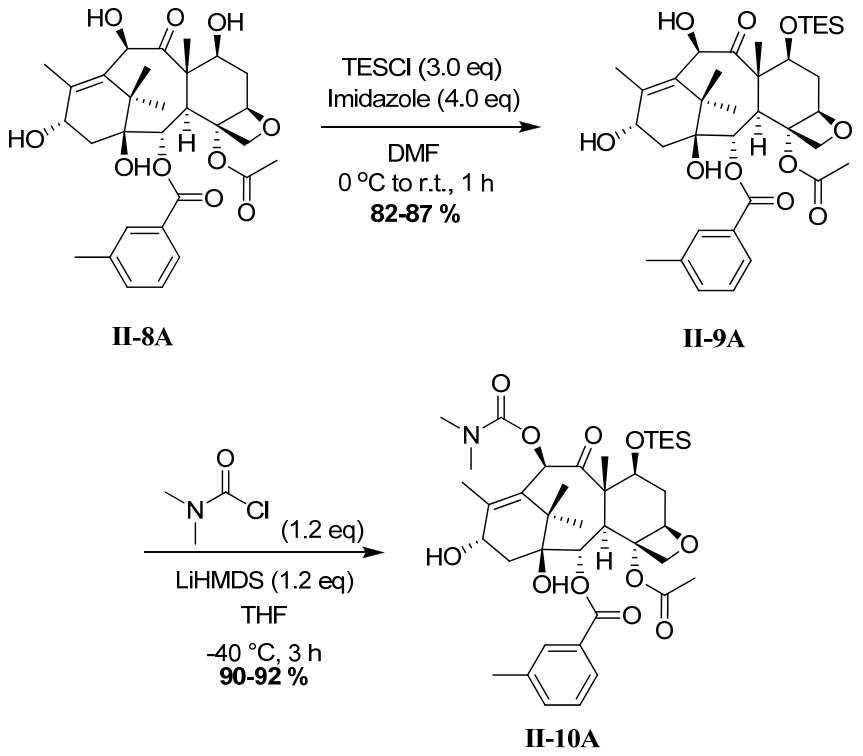

Scheme 18: Synthesis of C-10 modified 3-methyl-DAB.

The C-7 position of 2-m-methylbenzyol-DAB was selectivity protected with TES using triethylsilyl chloride (TESCl) and imidazole in dimethylforamide (DMF) that afforded 2-m-methylbenzyol-7-TES-DAB, **II-9A**, in good yields. Subsequent C-10 modification was done using dimethylcarbamoyl chloride in the presence of LiHMDS, which gave 2-m-methylbenzyol-7-TES-10- dimethylcarbamoyl–Baccatin, **II-10A**, in excellent yields. This C-10 acylation reaction was slow and did not show any evidence of disubsitituted side product, which was observed in C-10 modification on DAB using cyclopropanecarboxylic acid chloride for the synthesis of SB-T-1214. Thus, dimethylcarbamoyl chloride must be relatively stable at the low temperature and also because of the stable nitrogen-carbon bond in the structure may contribute its stability.

Modification of the C-10 position was also achieved by an alternative protocol as shown in **scheme 19**.

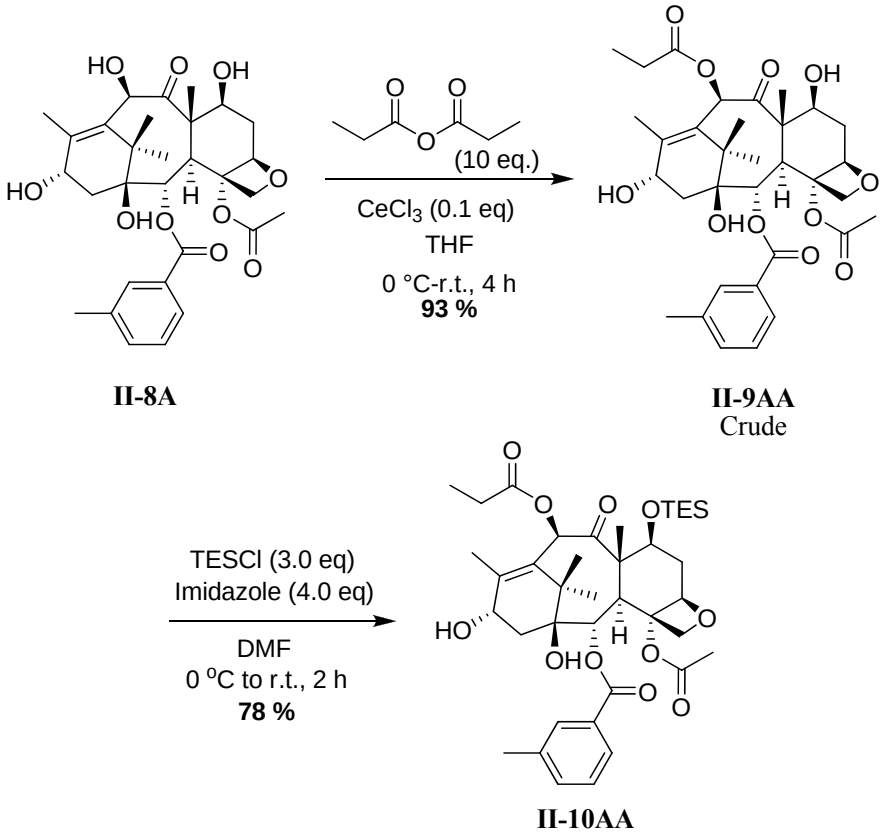

Scheme 19: Alternate protocol for C-10 modification using acid anhydrides.

In the presence of cerium trichloride, acid anhydrides selectivity reacts with the C-10 position on the baccatin core to yield C-10 acylated baccatin. Excess amounts of propionic anhydrides were reacted with **II-8A** in the presence of cerium trichloride that gave compound **II-9AA** in excellent yields. Normally, the C-7 hydroxyl group is more reactive than the C-10 hydroxyl group towards esterification; however, in the presence of cerium trichloride, the C-10 position is selectively acylated. A possible explanation for this selective acylation is that the

Lewis acid, cerium, forms a chelate with the acetylating agent, and the C-7 hydroxyl and C-9 carbonyl groups on DAB, which allows for C-10 acylation (**Figure 10**).[44]

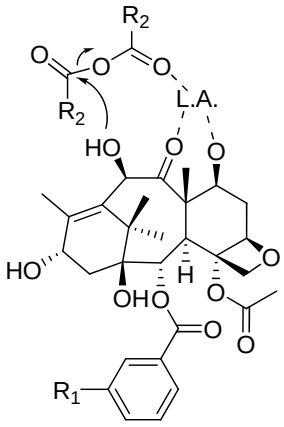

Figure 10: Mechanism for selective C-10 acylation using a Lewis Acid.[11]

This alternative protocol is very attractive for the acylation of the C-10 position because this reaction will not give undesirable di or tri acylated side products. The free C-7 hydroxyl group was used crudely in subsequent protection with TES that produced **II-10AA** in good yields.

Compounds **II-10A** and **II-10AA** were then subjected to the Ojima-Holton coupling protocol and subsequent deprotection that gave 3rd generation taxoids, SB-T-121602, **II-12A**, and SB-T-121302, **II-12AA** (**Scheme 19**) in moderate yields. The β-Lactam used in the coupling reactions were >97 % ee and were previously prepared via chiral ester enolate-imine cyclocondensation or Staudinger [2+2] cycloaddition followed by enzymatic resolution protocols.

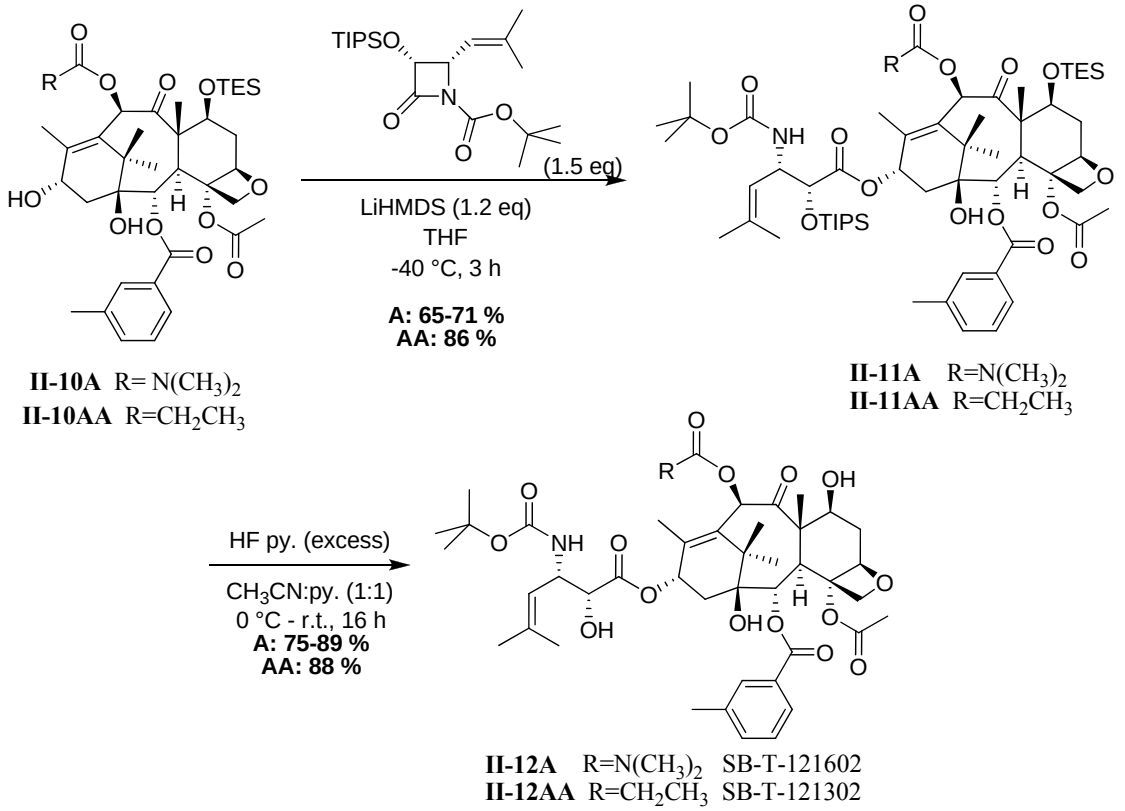

Scheme 20: Synthesis of 3rd generation taxanes, SB-T-121602 and SB-T-121302, via Ojima-Holton coupling Protocol.

§1.4.3 Synthesis of a Taxane construct

§1.4.3.1 Introduction

New generation taxanes were synthesized in high yields from the Ojima-Holton coupling protocol using modified baccatins and enantiopure β-lactams. However, synthesizing a library of new generation taxanes can be a lengthy process considering that it takes 8 steps to synthesize 3rd generation taxanes and each step requires purification via column chromatography. A practical and economical approach would be to synthesize a taxane construct which can be utilized in a few chemical reactions to yield a variety of next generation taxanes. The majority of next

generation taxanes synthesized in the Ojima lab contain modifications at the C-2 and C-10 positions on the baccatin core which gives rise for the diverse library of taxane analogs. A possible construct can be a taxane with an available C-10 position that can be easily acylated with various acyl chlorides to yield a diverse array of new generation taxanes. **Scheme 21** displays the rationale for the synthesis of new generation taxanes using the taxane construct.

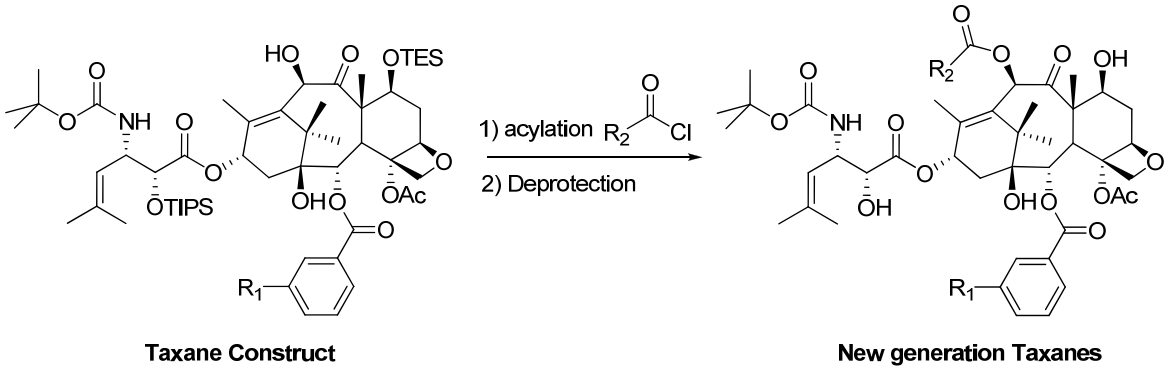

Scheme 21: Synthesis of New generation Taxanes using a Taxane construct.[41]

This taxane strategy has been employed in the Ojima lab.[41] Using this taxane construct strategy, one can synthesize new generation taxanes when needed in just two easy steps instead of synthesizing it from 10-DAB.

§1.4.3.2 Results and Discussion

The synthesis toward the taxane construct began with the selective acylation of 10-DAB, **III-1A**, and m-methoxy-DAB, **III-1B**, to eventually afford a 2nd and 3rd generation construct (**Scheme 22**).

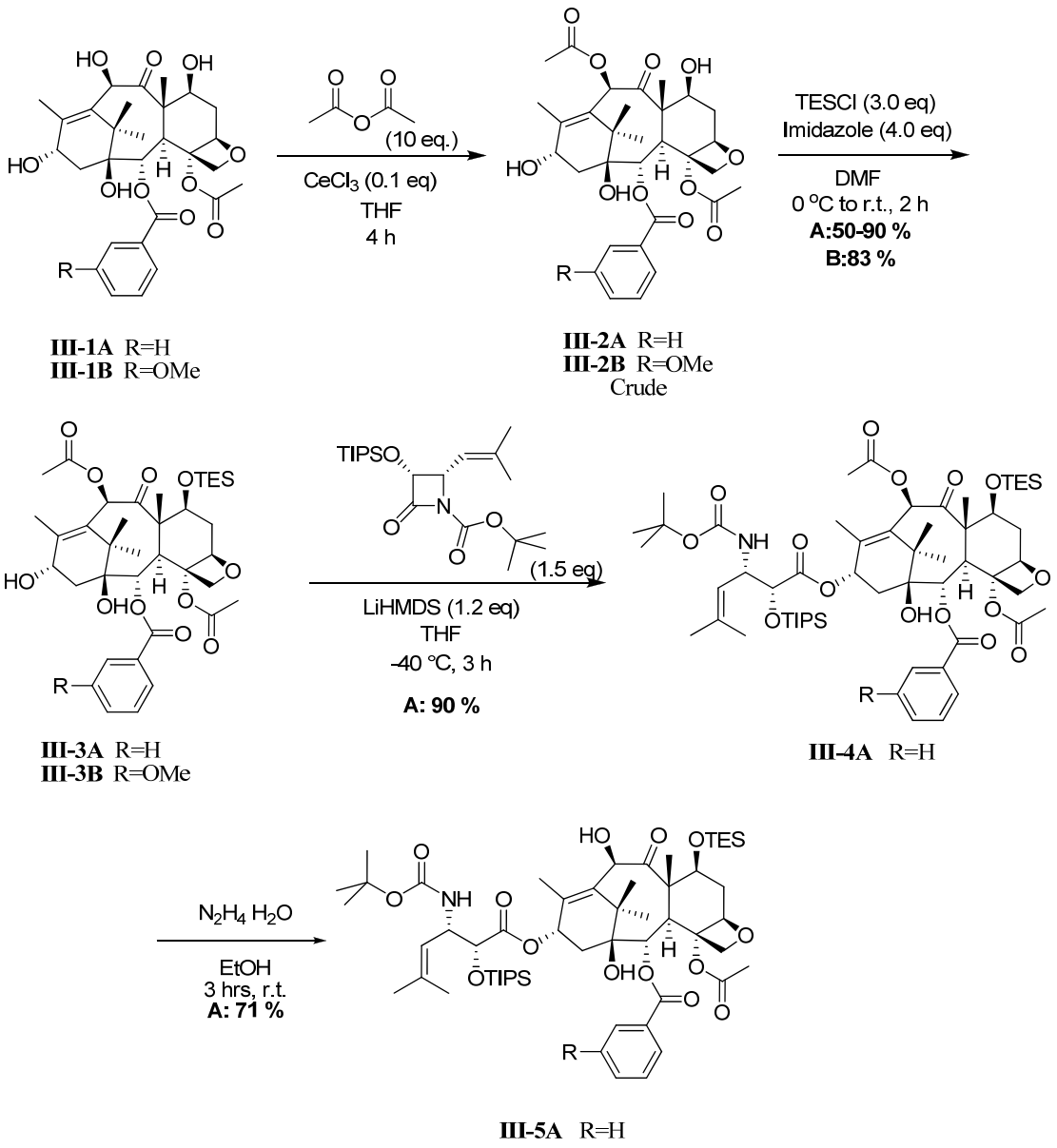

Scheme 22: Synthesis of Taxane Construct.[41]

C-10 acylation was achieved using acetic anhydride in the presence of cerium chloride that afforded compounds **III-2A** and **III-2B**. The free C-7 positions of these compounds were later silylated to afford **III-3A** and **III-3B** in good yields. A low yield of 50 % was observed for one experiment because the solvent (DMF) was wet, which prevented complete C-7 protection on compound **III-2A**. Compound **III-3A** was coupled to an optically pure, >97 % ee, β-lactam

via Ojima-Holton coupling protocol that afforded **III-4A** in excellent yields. Selective deacylation at C-10 position of compound **III-4A** was achieved using hydrazine monohydrate in ethanol. Initial attempts at this selective deacylation resulted in 0 % conversion; this was because the hydrazine monohydrate used was a very old bottle and may have been oxidized. A new bottle was used and afforded the desired product, **III-5A**, in moderate yields. However, this reaction produced a small amount of a side product, < 8 %. The side product was determined via FIA and ^{1}H-NMR analysis to be compound **III-5A** without the C-7 TES group attached to it. Thus, the reaction condition became too harsh due to the accumulation of acetohydrazide by-product which may have result in the cleavage of the bulky TES group.

With the second generation taxane construct in hand, various 2nd generation taxanes can be synthesized. The construct, **III-5A**, was used to synthesize 2nd generation taxoid, SB-T-1214 (**Scheme 23**).

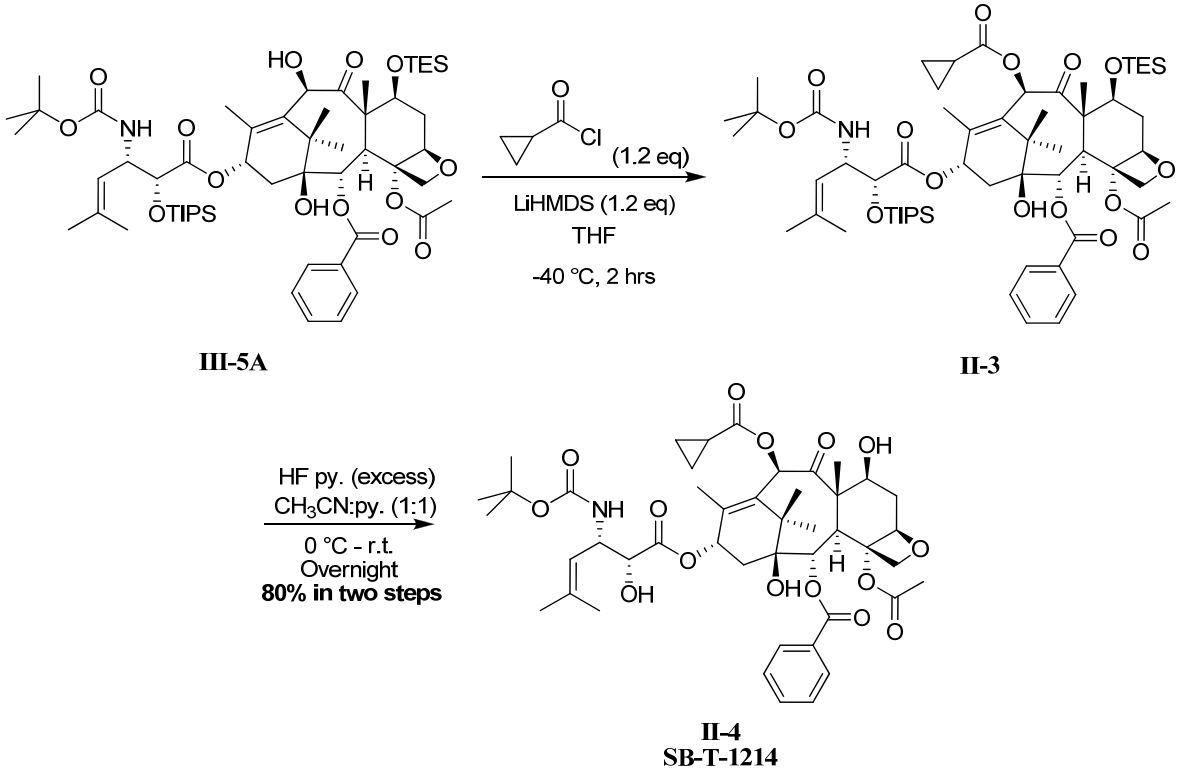

Scheme 23: Synthesis of SB-T-1214 from the Taxane construct.

Compound **III-5A** was acylated with cyclopropanecarboxylic acid chloride in the presence of LiHMDS to afford compound **II-3**. Subsequent deprotection gave SB-T-1214, **II-4**, in 80 % yield over two steps. However, another compound was observed in the deprotection reaction; the compound was isolated and characterized via ^{1}H-NMR and FIA. The compound was determined to be deprotected III-5A (C-10 hydroxyl taxoid). This evidence shows that the acylation of **III-5A** with cyclopropanecarboxylic acid chloride to yield **II-3** was not complete. This reaction was monitored via TLC analysis and ^{1}H-NMR. Monitoring this reaction can be difficult; TLC does not work well since there is minimal difference in polarity between compounds **III-5A** and **II-3** and ^{1}H-NMR may not always give accurate conversion values. As a result, this reaction should be monitored via HPLC to ensure completion and higher yields.

§1.5 Conclusions

The synthesis of a high optically pure β-lactam was done using two different synthetic routes; the standard Staudinger [2+2] cycloaddition followed by enzymatic resolution protocol, which has been well established in the Ojima lab and by new chiral ester enolate-imine cyclocondensation route that incorporates a new methodology by Sharpless and others for the synthesis of the chiral auxiliary used in the formation of the chiral ester. Both synthetic routes produced good quantities of β-lactams with high optical purity, however using the standard protocol, the β-lactam was afforded in 4 weeks due to the long and unreliable enzymatic resolution reaction. The new chiral ester enolate-imine cyclocondensation route produced larger quantities of β-lactam in just 2 weeks. The new protocol is a better and a more efficient way of synthesizing β-lactams with high optical purity.

In vivo studies and biological evaluation of new generation taxanes requires a large supply of taxanes, thus, highly potent second and third generation taxanes were synthesized. The promising second generation taxane, SB-T-1214, was synthesized in good yields. Third generation taxanes, SB-T-121602 and SB-T-121302 were synthesized in good yields. The synthesis of a taxane construct was also done. The rational for the taxane construct is that it can be used as an intermediate for the synthesis of diverse taxanes in a timely fashion. This construct was successfully synthesized and utilized to produce SB-T-1214 in good yields. This taxane construct can provide a better and faster means of synthesizing taxanes.

§1.6 Experimental Section

§1.6.1 General Methods and Materials

^{1}H and ^{13}C NMR spectra were measured on a Varian 300, 400 or 500 NMR spectrometer. Melting points were measured on a Thomas Hoover Capillary melting point apparatus and are uncorrected. Optical rotations were measured on a Perkin-Elmer Model 241 polarimeter. TLC was performed on Merck DC-alufolien with Kieselgel 60F-254 and column chromatography was carried out on silica gel 60 (Merck; 230-400 mesh ASTM). Mass to charge values were measured by flow injection analysis on an Agilent Technologies LC/MSD VL. In determining enantiopurity (% ee) of β-lactam, a Chiracel OD-H chiral column was used in normal phase, with an isocratic mixture of 85:15 Hexanes: IPA at a flow rate of 0.6 mL/min. In determining the purity of taxanes, a Phenomenex Jupiter 10 μ Proteo 9A column was used in reverse phase, with a mixture of 3:2 methanol: water at a flow rate of 0.4 mL/min.

The chemicals were purchased from Aldrich Co. and Sigma and purified before use by standard methods. Tetrahydrofuran was freshly distilled from sodium metal and benzophenone. Dichloromethane and methanol were also distilled immediately prior to use under nitrogen from calcium hydride. In addition, various dry solvents were degassed and dried using PureSolv™ solvent purification system (Innovative Technologies, Newburyport, MA).

§1.6.2 β-lactam

N-(4-Methoxyphenyl)-3-methyl-2-butenaldimine (I-1)[15]

A 4 g (32.3 mmol) aliquot of recrystallized *p*-anisidine and 13 g (64.6 mmol) of anhydrous Na_2SO_4 were dissolved in 50 mL dichloromethane under inert conditions. A 3.6 mL (42.0 mmol) aliquot of 3-methylbut-2-enal was added to the solution dropwise. The mixture was stirred at room temperature and monitored by TLC (3:1 hexane: ethyl acetate). After completion, the solvent was evaporated and concentrated *in vacuo* to yield **1-1** as a clear yellow oil (6.11 g, 32.3 mmol, quantitative yield), and was used immediately in the subsequent step; ^{1}H NMR (300 MHz, $CDCl_3$) δ 1.99 (d, J = 30 Hz, 6 H), 3.80 (s, 3 H), 6.21 (d, J = 15 Hz, 1 H), 6.85 (d, J = 3.75 Hz, 2 H) 7.08 (d, J = 3.75 Hz, 2 H), 8.39 (d, J = 4.25 Hz, 1 H). All data are in agreement with literature values.[15]

(±)-1-(4-Methoxyphenyl)-3-acetoxyl-4-(2-methylprop-1-enyl)azetidin-2-one (I-2)[45]

A 6.11 g (32.3 mol) aliquot of crude **I-1** was dissolved in 75 mL of dichloromethane. The mixture was cooled to -78 ˚C and maintained for at least 30 min under inert conditions. To the cooled solution, 9 mL of TEA (64.6 mmol) was added, followed by the slow and dropwise addition of acetoxyacetyl chloride (5.2 mL, 48.5 mmol). The -78 ˚C temperature of the mixture was maintained for at least 2 h. The mixture was stirred and allowed to warm slowly to room temperature overnight. The reaction was monitored by TLC (3:1 hexane: ethyl acetate). After completion, the reaction was quenched with 50 mL of saturated NH_4Cl. The organic layer was washed three times with brine (75 mL), dried over anhydrous $MgSO_4$, and concentrated *in vacuo,* producing a brown solid. Purification was done *via* column chromatography on silica gel (5:1 hexanes:ethyl acetate) to yield racemic **I-2 (**4.74 g, 51 % yield) as an off-white soild. ^{1}H NMR (300 MHz, $CDCl_3$) δ 1.79 (s, 3 H), 1.82 (s, 3 H), 2.11 (s, 3 H), 3.78 (s, 3 H), 4.9 (dd, *J* = 9.9Hz, 4.8 Hz, 1 H), 5.02 (d, *J* = 9.3 Hz, 1 H), 5.8 (d, *J* = 4.8 Hz, 1 H), 6.84 (d, *J* = 8.9 Hz, 2 H), 7.30 (d, *J* = 8.9 Hz, 2 H); m.p.= 101 – 103 ^{o}C. All data are consistent with literature values.[45]

Enzymatic Resolution of 1-2[34]

The racemic **I-2** mixture (4.74 g, 16.5 mmol) was dissolved in 600 mL of 0.2 M sodium phosphate buffer (pH 7.5) with 10 volume % acetonitrile and heated to 50 °C. A 2.59 g aliquot of PS-Amano Lipase was added to the solution. After addition, the mixture was stirred vigorously with a mechanical stirrer for 5 days at 50 ^{o}C. The reaction was monitored by TLC (3:1 hexanes: ethyl acetate) and ^{1}H-NMR, looked for 50% conversion of the acetate moiety to

the hydroxyl moiety. After 50% conversion, the remaining Lipase was filtered off *via* vacuum filtration and was washed with dichloromethane (50 mL). The organic layer was collected, washed 3 times with brine (100 mL), dried over anhydrous $MgSO_4$, and was concentrated *in vacuo* which produced yellow-white solid. Purification was done by column chromatography on silica gel (5:1 hexanes: ethyl acetate) to yield enantiopure **(+) I-2** (1.28 g, 28 % yield) as an off white solid and the resulting alcohol **(-) I-3** as a tan solid (not quantified). The enantiometric excess was determined to be >99 % *via* HPLC analysis on normal phase with a Chiracel OD-H column using Hexanes: Isopropanol (85:15, 0.6 mL/min): m.p.= 85-87 ^{o}C. ^{1}H NMR (300 MHz, $CDCl_3$) δ 1.79 (s, 3 H), 1.82 (s, 3 H), 2.11 (s, 3 H), 3.78 (s, 3 H), 4.9 (dd, *J* = 9.9Hz, 4.8 Hz, 1 H), 5.02 (d, *J* = 9.3 Hz, 1 H), 6.84 (d, *J* = 8.9 Hz, 2 H), 7.30 (d, *J* = 8.9 Hz, 2 H). All data are consistent with literature values.[34]

(3*R*,4*S*)-1-(4-Methoxyphenyl)-3-hydroxy-4-(2-methylprop-1-enyl)azetidin-2-one [(+) I-3][46]

A 1.24 g (4.32 mmol) aliquot of enantiomerically pure **(+) I-2** was dissolved in 20 mL of THF (~0.1 M) and cooled to 0 °C. A 1 M solution of KOH dissolved in 20 mL of THF was added to the mixture. The reaction mixture was stirred and monitored by TLC (3:1 hexanes: ethyl acetate). After completion, the reaction was quenched with 65 mL of saturated NH_4Cl and extracted with dichloromethane (75 mL). The organic layer was separated, washed three times with brine (200 mL), dried over anhydrous $MgSO_4$, and concentrated *in vacuo* to yield **(+) I-3** (1.04 g, 100 % yield) as a white solid: m.p.= 161-162 ^{o}C (lit.[46] 169-171 ^{o}C)^{1}H NMR (300 MHz, $CDCl_3$) δ 1.43 (s, 1H), 1.85 (s, 3 H), 2.27 (bs, 1H), 3.78 (s, 2 H), 4.82(t, *J* = 0.18 Hz, 1 H), 4.97

(s, 1 H), 5.20 (d, J = 6 Hz), 6.83 (d, J = 6 Hz), 7.33 (d, J = 5 Hz). All data are consistent with literature values.[46]

1-*p*-Methoxyphenyl-3-triisopropylsiloxy-4-(2-methylpropen-2-yl)azetidin-2-one [(+) I-4][15]

A 1.04 g (4.20 mmol) aliquot of **(+) I-3** and 154 mg (1.26 mmol) of DMAP were dissolved in 20 mL of dichloromethane (~0.1 M). The solution was cooled to 0 °C under inert conditions. A 1.2 mL (8.40 mmol) aliquot of TEA was added to the solution followed by the dropwise addition of 1.6 mL (6.30 mmol) of TIPSCl. The reaction mixture was stirred at room temperature and monitored by TLC (3:1 hexane: ethyl acetate). After completion the reaction was quenched with 40 mL of saturated NH_4Cl and extracted with dichloromethane (50 mL). The organic layer was collected, washed three times with brine (100 mL), dried over anhydrous $MgSO_4$, and concentrated *in vacuo*. Purification was done using column chromatography on silica gel (20:1 hexanes:ethyl acetate) to yield **(+) I-4** as a yellow solid. Recrystallization was performed using hexanes to yield **(+) I-4** (1.58 g, 90 % yield) as a white solid: m.p.= 92-94 ^{o}C; ^{1}H NMR δ ($CDCl_3$, 300 MHz) 0.99 (m, 21 H), 1.79 (d, J = 2.3 Hz, 3 H), 1.84 (d, J = 2.4 Hz, 3 H), 3.77 (s, 3 H), 4.41 (dd, J = 9.9, 5.1 Hz, 1 H), 5.04 (d, J = 5 Hz, 1 H), 5.30 (d, J = 9.8 Hz, 1 H), 6.82 (d, J = 8.1 Hz, 2 H), 7.30 (d, J = 8.5 Hz, 2 H). All data are consistent with literature values.[15]

3-Triisopropylsilyloxy-4-(2-methylpropen-2-yl)azetidin-2-one [(+) I-5][24]

A 1.30 g (3.21 mmol) aliquot of **(+) I-4** was dissolved in 105 mL of acetonitrile and cooled to -10 °C. To this solution, 6.17 g (11.3 mmol) of CAN dissolved previously dissolved in 105 mL

of H_2O was added dropwise over 1 hr *via* an addition funnel. The reaction temperature of -10 °C was maintained throughout the reaction. The reaction was monitored by TLC (3:1 hexanes: ethyl acetate, stained with PMA) and completed in 3 h. Upon completion, the reaction was quenched with saturated aqueous $NaHSO_3$ (100 mL). The aqueous layer was extracted with ethyl acetate (500 mL) and was washed three times with brine (200 mL). The organic layer was dried over anhydrous $MgSO_4$ and concentrated *in vacuo* that afforded a brown oil. The resulting crude oil was purified *via* column chromatography on silica gel with (85:15 hexanes:ethyl acetate) that yielded **(+) I-5** (0.90 g, 94 % yeild) as a white solid: m.p= 85-87 ^oC (lit.[24] 84.5-86 ^oC) ^1H NMR (300 MHz, $CDCl_3$) δ 1.06, (m, 18 H), 1.55 (s, 6 H), 1.7 (d, 6 H, *J*= 22 Hz), 2.24 (s), 4.12 (q),4.45 (dd, 1 H, *J*=5.4 Hz, 5.4 Hz), 4.98 (m, 1 H), 5.32 (d, 1 H, *J*= 15 Hz), 5.79 (bs, 1 H). All data are consistent with literature values.[24]

1-(*tert*-Butoxycarbonyl)-3-triisopropylsiloxy-4-(2-methylpropen-2-yl)azetidin-2-one [(+) I-6][24]

A 0.771 g (2.60 mmol) aliquot of **(+) I-5**, 0.095 g (3.90 mmol) of DMAP, and 0.720 ml (5.2 mmol) of TEA was dissolved in 13 mL of dichloromethane and cooled to 0 °C under inert conditions. A 0.85 g aliquot of di-*tert*-butyl dicarbonate was added to the mixture. The reaction mixture was stirred at room temperature overnight and monitored by TLC. Upon completion the reaction was quenched with 35 mL of saturated NH_4Cl and extracted twice with dimethylchloride (30 mL). The organic layer was washed three times with brine (50 mL), dried over anhydrous $MgSO_4$, and concentrated *in vacuo* that afforded a light brown oil. The resulting crude oil was purified *via* column chromatography on silica gel with (85:15 hexanes:ethyl

acetate) that yielded **(+) I-5** (01.03 g, 97 % yeild) as a clear oil. ^{1}H-NMR (300 Hz) δ 1.06, (m, 18 H), 1.48 (s, 9 H),1.67 (s, 6 H), 1.76 (d, 6 H, *J*= 9 Hz), 2.24 (s), 4.75 (dd, 1 H, *J*=6 Hz, 6 Hz), 4.95 (s, 1 H), 4.98 (s, 1 H), 5.28 (dt, 1 H, *J*= 0.3 Hz, 0.3 Hz). All data are consistent with literature values.[24]

(+)-(1*R*,2*S*)-1-phenylcyclohexane-*cis*-1,2-diol [I-7][38]

A 25 g (76 mmol) aliquot of potassium ferricyanide, 10.5 g (76 mmol) of potassium carbonate, and 2.40 (25 mmol) of methanesulfonamide were added to a 250 mL round bottomed flask. Then a mixture of 32 mL of *tert*-butanol dissolved in 48 mL of distilled water was added to the round bottom flask. Mixture appeared dark orange and was cooled down to 0 ^{o}C in an ice bath. Subsequently, 55 mg (0.15 mmol) of potassium osmate dehydrate and 0.4 g (0.6 mmol) of $DHQD_2PHAL$ ligand was added to the reaction mixture. After stirring for an additional 20 min, 4.3 g (14.50 mmol) of 1-phenylcyclohexene was added. This solution was warmed to room temperature and stirred for 48 h. The reaction mixture visibly changed from a dark orange color to a light yellow color as the potassium ferricyanide got reduced by the catalyst. After 48 h, 25 mL of ethyl acetate was added to the solution to stir for 15 min. The entire solution was then filtered to remove solid potassium ferrocyanide and then the resulting liquid was diluted with an additional 20 mL of ethyl acetate. The aqueous layer was discarded and the resulting organic layer was washed 3 times with 20 mL of 2M potassium hydroxide solution. This organic layer was then dried over anhydrous $MgSO_4$ and concentrated *in vacuo* that yielded a slightly yellow solid. This solid was pure enough by ^{1}H NMR for the next step without further purification: m.p. 77-80 ^{o}C, ^{1}H-NMR (300 Hz, $CDCl_3$) δ 1.47 (m, 5 H) 1.69 (m, 2 H), 1.85 (m, 1 H), 2.58 (s, 1 H),

3.89 (s, 2 H), 4.01 (dd, 2 H, *J*= 4.2 Hz, 5.1 Hz), 7.38 (m, 3 H), 7.54 (m, 2 H). All data are consistent with literature values.[38]

(-)-*trans*-2-phenyl-cyclohexanol (WCA) [I-8][38]

To a 500 mL round bottomed flask containing 4.8 g (25 mmol) of crude **I-7** and dissolved in 50 mL of ethanol. The reaction flask was purged with N_2. Then 85 mL of Raney®-Nickel 2800 catalyst in water was added to this solution. The reaction mixture was then refluxed at 100 ^oC for 3 h. The reaction was monitored by TLC (3:1 hexane: ethyl acetate, stain with PMA) with the diol appearing at an Rf of 0.2 and the dehydroxylated product appearing at an Rf of 0.4. After completion, the reaction mixture was cooled to room temperature and then filtered through a 3 mm bed of Celite, while taking care not to dry the solution (dry Raney nickel is pyrogenic and will ignite). The resulting black Ni solid was washed copiously with ethanol (60 mL) and then diluted with water and disposed in a proper container containing water. The resulting filtrate was concentrated *in vacuo* and then dissolved in 20 mL of ethyl acetate. The organic layer was washed three times with 50 mL of brine. The resulting organic layer was dried over anhydrous $MgSO_4$ and concentrated *in vacuo* to yield a white solid. This solid was purified by flash chromatography (9:1 hexanes: ethyl acetate). After column purification the desired product, **I-**8, was recrystallized with pentane that afforded white crystals (4.41 g, 50 % yield). The enantiometric excess was determined to be >99 % *via* HPLC analysis on normal phase with a Chiracel OD-H column using Hexanes: Isopropanol (85:15, 0.6 mL/min): m.p.= 64-66 ^oC (lit.[35] 62-65 ^oC, ^{1}H-NMR (300 Hz, $CDCl_3$) δ 1.50 (m, 5 H) 1.78 (m, 1 H), 1.88 (m, 1 H), 2.13 (m, 1

H), 2.43 (t, 1 H, *J*= 9 Hz), 3.67 (bm, 2 H), 7.23 (m, 3 H), 7.34 (m, 2 H). All data are consistent with literature values.[35]

TIPS-oxymethylglycolate[I-9][47]

A 2.3 g (26 mmol) aliquot of methyl-glycolate and 4.5 g (67 mmol) of imidazole was added to a 100 mL round bottomed flask. Then 11 mL of dry dimethylformamide was added with stirring. The solution was cooled down to 0 ^{o}C with an ice bath and 5.2 mL (24 mmol) of triisopropylsilyl chloride was added dropwise. This solution was stirred for 18 h and then quenched with saturated ammonium chloride (50 mL). The resulting solution was dissolved in 50 mL of ethyl acetate and washed two times with 50 mL of saturated ammonium chloride and three times with 50 mL of brine. The resulting organic layer was dried over anhydrous $MgSO_4$ and concentrated *in vacuo* to yield slightly yellow oil, **I-9** (6.3 g, quantitative yield). This oil was pure enough by ^{1}H-NMR for the next synthetic step without further purification. ^{1}H-NMR (300 Hz, $CDCl_3$) δ 1.06 (m, 18 H), 3.74 (s, 3 H), 4.32 (s, 2 H). All data are consistent with literature values.[47]

TIPS-oxyacetic acid [I-10][47]

A 6.3 g (26 mmol) aliquot of **I-9** was dissolved in 35 mL of 1 M LiOH and 35 mL of THF. The solution was stirred at room temperature overnight. Upon completion, THF was removed by a rotary evaporator. The resulting aqueous solution was then extracted with 10 mL of dichloromethane. The organic layer was discarded and the pH was adjusted to pH 2.0 with 1M HCl. The aqueous solution was then extracted with 50 mL of dichloromethane twice and washed

with brine (3x 60 mL). The resulting organic layer was dried anhydrous $MgSO_4$ and concentrated *in vacuo* that gave **I-10** (5.40 g, 90 % yield) as a clear oil. ^{1}H-NMR (300 Hz, $CDCl_3$) δ 1.09 (m, 18 H), 4.287 (s, 2 H). All data are consistent with literature values.[47]

TIPS-oxyacetyl chloride [I-11][47]

A 5.4 g (23 mmol) aliquot of **I-10** was dissolved in 230 mL of dry dichloromethane in inert conditions. To this solution, 2.5 mL (30 mmol) oxalyl chloride was added and the resulting solution was allowed to stir for 5 min. Then 6 drops of DMF was added and the resulting solution was stirred to completion at room temperature for 18 h. The reaction was monitored by TLC (3:1 hexane: ethyl acetate). After completion, the reaction was concentrated *in vacuo* to produce a pure yellow liquid, **I-11** (5.75 g, quantitative yield), that was used subsequently without further purification. ^{1}H-NMR (300 Hz, $CDCl_3$) δ 1.11 (m, 18 H), 4.62 (s, 2 H). All data are consistent with literature values.[47]

(1*R*, 2*S*)-(-)-2-Phenylcyclohexyl TIPS-oxyacetate [I-12][14]

A 2.18 g (12.4 mmol) aliquot of **I-8** and 1.66 g (13.6 mmol) of DMAP were dissolved in 20 mL of dichloromethane under inert conditions. To this solution, 1.50 mL (18.5 mmol) of dry pyridine was added and allowed to stir at room temperature. To this solution, 4.64 g (18.5 mmol) of **I-11** was added and the resulting mixture was stirred overnight until completion. The reaction was monitored by TLC (3:1 hexanes: ethyl acetate, stained with PMA). After completion the reaction was quenched with 40 mL of saturated sodium bicarbonate. Then 50 mL of dichloromethane was added and the resulting organic layer was washed with 100 mL of saturated sodium bicarbonate

twice, then 100 mL saturated cupric sulfate, then 100 mL of brine. The resulting organic layer was dried over anhydrous $MgSO_4$ and concentrated *in vacuo,* which gave a yellow oil. The crude oil was purified via column chromatography (9:1 hexane: ethyl acetate) that gave **I-12** as clear oil (4.46 g, 92 % yield). ^{1}H-NMR (300 Hz, $CDCl_3$) δ 0.97 (m, 18 H), 1.40 (m, 5 H), 1.83 (m, 3 H), 2.64 (t, 1H, *J*=12 Hz), 3.87-4.18 (q, 2 H), 5.08 (m, 1 H), 7.16 (m, 3 H), 7.22 (m, 2H). All data are consistent with literature values.[14]

(3*R*. 4*S*)-1-PMP-TIPSOxy-4S-(2-methylpropen-1-yl)azetidin-2-one [(+) I-4][14]

Dry THF (50 mL) and 2.27 mL (16.1 mmol) of diisopropylamine were added to a 250 mL round bottomed flask. This solution was cooled down to -15 ^{o}C with a cryocool and 10.1 mL (16.1 mmol) of (1.6 M *n*-BuLi in hexanes) was added dropwise to the solution. This solution was stirred for 1 h. Then the solution was cooled to -85 ^{o}C for 2 h. Then 4.84 g (12.4 mmol) of **I-12** in 30 mL of THF was added over 2 h with a syringe pump. The resulting solution was stirred for 10 h at -85 ^{o}C. Then 3.9 g (20.6 mmol) of **I-1**in 30 mL THF was added over 3 h with a syringe pump. The reaction mixture was allowed to stir for 7 h and then 10 mL of 1M LiHMDS in *tert*-butyl methyl ether was added and the reaction mixture was allowed to warm to room temperature overnight. The reaction was quenched with 100 mL of saturated ammonium chloride solution. The reaction mixture was then diluted with 100 mL of ethyl acetate and then washed with 100 mL of saturated ammonium chloride and three times with 100 mL of brine. The organic layer was separated and dried over anhydrous $MgSO_4$ and concentrated *in vacuo* to give a crude brown oil that was purified by column chromatography (20:1 hexanes: ethyl acetate) to yield a yellow oil. This was then subsequently recrystalized twice from pentane to yield a white crystalline solid, **(+) I-4** (1.76 g, 35 % yield): m.p.= 94-95 ^{o}C; ^{1}H NMR δ ($CDCl_3$, 300 MHz) 0.99 (m, 21

H), 1.79 (d, *J* = 2.3 Hz, 3 H), 1.84 (d, *J* = 2.4 Hz, 3 H), 3.77 (s, 3 H), 4.41 (dd, *J* = 9.9, 5.1 Hz, 1 H), 5.04 (d, *J* = 5 Hz, 1 H), 5.30 (d, *J* = 9.8 Hz, 1 H), 6.82 (d, *J* = 8.1 Hz, 2 H), 7.30 (d, *J* = 8.5 Hz, 2 H). All data are consistent with literature values.[15]

§ 1.6.3 New Generation Taxanes

7-(Triethylsilyl)-10-deacetylbaccatin III [II-1][48]

A 210 mg (0.39 mmol) aliquot of 10-deacetylbaccatin III (**10-DAB**) and a 105 mg (1.56 mmol) aliquot of imidazole was dissolved in 1 mL of *N*,*N*-dimethylformamide and was cooled to 0 °C in ice bath under inert conditions. At 0 ^{o}C, 0.2 mL (1.17 mmol) of chlorotriethylsilane was added dropwise. The mixture was stirred and allowed warm to room temperature. After completion, the reaction was quenched with saturated 10 mL of NH_4Cl and extracted with 20 mL of ethyl acetate. The organic layer was washed three times with brine (15 mL) and dried over anhydrous $MgSO_4$. Then, the solution was concentrated in *vacuo* to yield a white solid. Purification was done using column chromatography on silica gel (1:1 hexanes:ethyl acetate) that afforded 7-triethylsilyl-10-deacetylbaccatin III, **II-5**(234 mg, 91 % yield) as a white solid: m.p.= 242-244 ^{o}C (lit.[48] 256-257 ^{o}C); ^{1}H NMR (300 MHz, $CDCl_3$) δ 0.57 (m, 6 H), 0.93 (m, 9H), 1.04 (s, 3 H), 1.16 (s, 3 H), 1.67 (s, 3 H), 2.02 (s, 3 H), 2.33 (s, 3 H), 2.27 (s, 3 H), 2.51 (m, 1 H), 2.93 (s, 3 H), 3.07 (s, 3 H), 3.89 (d, *J* = 7.6 Hz, 1 H), 4.14 (d, *J* = 8.2 Hz, 1 H), 4.29 (d, *J* = 8.0 Hz, 1 H), 4.48 (dd, *J* = 10.2, 6.7 Hz, 1 H), 4.82 (t, *J* = 7.6 Hz, 1 H), 4.95 (d, *J* = 8.8 Hz, 1 H), 5.63 (d, *J* = 6.8 Hz, 1 H), 7.46 (t, *J* = 8.0 Hz, 2 H), 7.59 (t, *J* = 7.2 Hz, 1 H), 8.10 (d, *J* = 7.2 Hz, 1 H). All data are consistent with literature values.[48]

10-Cyclopropanecarbonyl-7-(Triethylsilyl)-10-deacetylbaccatin III [II-2][24]

A solution of 308 mg (0.468 mmol) of **II-1** dissolved in 2.13 mL THF was cooled to -40 °C under inert conditions. After 10 min at -40 °C, 0.470 mL (0.468 mmol) LiHMDS was added dropwise and stirred for an additional 10 min. Subsequently, 0.0465 mL (0.510 mmol) cyclopropanecarboxylic acid chloride was added dropwise to the mixture and stirred, producing a yellow solution. The reaction was monitored via TLC (1:1 hexane:ethyl acetate). After 20 min, the reaction was quenched with 5 mL saturated NH_4Cl and extracted with 20 mL of ethyl acetate. The organic layer was washed three times with brine (35 mL), dried over anhydrous $MgSO_4$, and concentrated *in vacuo*. Purification was done using column chromatography on silica gel (2:1 hexanes:ethyl acetate) to yield C-10-modified 7-TES-baccatin III, **II-2** (243 mg, 68%), as a white solid: m.p.= 210-212 ^oC; ^1H NMR (300 MHz, $CDCl_3$) δ 0.57 (m, 6 H), 0.90 (m, 9 H), 1.04 (s, 3 H), 1.16 (s, 3 H), 1.67 (s, 3 H), 1.83 (m, 1 H), 2.02 (s, 3 H), 2.18 (m, 3 H), 2.33 (s, 3 H), 2.27 (s, 3 H), 2.51 (m, 1 H), 2.93 (s, 3 H), 3.07 (s, 3 H), 3.89 (d, J = 7.6 Hz, 1 H), 4.14 (d, J = 8.2 Hz, 1 H), 4.29 (d, J = 8.0 Hz, 1 H), 4.48 (dd, J = 10.2, 6.7 Hz, 1 H), 4.82 (t, J = 7.6 Hz, 1 H), 4.95 (d, J = 8.8 Hz, 1 H), 5.63 (d, J = 6.8 Hz, 1 H), 6.37 (s, 1 H), 7.46 (t, J = 8.0 Hz, 2 H), 7.59 (t, J = 7.2 Hz, 1 H), 8.10 (d, J = 7.2 Hz, 1 H). All data are consistent with literature reported values.[24]

2'-Triisopropylsilyl-3'-dephenyl-10-(cyclopropylcarbonyl)-3'-(2-methyl-propen-1-yl)docetaxel [II-3][24]

A mixture of 243 mg (0.34 mmol) **II-2** and 147 mg (0.37 mmol) of **I-6** was dissolved in 13 mL THF was cooled to -40 °C under inert conditions. After 10 min, 0.37 mL (0.369 mmol) LiHMDS in 1.0 M THF was added dropwise to the mixture and stirred producing a yellow solution. The reaction was monitored by TLC (3:1 hexanes:ethyl acetate). After 2 h, the reaction was quenched with 10 mL saturated NH_4Cl. The mixture was extracted using ethyl acetate (35 mL) and the organic layer was washed with saturated NH_4Cl and brine (3 x 50 mL), dried over $MgSO_4$, and concentrated *in vacuo*. Purification was done using column chromatography on silica gel (5: 1 hexanes:ethyl acetate) to yield **II-3** (331 mg, 89%) as a white solid: m.p.= 189-193 ^oC; ^1H NMR (300 MHz, $CDCl_3$) δ 0.57 (m, 6 H), 0.91 (m, 9 H), 1.10 (s, 3 H), 1.19 (s, 3 H), 1.68 (s, 3 H), 1.83 (m, 1 H), 2.00 (s, 3 H), 2.18 (m, 3 H), 2.35 (s, 3 H), 2.40 (s, 3 H), 2.51 (m, 1 H), 2.93 (s, 3 H), 3.07 (s, 3 H), 3.83 (d, *J* = 7.6 Hz, 1 H), 4.18 (d, *J* = 8.2 Hz, 1 H), 4.28 (d, *J* = 8.0 Hz, 1 H), 4.45 (dd, *J* = 10.2, 6.7 Hz, 1 H), 4.81 (t, *J* = 7.6 Hz, 1 H), 4.95 (d, *J* = 8.8 Hz, 1 H), 5.67 (d, *J* = 6.8 Hz, 1 H), 6.47 (s, 1 H), 7.45 (t, *J* = 8.0 Hz, 2 H), 7.59 (t, *J* = 7.2 Hz, 1 H), 8.10 (d, *J* = 7.2 Hz, 1 H). All data are consistent with literature reported values.[24]

3'-Dephenyl-10-(cyclopropanecarbonyl)-3'-(2-methyl-2-propenyl)docetaxel (SB-T-1214) [II-4][24]

A solution of 331 mg (0.30 mmol) **II-3** dissolved in 6.6 mL acetonitrile and 6.6 mL pyridine was cooled to 0 °C under inert conditions. Then 2 mL HF/pyridine was added dropwise producing a

colorless solution and stirred at room temperature overnight. The reaction was monitored via TLC (1:1 hexanes:ethyl acetate). After 24 hours, the reaction was quenched with 10 mL of 10 % citric acid and extracted with 10 mL ethyl acetate three times. The mixture was extracted and the organic layer was washed three times with 30 mL saturated $CuSO_4$ and three times with brine (50 mL), dried over $MgSO_4$, and concentrated *in vacuo*. Purification was done using column chromatography on silica gel (1:1 hexanes:ethyl acetate) to yield **SB-T-1214 (II-4)** (248 mg, 99%), as a white solid: Purity was determined to be 92% % *via* HPLC analysis on reverse phase with a Jupiter proteo column using methanol: water (2:3, 0.4 mL/min); m.p.= 158-160 ^{o}C (lit.[24] 157-160 ^{o}C); ^{1}H NMR (300 MHz, $CDCl_3$) δ 0.99 (m, 2 H), 1.02 (m, 2H), 1.16 (s, 3 H), 1.26 (s, 3 H), 1.33 (s, 9 H), 1.67 (s, 4 H), 1.76 (m, 6 H), 1.89 (m, 1 H), 2.04 (s, 3 H), 2.35 (m, 4 H), 2.54 (m, 2 H), 3.36 (s, 1H), 3.82 (s, 1 H), 4.14 (d, J = 7.0 Hz, 1 H), 4.20 (m, 1 H), 4.30 (d, J = 9.0 Hz, 1 H), 4.44 (m, 1 H), 4.75 (s, 2 H), 4.96 (d, J = 7.5 Hz, 1 H), 5.34 (s, 1 H), 5.67 (d, J = 6.5 Hz, 1 H), 6.18 (t, J = 8.0 Hz, 1 H), 6.30 (s, 1 H), 7.47 (t, J = 6 Hz, 2 H), 7.58 (t, J = 8.0 Hz, 1 H), 8.09 (d, J = 7.5 Hz, 2 H). All data are consistent with literature reported values.[24]

7,10,13-Tris(triethylsilyl)-10-deacetylbaccatin III [II-5][41]

A 0.745 g (1.40 mmol) aliquot of 10-deacetylbaccatin III (**10-DAB)** and a 0.465 g (6.80 mmol) aliquot of imidazole was dissolved in 1.7 mL of *N*,*N*-dimethylformamide and was cooled to 0 °C in ice bath under inert conditions. At 0 ^{o}C, 1.14 mL (6.80 mmol) of chlorotriethylsilane was added dropwise. The mixture was stirred and allowed to warm to room temperature over 36 h. Reaction was monitored by TLC (3:1 hexane: ethyl acetate). After completion, the mixture was quenched with 30 mL of saturated NH_4Cl and extracted with 50 mL of ethyl acetate. The organic layer was washed three times with brine (50 mL) and dried over anhydrous $MgSO_4$.

Then, the solution was concentrated in *vacuo* to yield a white solid. Purification was done using column chromatography on silica gel (10:1 hexanes:ethyl acetate) that afforded **II-5** (1.03 g, 84 % yield) as a white solid: m.p.= 205-208 ^{o}C; ^{1}H NMR (300 MHz, $CDCl_3$) δ 0.57 (m, 18 H), 0.93 (m, 27 H), 1.04 (s, 3 H), 1.16 (s, 3 H), 1.67 (s, 3 H), 2.02 (s, 3 H), 2.33 (s, 3 H), 2.27 (s, 3 H), 2.51 (m, 1 H), 2.93 (s, 3 H), 3.07 (s, 3 H), 3.89 (d, *J* = 7.6 Hz, 1 H), 4.14 (d, *J* = 8.2 Hz, 1 H), 4.29 (d, *J* = 8.0 Hz, 1 H), 4.48 (dd, *J* = 10.2, 6.7 Hz, 1 H), 4.82 (t, *J* = 7.6 Hz, 1 H), 4.95 (d, *J* = 8.8 Hz, 1 H), 5.63 (d, *J* = 6.8 Hz, 1 H), 7.46 (t, *J* = 8.0 Hz, 2 H), 7.59 (t, *J* = 7.2 Hz, 1 H), 8.10 (d, *J* = 7.2 Hz, 1 H). All data are consistent with literature reported values.[24]

7,10,13-Tris(triethylsilyl)-2-debenzoyl-10-deacetylbaccatin III [II-6][24]

A 1.0 g (1.1 mmol) aliquot of **II-5** was dissolved in 15 mL of dry THF and was cooled to -50 ^{o}C using a Cryocool and kept under inert conditions. A 0.54 mL (3.3 mmol) aliquot of Sodium bis(2-methoxyethyoxy) aluminum hydride, 65 wt% in toluene was added to the solution dropwise. The reaction was monitored by TLC (3:1 hexane: ethyl acetate). Upon completion, the reaction was quenched with 15 mL of saturated NH_4Cl and extracted with 20 mL of ethyl acetate. The organic layer was washed with brine (3 x 30 mL), dried over anhydrous $MgSO_4$, and was concentrated in *vacuo*, which yielded a crude oil. Purification was done using column chromatography on silica gel (3: 2 hexanes: ethyl acetate) that afforded **II-6** (0.86 g, 98 % yield) as a white solid: m.p.= 68-71 ^{o}C; ^{1}H NMR (300 MHz, $CDCl_3$) δ 0.57 (m, 18 H), 0.93 (m, 27 H), 1.04 (s, 3 H), 1.16 (s, 3 H), 1.67 (s, 3 H), 2.02 (s, 3 H), 2.33 (s, 3 H), 2.27 (s, 3 H), 2.51 (m, 1 H), 2.93 (s, 3 H), 3.4 (d, *J*=7.2, 3 H), 3.87 (d, *J* = 7.6 Hz, 1 H), 4.14 (d, *J* = 8.2 Hz, 1 H), 4.35 (m, 1 H), 4.61 (q, 9 Hz, 1 H), 4.96 (bt, *J* = 11.1 Hz, 1 H), 5.11 (s, 1 H). All data are consistent with literature reported values.[24]

7,10,13-Tris(triethylsilyl)-2-debenzoyl-2-(3-methylbenzoyl)-10-deacetylbaccatin III [II-7A][49]

A 280 mg (0.360 mmol) aliquot of **II-6**, a 354 mg (2.90 mmol) aliquot of DMAP, and 390 mg (2.90 mmol) of 3-methylbenzoic acid was dissolved in 3.5 mL of dichloromethane under inert conditions. A 0.45 mL (2.9 mmol) aliquot of DIC was added to the mixture dropwise and was allowed to stir at room temperature for 5 days. The reaction was monitored by TLC (3:1 hexane: ethyl acetate). Upon completion, the reaction was quenched with saturated 15 mL of saturated NH_4Cl and extracted with 35 mL of ethyl acetate. The organic layer was washed with brine (3x30 mL), dried over anhydrous $MgSO_4$, and was concentrated in *vacuo* that yielded a yellow solid. Purification was done using column chromatography on silica gel (9:1 hexanes:ethyl acetate) that afforded **II-7A** (312 mg, 87 % yield) as a white solid: m.p.= 178-182 ^oC; ^1H NMR (300 MHz, $CDCl_3$) δ 0.57 (m, 18 H), 0.93 (m, 27 H), 1.04 (s, 3 H), 1.16 (s, 3 H), 1.67 (s, 3 H), 2.02 (s, 3 H), 2.33 (s, 3 H), 2.27 (s, 3 H), 2.51 (m, 1 H), 2.93 (s, 3 H), 3.4 (d, *J*=7.2, 3 H), 3.87 (d, *J* = 7.6 Hz, 1 H), 4.14 (d, *J* = 8.2 Hz, 1 H), 4.35 (m, 1 H), 4.61 (q, 9 Hz, 1 H), 4.96 (bt, *J* = 11.1 Hz, 1 H), 5.21 (s, 1 H), 5.89 (d, *J*=7.2 Hz, 1 H*)* 7.36 (m, 2 H), 7.92 (t, *J* = 9 Hz, 2 H). All data are consistent with literature reported values.[48]

7,10,13-Tris(triethylsilyl)-2-debenzoyl-2-(3-methoxybenzoyl)-10-deacetylbaccatin III (II-7B)[41]

A 542 mg (0.700 mmol) aliquot of **II-6**, a 683 mg (5.60 mmol) aliquot of DMAP, and 856 mg (5.60 mmol) of 3-methoxybenzoic acid was dissolved in 7 mL of dichloromethane under inert conditions. A 0.87 mL (5.6 mmol) aliquot of DIC was added to the mixture dropwise and was allowed to stir at room temperature for 5 days. The reaction was monitored by TLC (3:1 hexane:

ethyl acetate). Upon completion, the reaction was quenched with saturated 15 mL NH_4Cl and extracted with 35 mL of ethyl acetate. The organic layer was washed with brine (3x30 mL), dried over anhydrous $MgSO_4$, and was concentrated in *vacuo* to yield a yellow solid. Purification was done using column chromatography on silica gel (9:1 hexanes: ethyl acetate) that afforded **II-7B** (560 mg, 88 % yield) as a white solid: m.p. = 208-210 ^oC. ^1H NMR (300 MHz, $CDCl_3$) δ 0.57 (m, 18 H), 0.93 (m, 27 H), 1.04 (s, 3 H), 1.16 (s, 3 H), 1.67 (s, 3 H), 2.02 (s, 3 H), 2.33 (s, 3 H), 2.27 (s, 3 H), 2.51 (m, 1 H), 2.93 (s, 3 H), 3.4 (d, *J*=7.2, 3 H), 3.87 (d, *J* = 7.6 Hz, 1 H), 4.14 (d, *J* = 8.2 Hz, 1 H), 4.35 (m, 1 H), 4.61 (q, 9 Hz, 1 H), 4.96 (bt, *J* = 11.1 Hz, 1 H), 5.21 (s, 1 H), 5.89 (d, *J*=7.2 Hz, 1 H*)*, 7.36 (t, J= 8.1, 1H) 7.62 (m, 2 H), 7.78 (d, *J* =7.2Hz, 1 H). All data are consistent with literature reported values.[41]

2-Debenzoyl-2-(3-methylbenzoyl)-10-deacetylbaccatin III [II-8A][48]

An 0.50 g (0.56 mmol) aliquot of **II-7A** was dissolved in a 1:1 mixture of acetonitrile:pyridine (10 mL each) and was cooled to 0 °C under inert conditions. A 6 mL aliquot of HF/pyridine was added dropwise and allowed to stir at room temperature. The reaction was monitored by TLC (3:1 hexane: ethyl acetate). After completion, the reaction was quenched with 50 mL of 10 % citric acid and was extracted with 50 mL ethyl acetate two times. The organic layer was washed three times with saturated $CuSO_4$ (100 mL) and three times with brine (100 mL), dried over anhydrous $MgSO_4$, and concentrated *in vacuo*. Purification was done using column chromatography on silica gel (2:1 hexanes:ethyl acetate) to yield **II-8A** (283 mg, 91 % yield) as a white solid: m.p.=198-200 ^oC; ^1H NMR (300 MHz, $CDCl_3$) δ 1.04 (s, 3 H), 1.16 (s, 3 H), 1.67 (s, 3 H), 1.83 (m, 1 H), 2.02 (s, 3 H), 2.18 (m, 3 H), 2.33 (s, 3 H), 2.27 (s, 3 H), 2.51 (m, 1 H), 2.93 (s, 3 H), 3.07 (s, 3 H), 3.89 (d, *J* = 7.6 Hz, 1 H), 4.14 (d, *J* = 8.2 Hz, 1 H), 4.29 (d, *J* = 8.0 Hz, 1 H), 4.48 (dd, *J* = 10.2, 6.7 Hz, 1 H), 4.82 (t, *J* = 7.6 Hz, 1 H), 4.95 (d, *J* = 8.8 Hz, 1 H),

5.28 (s, 1H), 5.63 (d, *J* = 6.8 Hz, 1 H), 7.36 (m, 2 H), 7.92 (t, *J* = 9 Hz, 2 H). All data are consistent with literature reported values.[48]

2-Debenzoyl-2-(3-methoxylbenzoyl)-10-deacetylbaccatin III [II-8B][41]

An 465 mg (0.510 mmol) aliquot of **II-7B** was dissolved in a 1:1 mixture of acetonitrile:pyridine (8 mL each) and was cooled to 0 °C under inert conditions. A 5 mL aliquot of HF/pyridine was added dropwise and allowed to stir at room temperature. The reaction was monitored by TLC (3:1 hexane: ethyl acetate). After completion, the reaction was quenched with 18 mL of 10 % citric acid and was extracted with 25 mL ethyl acetate three times. The organic layer was washed three times with saturated $CuSO_4$ (30 mL) and three times with brine (30 mL), dried over $MgSO_4$, and concentrated *in vacuo*. Purification was done using column chromatography on silica gel (2:1 hexanes:ethyl acetate) to yield **II-8B** (280 mg, 95 % yield) as a white solid: m.p.= 202-205 ^oC; ^1H NMR (300 MHz, $CDCl_3$) δ 1.04 (s, 3 H), 1.16 (s, 3 H), 1.67 (s, 3 H), 1.83 (m, 1 H), 2.02 (s, 3 H), 2.18 (m, 3 H), 2.33 (s, 3 H), 2.27 (s, 3 H), 2.51 (m, 1 H), 2.93 (s, 3 H), 3.07 (s, 3 H), 3.89 (d, *J* = 7.6 Hz, 1 H), 4.14 (d, *J* = 8.2 Hz, 1 H), 4.29 (d, *J* = 8.0 Hz, 1 H), 4.48 (dd, *J* = 10.2, 6.7 Hz, 1 H), 4.82 (t, *J* = 7.6 Hz, 1 H), 4.95 (d, *J* = 8.8 Hz, 1 H), 5.28 (s, 1H), 5.63 (d, *J* = 6.8 Hz, 1 H), 7.36 (t, J= 8.1, 1H) 7.62 (m, 2 H), 7.78 (d, *J* =7.2Hz, 1 H). All data are consistent with literature reported values.[41]

2-Debenzoyl-2-(3-methylbenzoyl)-7-triethylsilyl-10-deacetylbaccatin III (II-9A)[48]

An 100 mg (0.180 mmol) aliquot of **II-8A** and a 49 mg (0.72 mmol) of aliquot of imidazole was dissolved in 3.5 mL *N*,*N*-dimethylformamide and was cooled to 0 °C under inert conditions. At 0 ^oC, 0.09 mL (0.54 mmol) of chlorotriethylsilane was added dropwise. The mixture was stirred and allowed to warm to room temperature. The reaction was monitored by TLC (1:1 hexane:

ethyl acetate). After completion, the mixture was quenched with 12 mL of saturated NH_4Cl and extracted with 35 mL of ethyl acetate. The organic layer was washed with 30 mL of brine three times, dried over anhydrous $MgSO_4$, and was concentrated in *vacuo* to afford a clear oil. Purification was done using column chromatography on silica gel (1:1 hexanes:ethyl acetate) to yield **II-9A** (100 mg, 83 % yield) as a white solid: m.p.= 196-198 ^oC; ^1H NMR (300 MHz, $CDCl_3$) δ 0.57 (m, 6 H), 0.90 (m, 9 H), 1.04 (s, 3 H), 1.16 (s, 3 H), 1.67 (s, 3 H), 1.83 (m, 1 H), 2.02 (s, 3 H), 2.18 (m, 3 H), 2.33 (s, 3 H), 2.27 (s, 3 H), 2.51 (m, 1 H), 2.93 (s, 3 H), 3.07 (s, 3 H), 3.89 (d, *J* = 7.6 Hz, 1 H), 4.14 (d, *J* = 8.2 Hz, 1 H), 4.29 (d, *J* = 8.0 Hz, 1 H), 4.48 (dd, *J* = 10.2, 6.7 Hz, 1 H), 4.82 (t, *J* = 7.6 Hz, 1 H), 4.95 (d, *J* = 8.8 Hz, 1 H), 5.63 (d, *J* = 6.8 Hz, 1 H), 7.36 (m, 2 H), 7.92 (t, *J* = 9 Hz, 2 H). All data are consistent with literature reported values.[48]

2-Debenzoyl-2-(3-methylbenzoyl)-7-triethylsilyl-10-(*N,N*-dimethylcarbamoyl)-10-deacetylbaccatin III (II-10A)[50]

A 95 mg (0.14 mmol) aliquot of **II-9A** was dissolved in 2.8 mL of THF and was cooled to -40 °C under inert conditions. After 10 min at -40 °C, 0.16 mL (0.16 mmol) of LiHMDS was added dropwise and allowed to stir for an additional 10 min. Subsequently, a 0.017 mL (0.18 mmol) aliquot of *N,N*-dimethylcarbamoyl chloride was added dropwise to the mixture and allowed to stir for 3 h. The reaction was monitored by TLC (9:1 dichloromethane:methanol, 6 inch TLC) and ^1H-NMR. After completion, the reaction was quenched with 12 mL saturated NH_4Cl and extracted with 25 mL of ethyl acetate. The organic layer was washed with brine (3x30 mL), dried over anhydrous $MgSO_4$, and concentrated *in vacuo*. Purification was done using column chromatography on silica gel (1:1 hexanes:ethyl acetate) to yield **II-10A** (104 mg, 92 % yield) as a white solid: m.p.= 208-212 ^oC ^1H NMR (300 MHz, $CDCl_3$) δ 0.57 (m, 6 H), 0.90 (m, 9 H), 1.04 (s, 3 H), 1.16 (s, 3 H), 1.67 (s, 3 H), 1.83 (m, 1 H), 2.02 (s, 3 H), 2.18 (m, 3 H), 2.33 (s, 3

H), 2.27 (s, 3 H), 2.51 (m, 1 H), 2.93 (s, 3 H), 3.07 (s, 3 H), 3.89 (d, *J* = 7.6 Hz, 1 H), 4.14 (d, *J* = 8.2 Hz, 1 H), 4.29 (d, *J* = 8.0 Hz, 1 H), 4.48 (dd, *J* = 10.2, 6.7 Hz, 1 H), 4.82 (t, *J* = 7.6 Hz, 1 H), 4.95 (d, *J* = 8.8 Hz, 1 H), 5.63 (d, *J* = 6.8 Hz, 1 H), 6.37 (s, 1 H), 7.36 (m, 2 H), 7.92 (t, *J* = 9 Hz, 2 H). All data are consistent with literature reported values.[50]

2-Debenzoyl-2-(3-methylbenzoyl)-10-(propanoyl)-10-deacetylbaccatin III (II-9AA)[50]

A 116 mg (0.213 mmol) aliquot of **II-8A** and a 12 mg (0.021) aliquot of cerium chloride were dissolved in 9 mL of THF and cooled to 0 °C under inert conditions. After 10 min at 0 °C, 0.273 mL (2.13 mmol) of propionic anhydride was added dropwise and allowed to warm to room temperature. The mixture was allowed to stir for 4 h. The reaction was monitored by TLC (1:1 hexane: ethyl acetate). After completion, the reaction was quenched with 20 mL saturated $NaHCO_3$ and extracted with 25 mL of ethyl acetate. The organic layer was washed with brine (3x30 mL), dried over anhydrous $MgSO_4$, and concentrated *in vacuo* to yield **II-9AA** (122 mg, 93 % yield) as a white solid**.** This compound was used crude in the subsequent reaction. ^{1}H NMR (300 MHz, $CDCl_3$) 1.04 (s, 3 H), 1.16 (s, 3 H), 1.67 (s, 3 H), 1.83 (m, 1 H), 2.02 (s, 3 H), 2.18 (m, 3 H), 2.33 (s, 3 H), 2.27 (s, 3 H), 2.51 (m, 1 H), 3.89 (d, *J* = 7.6 Hz, 1 H), 4.14 (d, *J* = 8.2 Hz, 1 H), 4.29 (d, *J* = 8.0 Hz, 1 H), 4.48 (dd, *J* = 10.2, 6.7 Hz, 1 H), 4.82 (t, *J* = 7.6 Hz, 1 H), 4.95 (d, *J* = 8.8 Hz, 1 H), 5.63 (d, *J* = 6.8 Hz, 1 H), 6.37 (s, 1 H), 7.36 (m, 2 H), 7.92 (t, *J* = 9 Hz, 2 H). All data are consistent with literature reported values.[50]

2-debenzoyl-2-(3-methylbenzoyl)-7-Triethylsilyl-10-(propanoyl)-10-deacetylbaccatin III (II-10AA)[50]

An 122 mg (0.200 mmol) aliquot of crude **II-9AA** and a 54.0 mg (0.800 mmol) of aliquot of imidazole was dissolved in 3 mL *N*,*N*-dimethylformamide and was cooled to 0 °C under inert conditions. At 0 ^{o}C, 0.10 mL (0.60 mmol) of chlorotriethylsilane was added dropwise. The mixture was stirred and allowed to warm to room temperature. The reaction was monitored by TLC (1:1 hexane: ethyl acetate). After completion, the mixture was quenched with 12 mL of saturated NH_4Cl and extracted with 35 mL of ethyl acetate. The organic layer was washed with 30 mL of brine three times, dried over anhydrous $MgSO_4$, and was concentrated in *vacuo* to afford a yellow oil. Purification was done using column chromatography on silica gel (3:1 hexanes:ethyl acetate) to yield **II-10AA** (105 mg, 78 % yield) as a white solid: m.p.= 208-210 ^{o}C; ^{1}H NMR (300 MHz, $CDCl_3$) δ 0.57 (m, 6 H), 0.90 (m, 9 H), 1.04 (s, 3 H), 1.16 (s, 3 H), 1.67 (s, 3 H), 1.83 (m, 1 H), 2.02 (s, 3 H), 2.18 (m, 3 H), 2.33 (s, 3 H), 2.27 (s, 3 H), 2.51 (m, 1 H), 3.89 (d, *J* = 7.6 Hz, 1 H), 4.14 (d, *J* = 8.2 Hz, 1 H), 4.29 (d, *J* = 8.0 Hz, 1 H), 4.48 (dd, *J* = 10.2, 6.7 Hz, 1 H), 4.82 (t, *J* = 7.6 Hz, 1 H), 4.95 (d, *J* = 8.8 Hz, 1 H), 5.63 (d, *J* = 6.8 Hz, 1 H), 6.37 (s, 1 H), 7.36 (m, 2 H), 7.92 (t, *J* = 9 Hz, 2 H). All data are consistent with literature reported values.[50]

2'-Triisopropylsilyl-3'-dephenyl-3'-(2-methylpropen-1-yl)-2-debenzoyl-2-(3-methylbenzoyl)-7-triethylsilyl-10-(*N*,*N*-dimethylcarbamoyl)docetaxel (II-11A)[50]

A mixture of 160 mg (0.215 mmol) of **II-10A** and 111 mg (0.280 mmol) of **(+) I-6** was dissolved in 8 mL of dry THF and was cooled to -40 °C under inert conditions. After 10 minutes, 0.26 mL

(0.258 mmol) LiHMDS in 1.0 M THF was added dropwise to the mixture with stirring. The reaction was monitored by TLC (3:1 hexanes: ethyl acetate). After 2 hours, the reaction was quenched with 10 mL of saturated NH_4Cl. The mixture was extracted using ethyl acetate (60 mL) and the organic layer was washed with saturated NH_4Cl (30 mL) and brine (3 X 30 mL), dried over anhydrous $MgSO_4$, and concentrated *in vacuo*. Purification was done using column chromatography on silica gel (3:1 hexanes: ethyl acetate) to yield **II-11A** (168 mg, 70 %) as a white solid: m.p.= 182-186 ^oC; ^1H NMR (300 MHz, $CDCl_3$) δ 0.57 (m, 6 H), 0.91 (m, 9 H), 1.10 (s, 3 H), 1.19 (s, 3 H), 1.68 (s, 3 H), 1.83 (m, 1 H), 2.00 (s, 3 H), 2.18 (m, 3 H), 2.35 (s, 3 H), 2.40 (s, 3 H), 2.51 (m, 1 H), 2.93 (s, 3 H), 3.07 (s, 3 H), 3.83 (d, J = 7.6 Hz, 1 H), 4.18 (d, J = 8.2 Hz, 1 H), 4.28 (d, J = 8.0 Hz, 1 H), 4.45 (dd, J = 10.2, 6.7 Hz, 1 H), 4.81 (t, J = 7.6 Hz, 1 H), 4.95 (d, J = 8.8 Hz, 1 H), 5.67 (d, J = 6.8 Hz, 1 H), 6.47 (s, 1 H), 7.36 (m, 2 H), 7.92 (t, J = 9 Hz, 2 H). All data are consistent with literature reported values.[50]

2'-Triisopropylsilyl-3'-dephenyl-3'-(2-methylpropen-1-yl)-2-debenzoyl-2-(3-methylbenzoyl)-7-triethylsilyl-10-(propanoyl)docetaxel (II-11AA)[50]

A mixture of 105 mg (0.144 mmol) of **II-10AA** and 75 mg (0.19 mmol) of **(+) I-6** was dissolved in 8 mL of dry THF and was cooled to -40 °C under inert conditions. After 10 min, 0.18 mL (0.18 mmol) LiHMDS in 1.0 M THF was added dropwise to the mixture with stirring. The reaction was monitored by TLC (3:1 hexanes:ethyl acetate). After 2 h, the reaction was quenched with 10 mL of saturated NH_4Cl. The mixture was extracted using ethyl acetate (35 mL) and the organic layer was washed with saturated NH_4Cl (20 mL) and brine (3 X 30 mL), dried over anhydrous $MgSO_4$, and concentrated *in vacuo*. Purification was done using column

chromatography on silica gel (3:1 hexanes: ethyl acetate) to yield **II-11AA** (140 mg, 86 %) as a white solid: m.p.= 182-188 ^{o}C; ^{1}H NMR (300 MHz, $CDCl_3$) δ 0.57 (m, 6 H), 0.91 (m, 9 H), 1.10 (s, 3 H), 1.19 (s, 3 H), 1.68 (s, 3 H), 1.83 (m, 1 H), 2.00 (s, 3 H), 2.18 (m, 3 H), 2.35 (s, 3 H), 2.40 (s, 3 H), 2.51 (m, 1 H), 2.93 (s, 3 H), 3.07 (s, 3 H), 3.83 (d, *J* = 7.6 Hz, 1 H), 4.18 (d, *J* = 8.2 Hz, 1 H), 4.28 (d, *J* = 8.0 Hz, 1 H), 4.45 (dd, *J* = 10.2, 6.7 Hz, 1 H), 4.81 (t, *J* = 7.6 Hz, 1 H), 4.95 (d, *J* = 8.8 Hz, 1 H), 5.67 (d, *J* = 6.8 Hz, 1 H), 6.47 (s, 1 H), 7.36 (m, 2 H), 7.92 (t, *J* = 9 Hz, 2 H). All data are consistent with literature reported values.[50]

3'-Dephenyl-3'-(2-methylpropen-1-yl)-2-debenzoyl-2-(3-methylbenzoyl)-10-(*N,N*-dimethylcarbamoyl)docetaxel (SB-T-121602) (II-12A)

A solution of 168 mg (0.147 mmol) **II-11A** dissolved in 3.5 mL acetonitrile and 3.5 mL pyridine was cooled to 0 °C under inert conditions. Then 2 mL HF/pyridine was added dropwise, producing a colorless solution and stirred at room temperature overnight. The reaction was monitored by TLC (3:1 hexanes:ethyl acetate). After 24 h, the reaction was quenched with 10 mL of 10 % citric acid and extracted with 10 mL ethyl acetate three times. The mixture was extracted and the organic layer was washed three times with 30 mL saturated $CuSO_4$ and three times with brine (30 mL), dried over anhydrous $MgSO_4$, and concentrated *in vacuo*. Purification was done using column chromatography on silica gel (1:1 hexanes: ethyl acetate) to yield **SB-T-121602 (II-12A)** (103 mg, 86%) as a white solid: m.p.= 165 ^{o}C-168 ^{o}C; $[\alpha]^{22}_{D}$ -13 (c 0.4, CH_2Cl_2); ^{1}H NMR (500 MHz, $CDCl_3$) δ 0.86 (m, 1 H), 0.99 (m, 2 H), 1.02 (m, 2H), 1.16 (s, 3 H), 1.26 (s, 3 H), 1.33 (s, 9 H), 1.67 (s, 4 H), 1.76 (m, 6 H), 1.92 (m, 1 H), 2.04 (s, 3 H), 2.35 (m, 4 H), 2.54 (m, 2 H), 2.95 (s, 1 H), 3.04 (s, 1H), 3.18 (s, 1 H), 3.37 (bs, 1 H), 3.81 (s, 1 H), 4.17

(d, *J* = 10 Hz, 1 H), 4.20 (m, 1 H), 4.31 (d, *J* = 5.0 Hz, 1 H), 4.75 (t, *J*=5 Hz, 2 H), 4.97 (d, *J* = 10 Hz, 1 H), 5.33 (s, 1 H), 5.65 (d, *J* = 5 Hz, 1 H), 6.19 (t, *J* = 10 Hz, 1 H), 6.26 (s, 1 H), 7.36 (m, 2 H), 7.92 (t, *J* = 10 Hz, 2 H); ^{13}C NMR (500 MHz, $CDCl_3$) δ 12.0, 17.6, 21.2, 23.9, 24.9, 25.0, 28.3, 29.5, 30.8, 38.1, 38.3, 38.6, 39.3, 45.9, 48.3, 54.3, 61.2, 75.0, 75.1, 77.9, 78.9, 79.1, 79.4, 79.6, 79.9, 81.9, 82.5, 83.9, 87.3, 123.4, 129.9, 130.1, 131.1, 131.9, 133.5, 137.0, 140.5, 140.9, 145.2, 158.0, 158.8, 169.7, 172.6, 208.3; LC/MS (positive mode) [M^{+1}] 871.3 m/z (major peak), [M^{+2}] 872.3, [M^{+3}] 873.3; Purity was determined to be 91% *via* HPLC analysis on reverse phase with a Jupiter proteo column using methanol: water (2:3, 0.4 mL/min).

3'-Dephenyl-3'-(2-methylpropen-1-yl)-2-debenzoyl-2-(3-methylbenzoyl)-10-(propanoyl)docetaxel (SB-T-121302) (II-12AA)

A solution of 124 mg (0.140 mmol) **II-11A** dissolved in 2.5 mL acetonitrile and 2.5 mL pyridine was cooled to 0 °C under inert conditions. Then 1.5 mL HF/pyridine was added dropwise, producing a colorless solution and stirred at room temperature overnight. The reaction was monitored by TLC (3:1 hexanes:ethyl acetate). After 24 h, the reaction was quenched with 10 mL of 10 % citric acid and extracted with 10 mL ethyl acetate three times. The mixture was extracted and the organic layer was washed three times with 30 mL saturated $CuSO_4$ and three times with brine (30 mL), dried over anhydrous $MgSO_4$, and concentrated *in vacuo*. Purification was done using column chromatography on silica gel (1:1 hexanes: ethyl acetate) to yield **SB-T-121302 (II-12AA)** (80 mg, 70%) as a white solid: m.p.= 152 ^{o}C-155 ^{o}C; $[\alpha]^{22}_{D}$ -73 (c 0.3, CH_2Cl_2); ^{1}H NMR (500 MHz, $CDCl_3$) δ 0.86 (m, 1 H), 0.97 (m, 2 H), 1.16 (s, 3 H), 1.28 (s, 3 H), 1.33 (m, 9 H), 1.67 (s, 4 H), 1.76 (m, 6 H), 1.92 (m, 1 H), 2.04 (s, 3 H), 2.35 (m, 4 H), 2.54 (m, 2

H), 2.95 (s, 1 H), 3.42 (bs, 1 H), 3.81 (s, 1 H), 4.17 (d, *J* = 10 Hz, 1 H), 4.20 (m, 1 H), 4.31 (d, *J* = 5.0 Hz, 1 H), 4.75 (t, *J*=5 Hz, 2 H), 4.97 (d, *J* = 10 Hz, 1 H), 5.33 (s, 1 H), 5.65 (d, *J* = 5 Hz, 1 H), 6.16 (t, *J* = 10 Hz, 1 H), 6.32 (s, 1 H), 7.36 (m, 2 H), 7.92 (t, *J* = 10 Hz, 2 H); ^{13}C NMR (400 MHz, $CDCl_3$) δ 9.2, 9.3, 9.7, 9.8, 14.3, 15.1, 18.7, 21.5, 22.0, 22.5, 22.6, 22.8, 25.9, 26.8, 27.8, 28.4, 29.9, 31.8, 35.8, 43.4, 45.9, 48.3, 58.8, 64.5, 72.5, 73.9, 75.1, 75.7, 79.3, 80.1, 81.3, 82.5, 84.7, 120.9, 127.5, 128.8, 129.3, 130.9, 133.2, 134.6, 137.9, 138.5, 142.6, 15536, 167.2, 170.2, 173.3, 174.8, 204.0; Purity was determined to be 72% *via* HPLC analysis on reverse phase with a Jupiter proteo column using methanol: water (2:3, 0.4 mL/min).

§ 1.6.4 Taxane Construct

Baccatin III (III-2A)

A 100 mg (0.18 mmol) aliquot of **10-DAB** and a 10 mg (0.018 mmol) aliquot of cerium chloride were dissolved in 5 mL of THF and cooled to 0 °C under inert conditions. After 10 min at 0 °C, 0.115 mL (1.8 mmol) of acetic anhydride was added dropwise and allowed to warm to room temperature. The mixture was allowed to stir for 4 h. The reaction was monitored by TLC (1:1 hexane: ethyl acetate, stain). After completion, the reaction was quenched with 20 mL saturated $NaHCO_3$ and extracted with 25 mL of ethyl acetate. The organic layer was washed with brine (3x30 mL), dried over anhydrous $MgSO_4$, and concentrated *in vacuo* to yield **III-2B (**50 mg, 94 %) as an off white solid. It was used crude in the subsequent reaction. m.p.= 220-222 ^{o}C. ^{1}H NMR (300 MHz, $CDCl_3$) 1.11 (s, 6 H), 1.25 (t, *J*=3 Hz, 2H), 1.60 (s, 3 H), 2.02 (s, 3 H), 2.18 (m, 3 H), 2.33 (s, 3 H), 2.27 (s, 3 H), 2.51 (m, 1 H), 3.89 (d, *J* = 7.6 Hz, 1 H), 4.14 (d, *J* = 8.2 Hz, 1 H), 4.29 (d, *J* = 8.0 Hz, 1 H), 4.48 (dd, *J* = 10.2, 6.7 Hz, 1 H), 4.90 (t, *J* = 7.6 Hz, 1 H), 4.97 (d,

J = 8.8 Hz, 1 H), 5.63 (d, *J* = 6.8 Hz, 1 H), 6.37 (s, 1 H), 7.49 (m, 2 H), 7.6 (m, 1 H), 8.11 (d, *J*= 12 Hz, 2H). All data are consistent with literature reported values.[13]

Debenzoyl-2-(3-methoxybenzoyl)-baccatin III (III-2B)[50]

A 170 mg (0.30 mmol) aliquot of **II-8B** and a 17 mg (0.03 mmol) aliquot of cerium chloride were dissolved in 10 mL of THF and cooled to 0 °C under inert conditions. After 10 min at 0 °C, 0.283 mL (3.0 mmol) of acetic anhydride was added dropwise and allowed to warm to room temperature. The mixture was allowed to stir for 4 h. The reaction was monitored by TLC (1:1 hexane: ethyl acetate). After completion, the reaction was quenched with 20 mL saturated $NaHCO_3$ and extracted with 25 mL of ethyl acetate. The organic layer was washed with brine (3x30 mL), dried over anhydrous $MgSO_4$, and concentrated *in vacuo* to yield **III-2B** (170 mg, 89 % yield) as a white solid. It was used crude in the subsequent reaction. m.p.= 210-215 ^oC. ^1H NMR (300 MHz, $CDCl_3$) 1.11 (s, 6 H), 1.25 (t, *J*=3 Hz, 2H), 1.42 (s, 2H), 1.57 (s, 3 H), 2.05 (s, 3 H), 2.18 (m, 3 H), 2.30 (s, 3 H), 2.27 (s, 3 H), 2.51 (m, 1 H), 3.87 (d, *J* = 7.6 Hz, 1 H), 4.14 (d, *J* = 8.2 Hz, 1 H), 4.29 (d, *J* = 8.0 Hz, 1 H), 4.36 (dd, *J* = 10.2, 6.7 Hz, 1 H), 4.97 (t, *J* = 7.6 Hz, 1 H), 5.02 (d, *J* = 8.8 Hz, 1 H), 5.62 (d, *J* = 6.8 Hz, 1 H), 6.32 (s, 1 H), 7.16 (m, 1 H), 7.38 (t, *J*= 9 Hz, 1 H), 7.64 (s, 1 H), 7.69 (d, *J*= 9 Hz, 1H).

7-Triethylsilyl-baccatin III (III-3A)[48]

An 50 mg (0.09 mmol) aliquot of **III-2A** and a 25 mg (0.36 mmol) of aliquot of imidazole was dissolved in 1 mL *N*,*N*-dimethylformamide and was cooled to 0 °C under inert conditions. At 0 ^oC, 0.08 mL (0.45 mmol) of chlorotriethylsilane was added dropwise. The mixture was stirred and allowed to warm to room temperature. The reaction was monitored by TLC (1:1 hexane: ethyl acetate). After completion, the mixture was quenched with 12 mL of saturated NH_4Cl and

extracted with 35 mL of ethyl acetate. The organic layer was washed three times with 30 mL of brine, dried over anhydrous $MgSO_4$, and concentrated in *vacuo* that afforded a yellow oil. Purification was done using column chromatography on silica gel (3:1 hexanes:ethyl acetate) to yield **III-3A** (57 mg, 90 % yield)as a off-white solid: m.p.= 210-212 ^oC; ^1H NMR (300 MHz, $CDCl_3$) δ 0.57 (m, 6 H), 0.90 (m, 9 H), 1.04 (s, 3 H), 1.16 (s, 3 H), 1.67 (s, 3 H), 1.83 (m, 1 H), 2.02 (s, 3 H), 2.18 (m, 3 H), 2.33 (s, 3 H), 2.27 (s, 3 H), 2.51 (m, 1 H), 3.89 (d, *J* = 7.6 Hz, 1 H), 4.14 (d, *J* = 8.2 Hz, 1 H), 4.29 (d, *J* = 8.0 Hz, 1 H), 4.48 (dd, *J* = 10.2, 6.7 Hz, 1 H), 4.82 (t, *J* = 8.1 Hz, 1 H), 4.95 (d, *J* = 8.8 Hz, 1 H), 5.63 (d, *J* = 8 Hz, 1 H), 6.34 (s, 1 H), 7.46 (t, *J* = 8.0 Hz, 2 H), 7.59 (t, *J* = 7.2 Hz, 1 H), 8.08 (d, *J* = 7.2 Hz, 1 H). All data are consistent with literature reported values.[13]

2'-Triisopropylsilyl-3'-dephenyl-3'-(2-methyl-2-propenyl)-7-triethylsilyl-10-acetyl-docetaxel [III-4A][41]

A mixture of 100 mg (0.185 mmol) **III-3A** and 95 mg (0.240 mmol) of **(+) I-6** was dissolved in 7 mL of THF was cooled to -40 °C under inert conditions. After 10 min, 0.22 mL (0.22 mmol) of LiHMDS in 1.0 M THF was added dropwise to the mixture. The reaction was monitored by TLC (3:1 hexanes:ethyl acetate). After 2 h, the reaction was quenched with 10 mL saturated NH_4Cl. The mixture was extracted using ethyl acetate (60 mL) and the organic layer was washed with saturated NH_4Cl (50 mL) and brine (3 X 50 mL), dried over anhydrous $MgSO_4$, and concentrated *in vacuo*. Purification was done using column chromatography on silica gel (3:1 hexanes: ethyl acetate) to yield **III-4A** (157 mg, 98%) as a white solid: m.p.=172-175 ^oC; ^1H NMR (300 MHz, $CDCl_3$) δ 0.57 (m, 6 H), 0.91 (m, 9 H), 1.10 (s, 3 H), 1.19 (s, 3 H), 1.68 (s, 3

H), 1.83 (m, 1 H), 2.00 (s, 3 H), 2.18 (m, 3 H), 2.35 (s, 3 H), 2.40 (s, 3 H), 2.51 (m, 1 H), 2.93 (s, 3 H), 3.07 (s, 3 H), 3.83 (d, *J* = 7.6 Hz, 1 H), 4.18 (d, *J* = 8.2 Hz, 1 H), 4.28 (d, *J* = 8.0 Hz, 1 H), 4.45 (dd, *J* = 10.2, 6.7 Hz, 1 H), 4.81 (t, *J* = 7.6 Hz, 1 H), 4.95 (d, *J* = 8.8 Hz, 1 H), 5.67 (d, *J* = 6.8 Hz, 1 H), 6.47 (s, 1 H), 7.46 (t, *J* = 8.0 Hz, 2 H), 7.59 (t, *J* = 7.2 Hz, 1 H), 8.08 (d, *J* = 7.2 Hz, 1 H). All data are consistent with literature reported values.[41]

2'-Triisopropylsilyl-3'-dephenyl-3'-(2-methyl-2-propenyl)-7-triethylsilyl-docetaxel [III-5A][41]

A 150 mg (0.140 mmol) aliquot of **III-4A** was dissolved in 12 mL of ethanol. After 10 min, 5.0 mL hydrazine monohydrate was added dropwise to the mixture. The reaction was monitored by ^{1}H-NMR. After 3 h, the reaction was quenched with 10 mL saturated NH_4Cl. The mixture was extracted using ethyl acetate (35 mL) and the organic layer was washed with saturated NH_4Cl (50 mL) and brine (3 X 30 mL), dried over anhydrous $MgSO_4$, and concentrated *in vacuo*. Purification was done using column chromatography on silica gel (3:1 hexanes:ethyl acetate) to yield **III-5A** (101 mg, 70%) as a white solid: m.p.= 163-168 ^oC; ^{1}H NMR (300 MHz, $CDCl_3$) δ 0.57 (m, 6 H), 0.91 (m, 9 H), 1.10 (s, 3 H), 1.19 (s, 3 H), 1.68 (s, 3 H), 1.83 (m, 1 H), 2.00 (s, 3 H), 2.18 (m, 3 H), 2.35 (s, 3 H), 2.40 (s, 3 H), 2.51 (m, 1 H), 2.93 (s, 3 H), 3.07 (s, 3 H), 3.83 (d, *J* = 7.6 Hz, 1 H), 4.18 (d, *J* = 8.2 Hz, 1 H), 4.28 (d, *J* = 8.0 Hz, 1 H), 4.45 (dd, *J* = 10.2, 6.7 Hz, 1 H), 4.81 (t, *J* = 7.6 Hz, 1 H), 4.95 (d, *J* = 8.8 Hz, 1 H), 5.67 (d, *J* = 6.8 Hz, 1 H), 7.46 (t, *J* = 8.0 Hz, 2 H), 7.59 (t, *J* = 7.2 Hz, 1 H), 8.08 (d, *J* = 7.2 Hz, 1 H). LC/MS (positive mode)= [M^{+1}] 1056.6 m/z, [M^{+2}] 1057.6 m/z, [M^{+3}] 1058.6 m/z. All data are consistent with literature reported values.[41]

Chapter II

Synthesis of Tumor-Targeting Taxane-Based Drug Conjugates using Linolenic Acid as Tumor-Targeting Module

Table of Contents

§2.1. Targeted Chemotherapy

§2.1.1 Introduction

Traditional chemotherapy functions on the assumption that cytotoxic agents will distinguish cancer cell from normal cell and destroy them. However, cytotoxic agents cannot differentiate between cancer cells and normal cells and as a result both cells are destroyed. Thus, a prevailing problem in cancer chemotherapy is that most cytotoxic agents lack specificity and causes systemic toxicity. Systemic toxicity results in the destruction of normal cell and causes harmful side effects such as hair loss, depression of the immune system, and damage to the liver, kidney and bone marrow. Modern drug discovery attempts to make cytotoxic agents more specific to tumor cells to prevent the destruction of normal cells, which can improve the quality of life for patients.

§2.1.1 Targeted Chemotherapeutics

Targeted therapy is a relatively new field in cancer treatment that uses drugs to specifically attack cancer cells. These therapies attack the cancer cells' inner workings, the programming that makes them different from normal, healthy cells. This approach may be more effective than current treatments.

Targeted cancer therapies that have been approved by the FDA are drugs that interfere with cell growth signals, disrupt tumor angiogenesis, induce specific death of cancer cells, and are delivered to cancer cells. Imatinib (Gleevec ®) and Erlotinib hydrochloride (Tarceva®) (**Figure 11**) are a few chemotherapeutic agents that act by specifically inhibiting certain tyrosine kinase enzymes that are characteristic of a particular cancer cell. Tyrosine kinases are involved

in a number cell processes including cell differentiation and cell division. Over activity of tyrosine kinases can lead to cancer of which makes it an attractive target for targeted chemotherapy.

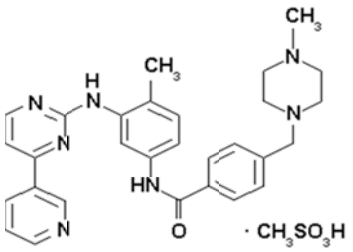

Imatinib Mesylate
Gleevec ®

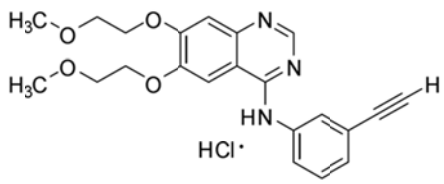

Erlotinib Hydrochloride
Tarceva ®

Figure 11: Structures of Gleevec ® and Tarceva ®

Imatinib received FDA approval in May 2001 and was considered the "Magic Bullet" to cure cancer because of its high specificity for cancer cells. It is marketed by Novartis and is used in treatment of chronic myelogenous leukemia (CML) and gastrointestinal stromal tumors (GISTs). It is a 2-phenylaminopyrimidine derivative which acts by inhibiting tyrosine kinase enzymes found in cancer cells. Imatinib is specific for the tyrosine kinase domain in the Abelson proto-oncogene (abl) and mutations of abl are associated with CML. In CML, the Philadelphia chromosome leads to a fusion protein of abl with bcr (breakpoint cluster region), which gives rise to a continuously active tyrosine kinase, termed bcr-abl. Imatinib is selective for bcr-abl and functions by selectively inhibiting the kinase activity of bcr-abl (**Figure 12**). The decreased activity of the kinase leads to remission of CML.

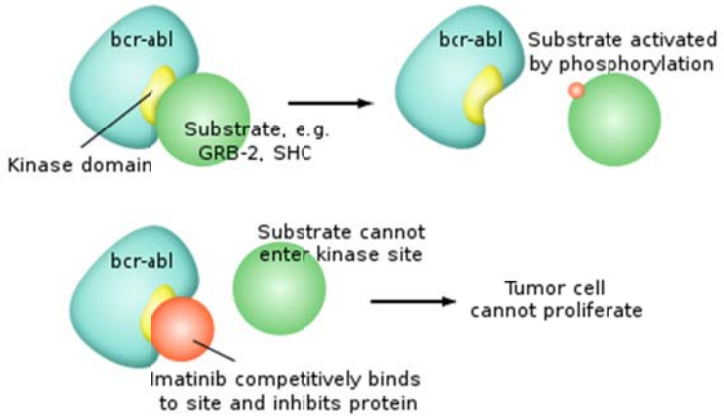

Figure 12: Mechanism of action of Gleevec ®.[51]

While this approach is effective in targeting cancer cells and reducing harmful side effects, these drugs can potentially cause the cell to develop resistance to them. Signal transduction pathways in mammalian cells are quite complex and have several secondary routes to transduce the same signal (**Figure 13**). By inhibiting one pathway, the cell can initiate or develop a secondary pathway to amplify the signal, causing a loss of efficacy of the drug.

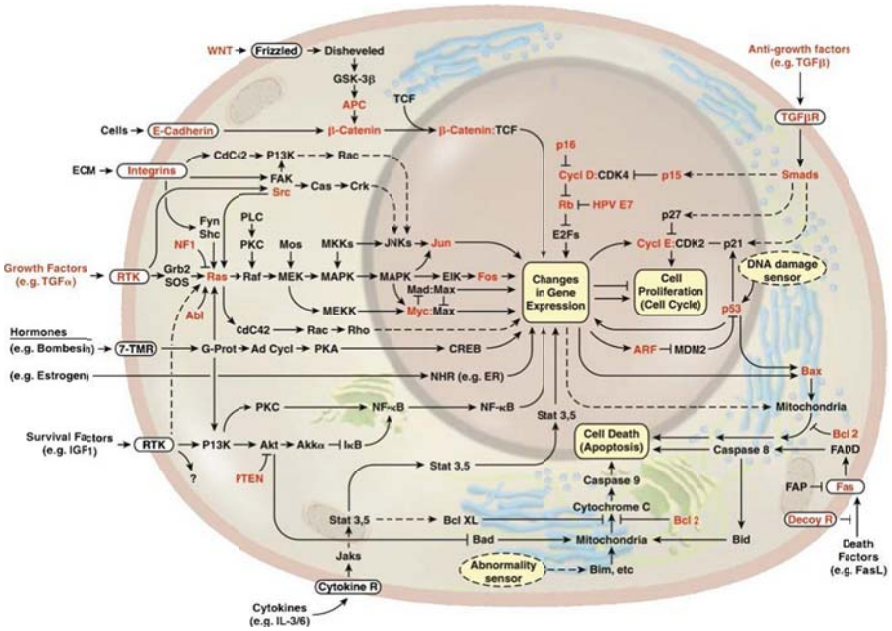

Figure 13: Signal Transduction Pathways in the Cell.[52]

Recently, Imatinib has shown to be resistant in some patients. Mutations within the bcr-abl kinase domain are a major cause of resistance. Mutations can cause a conformational change of the protein which reduces the affinity for binding of the drug. Studies have also shown that allosteric mutants disrupt inhibition caused by imatinib binding and produces activated kinases that are resistant to Imatinib.[53] Alternative methods should be explored to effectively target cancer cells.

§2.1.2 Tumor-Targeting Drug Conjugates

§2.1.2.1 Introduction

Another way to make anticancer agents more specific is to conjugate a tumor-targeting module (TTM) to an anticancer agent. This targeted approach uses tumor specific molecules to selectively deliver a cytotoxic agent to cancer cells. Tumor-targeting molecules take advantage of the differences in cancer and normal cells. Some examples of tumor-targeting modules are monoclonal anti-bodies, vitamins, and polyunsaturated fatty acids (PUFAs). Monoclonal anti-bodies have shown specificity for tumor-specific antigens and can be used as a targeting agent. Vitamins and polyunsaturated fatty acids can also be used as effective TTM based on the fact that tumor cells need more vitamins and nutrients than normal cells to maintain their limitless growth potential. These TTMs can be conjugated to the cytotoxic agent via suitable linker or directly if acceptable. These tumor-targeting drug conjugates should be stable in circulation, delivered and internalized by the cancer cell, and activated once internalized.

§2.1.2.2 Vitamins as Tumor-Targeting Modules

Cancer cells overexpress vitamin and nutrient receptors to maintain their limitless growth. Vitamins, such as biotin and folic acid, can be used as tumor targeting modules to ensure delivery to cancer cells without affecting normal cells. When conjugated to a TTM, the drug conjugate will be delivered specifically to the tumor site. At the tumor site, the conjugate will be internalized via receptor-mediated endocytosis (RME).[54]

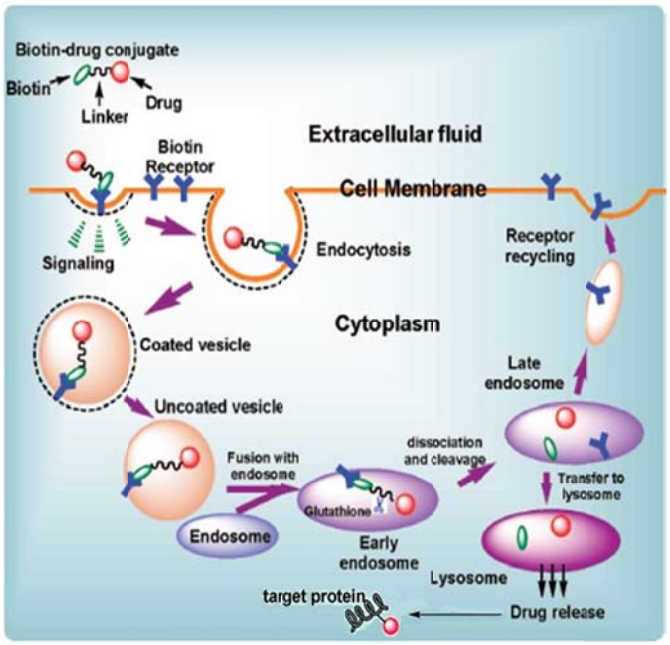

Figure 14: Receptor-Mediated Endocytosis.[54]

After internalization the linker is cleaved, releasing the cytotoxic agent in its free and active form to target proteins (**Figure 14**). The RME mechanism of internalization was confirmed by the Ojima lab with a biotin-linker-taxoid-fluorescein conjugate using confocal fluorescence microscopy (CFM).

§2.1.2.3 Omega-3 Fatty Acids as Tumor- Targeting Modules

Polyunsaturated fatty acids (PUFAs) have also exhibited anticancer activity in various cancer cell lines.[55,56] In addition, certain omega-3 fatty acids, such as linolenic acid (LNA), docosahexaenoic acid (DHA), and eicosapentaenoic acid (EPA), are readily taken up by tumor cells as biochemical precursors. Linolenic acid is an essential fatty acid which plays a crucial role in many metabolic processes and is readily incorporated into the lipid bilayer of tumor cells.

§2.1.2.4 Disulfide Linker

A suitable linker can be used to conjugate a TTM to a cytotoxic agent. These linkers can aid in masking the activity of the cytotoxicity of the agent while the drug conjugate in is circulation as well as a means to incorporate a TTM to the cytotoxic agent. Linkers should also be bi-functional; stable while in circulation and readily cleave after internalization. Disulfide linkers have been chosen as ideal linkers because they are cleaved by an intracellular thiol, usually glutathione, upon internalization in the cell. It has been observed that in tumor cells, the concentration of glutathione (GSH) is 1000 times greater than in blood plasma, therefore disulfide linkers will be readily cleaved inside the cell.[54] The GSH-triggered disulfide bond-cleavage generates to the formation of a phenylthiolate species which can attack the linker-drug ester bond, releasing the drug in its active form and generating a thiolactone side-product (**Figure 15**).[54,57]

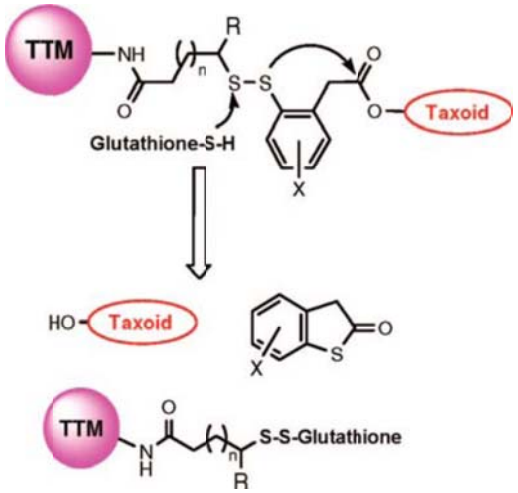

Figure 15: Thiolactonization Process and drug release.[54]

The thiolactonization processes is essentially an irreversible step due to both enthalpy and entropic favorability towards the exchange and self-attack, which ensures that all of the drug will be released from the system. After this process, the drug is able to bind to its targeted proteins, the biotin receptor is recycled and returns to the cell surface and the resulting thiolactone and new TTM-GSH moieties are broken down by the cell. The mechanism-based drug release of the disulfide linker was confirmed by the Ojima lab by monitoring the reaction of fluorine-labeled molecules with ^{19}F-NMR (**Figure 16**). [57]

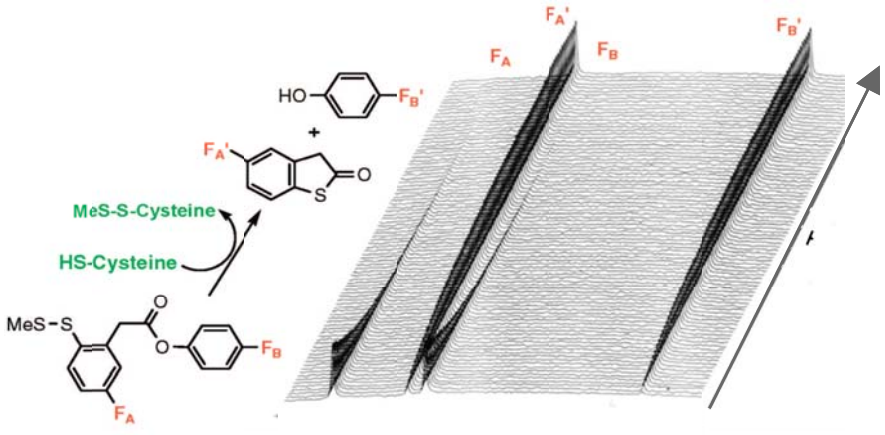

Figure 16: ^{19}F-NMR Validation of the Thiolactonization Process[57]

§2.2 Omega- 3 Polyunsaturated Fatty Acid-Drug Conjugates

§2.2.1 Introduction

Omega-3 polyunsaturated fatty acids are known to be nutritionally important and beneficial to human health and development. They are classified as essential fatty acids because they are not synthesized by the human body but are vital for normal metabolism. Essential fatty acids include α-linolenic acid (LNA), which is obtained from vegetable oils, and eicosapentaenoic acid (EPA) and docosahexaenoic acid (DHA), which are obtained from cold-water fish. The structures of these essential fatty acids are displayed in **Figure 17**.

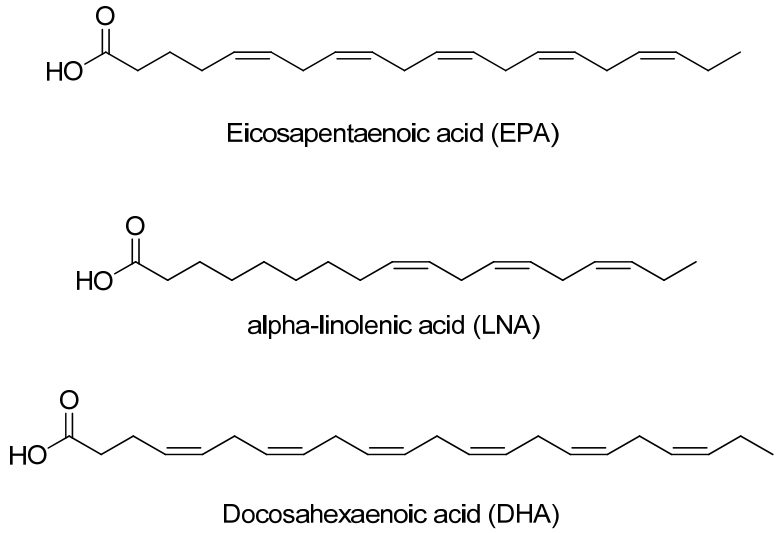

Figure 17: Structures of EPA, LNA, DHA.

Omega-3 fatty acids are thought to be beneficial in a number of diseases including, atherosclerosis, arthritis, neurological disorders, and in certain cancers. Tumors have been shown to greedily take up these ω-3 fatty acids as biochemical precursors, making them excellent tumor-targeting modules. In addition, ω-3 fatty acids have also exhibited anticancer

activity in several cancers particularly breast, colon, and prostate cancer.[58,59] When conjugated to a cytotoxic agent, ω-3 fatty acids can offer selective delivery to cancer cells and because of its anticancer properties, it may also provide synergism with the cytotoxic agent.

§2.2.2 DHA-Paclitaxel (Taxoprexin ®)

Paclitaxel is a common chemotherapeutic agent used for the treatment of lung, ovarian, and breast cancer, as well as advanced forms of Kaposi's sarcoma. It is a mitotic inhibitor and functions by hyper-stabilizing microtubules, causing cell division arrest and the initiation of apoptosis at the G2/M stage. Like most traditional chemotherapeutics, Paclitaxel is not specific; treatment of this drug will kill normal healthy cells in the process leading to a number of severe and harmful side effects. To manage its non-specificity and poor solubility in aqueous environments, numerous formulation of paclitaxel have been developed, including and DHA-paclitaxel or Taxoprexin ®.

DHA-paclitaxel is an investigational drug made by linking DHA to the C-2' position of paclitaxel by Protarga Inc. (**Figure 18**). DHA is a ω-3 fatty acid that is actively taken up by tumor cells making it an effective tumor targeting agent. This compound was shown to exhibit increased anti-tumor activity and reduced systemic toxicity. It was also shown that this conjugate is stable in circulation and maintained for long period of time, thus the drug is activated slowly, which increases the efficacy of the drug and reduces side effects.[60]

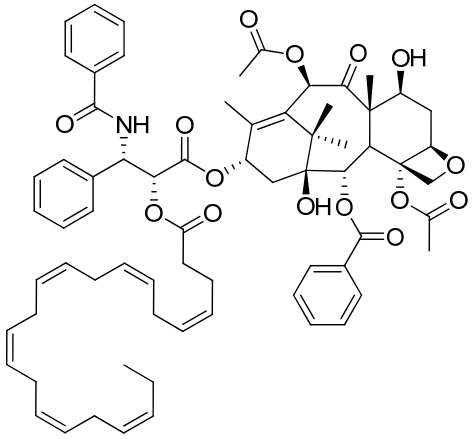

Figure 18: Structure of DHA-Paclitaxel.

The conjugation of cytotoxic drugs to DHA or other PUFAs has been found to drastically change the pharmacokinetics and distribution of the drug, resulting in accumulation of the drug conjugate in tumor-tissues. A hypothesized mechanism of the PUFA-drug conjugate delivery to tumor is shown in **Figure 19**.[61] Human serum albumin (HSA) is the most abundant protein in human blood plasma and is involved in the transport of PUFAs. The DHA component of the conjugate readily binds to HSA in the blood plasma, which forms a HSA-bounded conjugate by solubilizing the hydrophobic drug conjugate. The HSA-bounded conjugate is then recognized by glycoprotein 60 (gp-60), where it binds and undergoes transcytosis from the blood capillaries to the tumor interstitium.[62] Once accumulated in the tumor interstitium, the drug conjugate dissociates from HSA with the aid of secreted protein acidic and rich in cysteine (SPARC). The DHA-paclitaxel conjugate is assumed to be desorbed into the external membrane of the tumor cell and eventually internalized. After internalization in the tumor cell, the DHA-paclitaxel ester bond is cleaved, releasing the drug in the active form and DHA. It is anticipated that DHA and

its metabolites will further enhance the drug efficacy by interfering with a number of cellular processes.

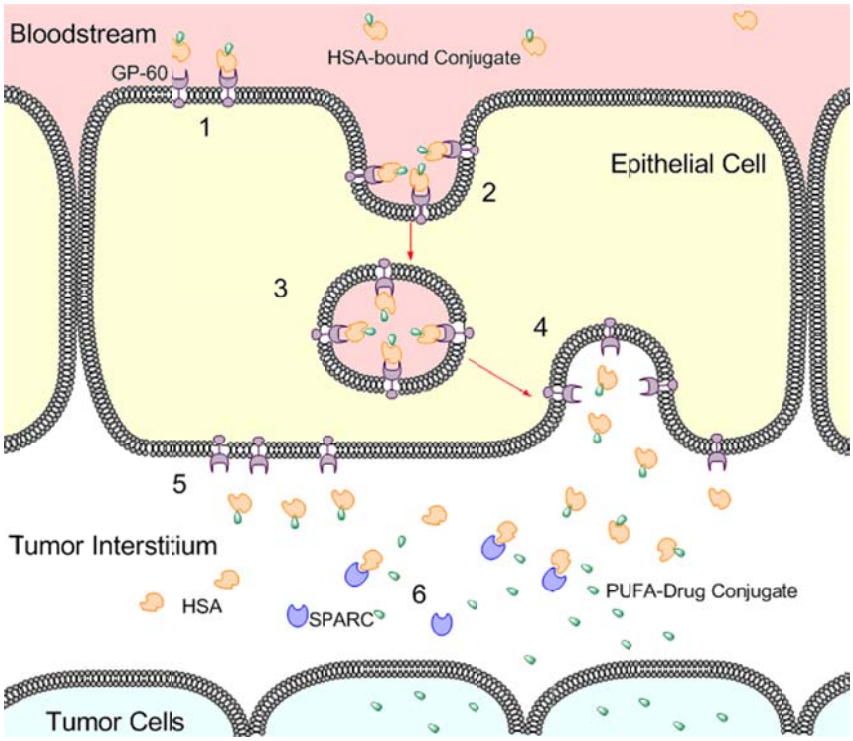

Figure 19: Internalization of PUFA-Drug Conjugates.[61]

Another hypothesized mechanism of PUFA-drug internalization in tumor cells is by the accumulation of these drugs in the tumor intersitium through tumor's abnormal blood vessels. Tumors can form abnormal blood vessels in order to gain nutrients from the blood stream. These tumor blood vessels have perivascular detachment, vessel dilation, holes, and irregular shape. It is hypothesized that the PUFA-drug conjugate will travel through the vascular system and fall through the holes in the tumor blood vessel; where it will be accumulated for a long period of time and slowly internalized by the tumor cell.

Taxoprexin ® takes advantage of the tumor-targeting properties of PUFA. This drug conjugate reduces the destruction of normal cells and may decrease the harmful side effects caused by traditional chemotherapeutics. Taxoprexin ® is a promising anticancer agent and is currently in phase III clinical trials.

§2.2.3 DHA-SB-T-1214

Although taxoprexin ® displays great anti-tumor activity and also reduces systemic toxicity, this drug will not be active in multi-drug resistant (MDR) cancer cell lines. The cytotoxic agent in this drug complex is paclitaxel; studies have shown that this drug produces drug resistance in cancer cell lines and is not active in multi-drug resistance (MDR) cancer cell lines.[63] P-glycoprotein (Pgp) and multidrug resistance-associated proteins (MRP) are two molecular pumps from the ABC family that have been associated with MDR. After internalization of taxoprexin ® in the tumor cell, the ester bond is cleaved releasing DHA and paclitaxel. If the tumor cell displays MDR, Paclitaxel will be recognized by pgp and will be removed out of the cell via efflux, which results in the loss of efficacy of the drug. The removal of cytotoxic agents in MDR cancer cell can be avoided by incorporating anticancer agents that are active in MDR expressing cancer cells to this PUFA-drug model. Ojima and co-workers have synthesized a wide array of 2nd and 3rd generation taxanes that are 2-3 orders of magnitude more potent than the paclitaxel in MDR expressing cells. Accordingly, Ojima *et. al.* synthesized drug conjugate a PUFA drug conjugate incorporating 2nd generation taxane, SB-T-1214, as the cytotoxic agent (**Figure 20**).[64]

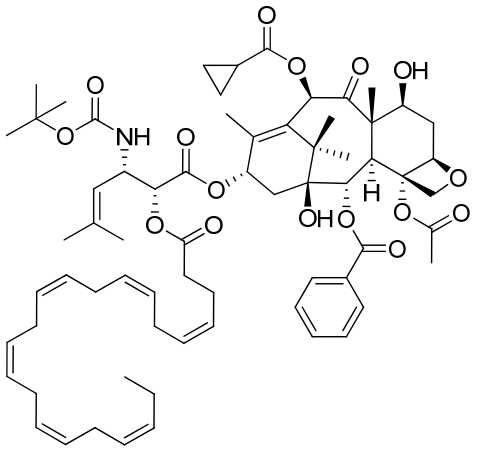

Figure 20: DHA-SB-T-1214 Drug conjugate.

The antitumor activity of DHA-SB-T-1214 was evaluated and compared to taxoprexin ® by the Ojima group. The PUFA drug conjugates were evaluated against the drug-sensitive A121 human ovarian tumor xenograft and the drug-resistant DLD-1 human colon tumor xenograft in SCID mice (**Figure 21**).[64] It was found that Taxoprexin ® was ineffective against the drug-resistant DLD-1 human colon tumor xenograft, whereas, DHA–SB-T-1214 showed complete regression of the tumor.

.

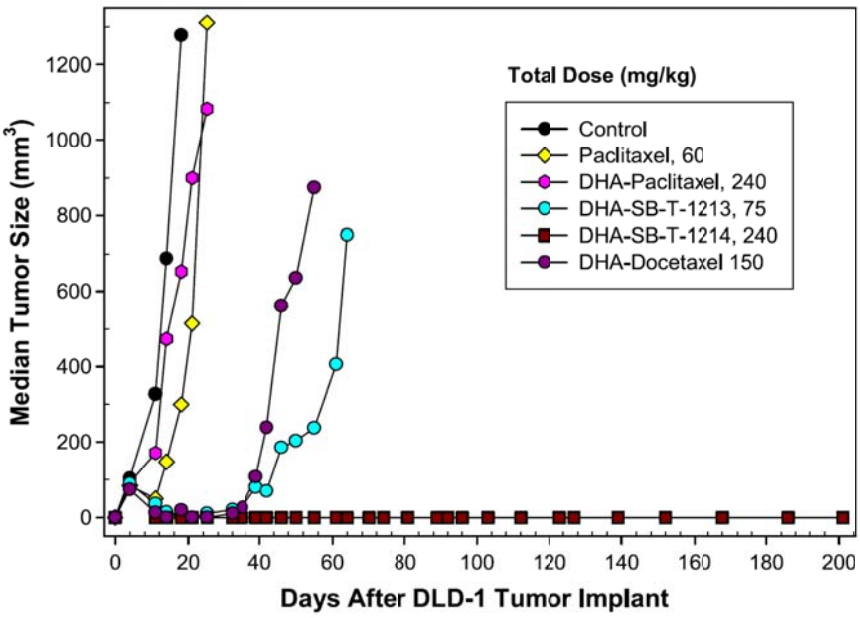

Figure 21: Evaluation of Anti-tumor activity of DHA-Paclitaxel and DHA-SB-T-1214 against DLD-1 human colon tumor xenograft.[14]

PUFA–taxoid conjugates have a high potential to become efficacious tumor-targeting chemotherapeutic agents in cancer therapy. These conjugates incorporates a tumor-targeting module to effectively deliver the cytotoxic agent to cancer cells, thus destroying them without causing systemic toxicity, thereby improving the quality of life for patients. The highly potent DHA-SB-T-1214 is a promising drug conjugate because it can be selectively delivered and the 2nd generation taxane will be active in MDR cancer cells. DHA-SB-T-1214 is currently in phase II clinical trials.

§2.3 Synthesis of 2nd and 3rd Generation Taxane-PUFA Conjugate

The synthesis of PUFA-Taxoid conjugates are of high interest in the Ojima lab. The syntheses of PUFA-Taxoid conjugate using α-linolenic acid (LNA) as tumor-targeting module and a 3rd generation taxoid is reported. LNA as the tumor tageting module functions in the same manner as DHA and is also more stable than DHA, making LNA a better PUFA to work with. Highly potent PUFA-3rd generation taxanes can be used as treatment if taxoprexin ® or PUFA-2nd generation taxanes fall to resistance in MDR cancer cells.

§2.3.1 Results and Discussion

The synthesis of LNA-taxoid conjugate is shown in (**Scheme 1).** The tumor-targeting moiety, LNA, was coupled to the C-2' position of the taxoid in the presence of DIC and DMAP that afforded the LNA-taxane conjugate in good yields.

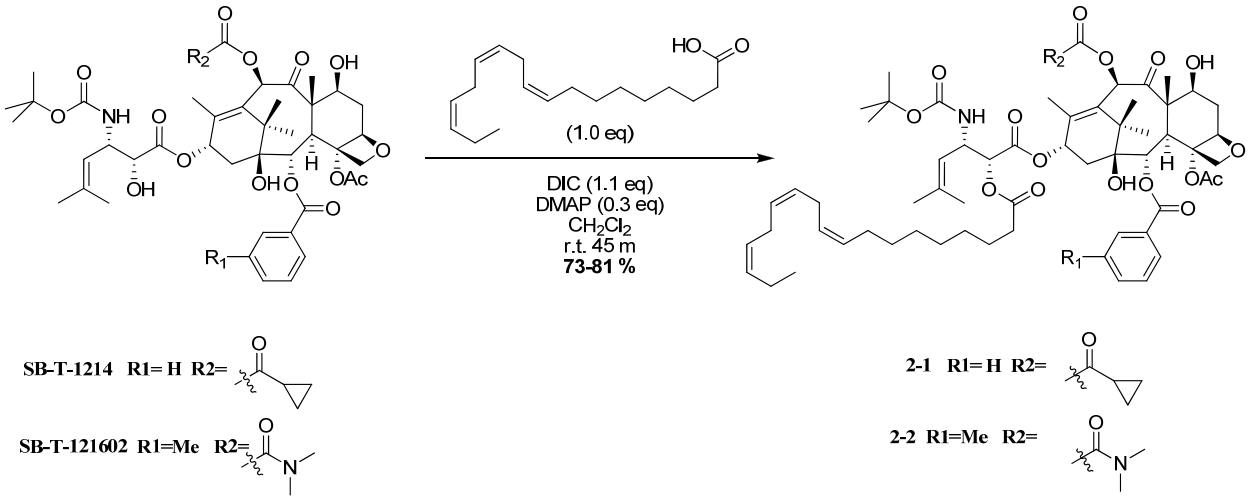

Scheme 1: Synthesis of LNA-SB-T-1214 and LNA-SB-T-121602.

This reaction must be monitored via TLC to prevent the functionalization of the available C-7 hydroxyl group. LNA was shown to be more stable during the course of the reaction and subsequent workup, whereas, it has been experimental observed that DHA is difficult to work with due to its instability.

§2.4 Synthesis of LNA-Linker-Taxoid Drug Conjugate

Linkers can be included in tumor-targeting drug conjugates to bridge a TTM with a cytotoxic agent and/or ensure the stability of the conjugate in circulation and rapid release upon internalization. A self-immolative methyl branched disulfide linker was determined to be a suitable linker to for drug conjugates by the Ojima group (**Figure 12**). The methyl moiety alpha to the disulfide bond may provide enough steric hindrance to prevent premature cleavage of the disulfide bond while in circulation. Increasing the length of the carbon-branch increases the stability of linker. Once the synthesis of the linker is achieved, subsequent attachment of the cytotoxic agent and TTM will afford the TTM-Linker-Drug conjugate.

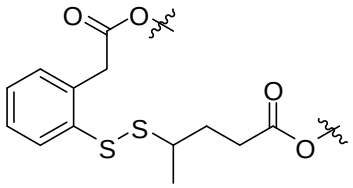

Figure 22: Methyl-Branched Disulfide Linker.

Attachment of SB-T-1214 to the linker and further modification complex will give the "Coupling-Ready" SB-T-1214-Linker Construct. This construct is a versatile moiety, containing all of the essential pieces needed to prepare tumor-targeting drug conjugates (**Figure 13**).

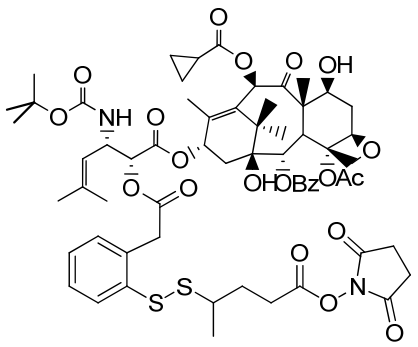

Figure 23: Coupling-Ready SB-T-1214-Linker Construct.[45]

The linker is attached to the drug via an ester bond at the C-2' position, which upon thiolactonization, it becomes cleaved, releasing the taxoid with a free C-2' hydroxyl moiety. The free hydroxyl moiety is essential for optimum activity. The succinimide activated ester is highly reactive towards nucleophillic groups, any tumor-targeting module containing a nucleophillic group can be conjugated at this position.

The incorporation of a disulfide linker to a tumor targeting drug conjugate is a novel approach to the synthesis of effective tumor-targeting drug conjugates. The methyl branched linker can provide more stability while in the conjugate is in circulation, which can prevent premature cleavage as in other drug conjugates. The linker can also ensure the complete and rapid delivery of the cytotoxic agent due to the irreversible thiolactonization process. The synthesis of a taxane-linker-TTM drug conjugate using α-linolenic acid as the TTM is reported.

§2.4.1 Synthesis of the Methyl-Branched Disulfide Linker

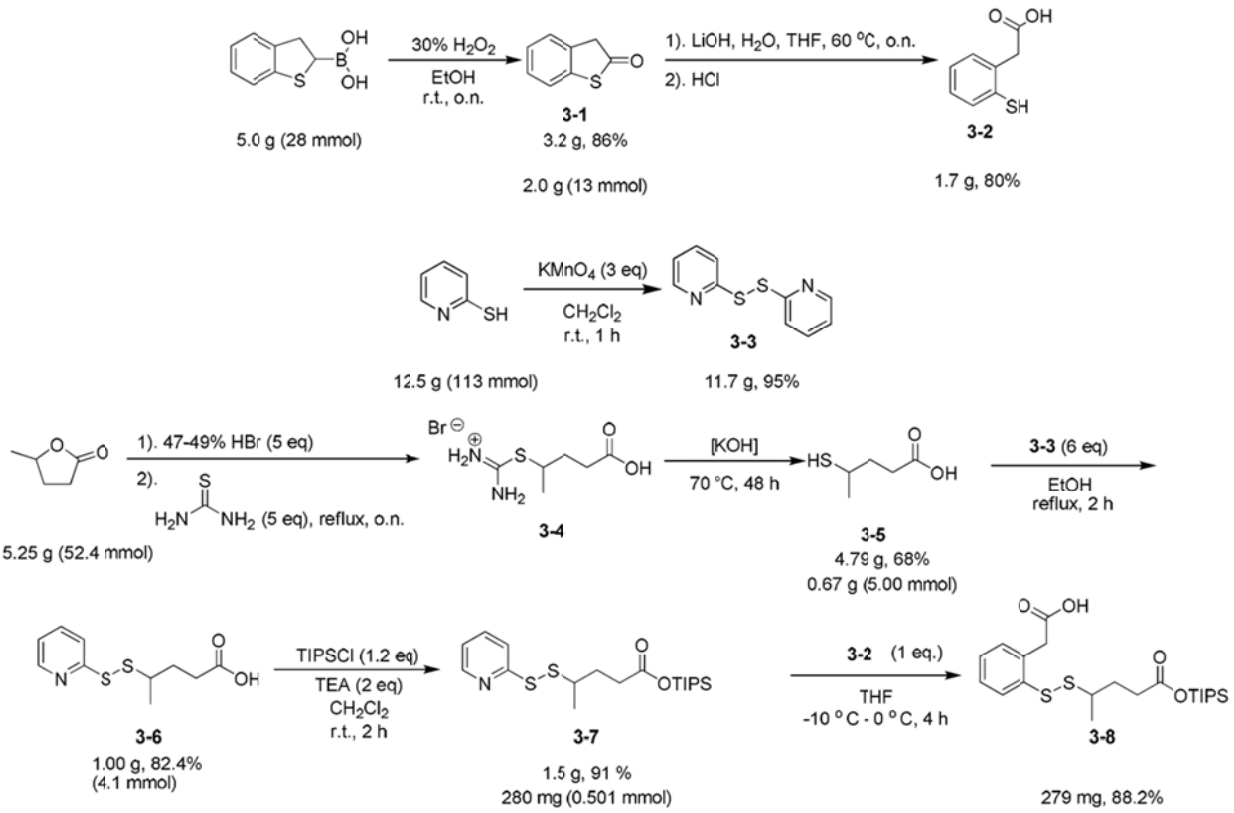

Scheme 2: Synthesis of the Methyl-Branched Disulfide Linker.[65,66,67,68,69]

The synthesis towards the novel methyl-branched disulfide linker is outlined in **scheme 2**. The synthesis of the methyl-branched disulfide linker began with the synthesis of key intermediates, **3-2** and **3-3**. These intermediates were needed for the two thiol-dilsulfide exchange reactions required to prepare the desired linker. The first key intermediate **3-2** was obtained via oxidation followed by ring opening. The synthesis of **3-3** occurred in two steps. In the first step, thianaphthene 2-boronic acid is oxidized in the presence of hydrogen peroxide to produce the thiolactone **3-2** in good yield. In the second step, the thiolactone underwent base-mediated ring opening and followed by acid work-up which produced the desired 3-2 in good

yeild. However, the compound was not isolated pure. The impurity was the disulfide dimer of **3-2** which was visible on TLC and was separated from the product via column chromatography.

The second key intermediate **3-3** was prepared *via* on oxidation using $KMnO_4$. Pyridine-2-thiol was oxidized in the presence of $KMnO_4$ which produced **3-3** in high yields. Purification of the product was easy; the crude product was filtered through celite and washed with CH_2Cl_2. However, the disposal of the remaining $KMnO_4$ was burdensome.

The synthesis towards the methyl branched disulfide linker began with the synthesis of 4-sufhydrylpentanoic acid. The synthesis of **3-5** occurred in two steps. In the first step, the starting material, γ-valerolactone was stirred under reflux conditions with HBr. HBr acts like a Brønsted acid and protonates the carbonyl functional group. The protonated functional group creates a dipole moment and pulls the electron density towards the carbonyl group. As a result, the tertiary position of the lactone is open for nucleophilic attack by thiourea. The crude salt was then subject to hydrolysis with sodium hydroxide to yield **3-5** in moderate to low yields. A problem with this reaction is that a significant amount of γ-valerolactone was recovered with the product. To correct this, more time was allotted for reflux at a higher temperature to force the γ-valerolactone to completely react. In addition, the formation of γ-valerolactone competes with the nucleophilic substitution of thiourea. Instead of the intermolecular nucleophilic attack, an intramolecular attack from the carboxylate anion will result in ring-closure. However, any formed γ-valerolactone and any excess thiourea was removed from the aqueous mixture containing **3-4** by washing the aqueous layer with CH_2Cl_2 followed by washing with ether.

Compound **3-5** was subject to the first thiol-disulfide exchange reaction to produce **3-6**. The addition of **3-5** to **3-3** in hot EtOH assured minimal dimer formation and formation of **3-6** in good yields. Column chromatography was performed to obtain pure **3-6**, excess **3-3** and the

pyridinyl thiol byproduct. Compound **3-6** was obtained in good yields (82.4%). However, separation of **3-6** by column chromatography was an extremely difficult process because the R_f values on TLC plate of the reactants and product were very close. A slow column was done in order to obtain pure isolated product.

With **3-6** in hand, TIPS protection of this compound was obtained in high yields **3-7.** The TIPS protection is needed to prevent drug coupling to the two different carboxylic acid positions in the disulfide linker. Compound **3-7** is stable under nitrogen and can be stored in the refrigerator for approximately 2 weeks.

Compound **3-7** was subject to the second thiol-disulfide exchange reaction with **3-2** which produced **3-8**. However, this exchange can be problematic. The reaction was done under slightly acidic conditions because of the presence of the carboxylic group in compound **3-2**. It has been experimentally observed that as the reaction length increases, the TIPS moiety is cleaved, rendering the disulfide linker obtained useless in the preparation of a drug conjugate, as two carboxylic acid moieties are present. With **3-8**, any other –OH bearing drug compound can be coupled to the free carboxylic acid moiety.

§2.4.2 Synthesis of the Coupling Ready Construct

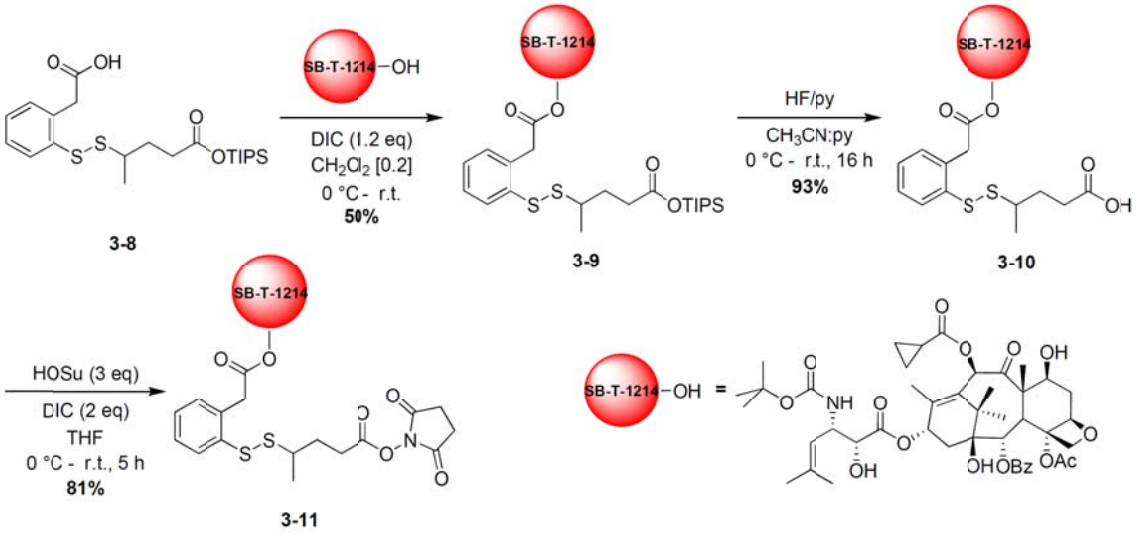

Scheme 3: Synthesis of the Coupling Ready Construct.[45]

The synthesis of the coupling ready construct is displayed in **scheme 3**. **SB-T-1214** was coupled to **3-8** via DIC coupling reagent to yield **3-9**. However, the product was obtained in low yields (50%) and a significant amount of **SB-T-1214** was also recovered. The low yield was attributed to the low purity of the taxane. Compound **3-9** was deprotected by HF in pyridine to yield **3-10**. Compound **3-10** was then activated by OSu coupling. The synthesis of the SB-T-1214-linker coupling-ready construct was done by treating **3-10** with HOSu in the presence of DIC that afforded the construct, **3-11**, in good yields (81%). The coupling ready construct, **3-11**, can be coupled to any tumor-targeting module which bears free amine.

§2.4.3 Synthesis of the Drug Linker Conjugate with LNA as TTM

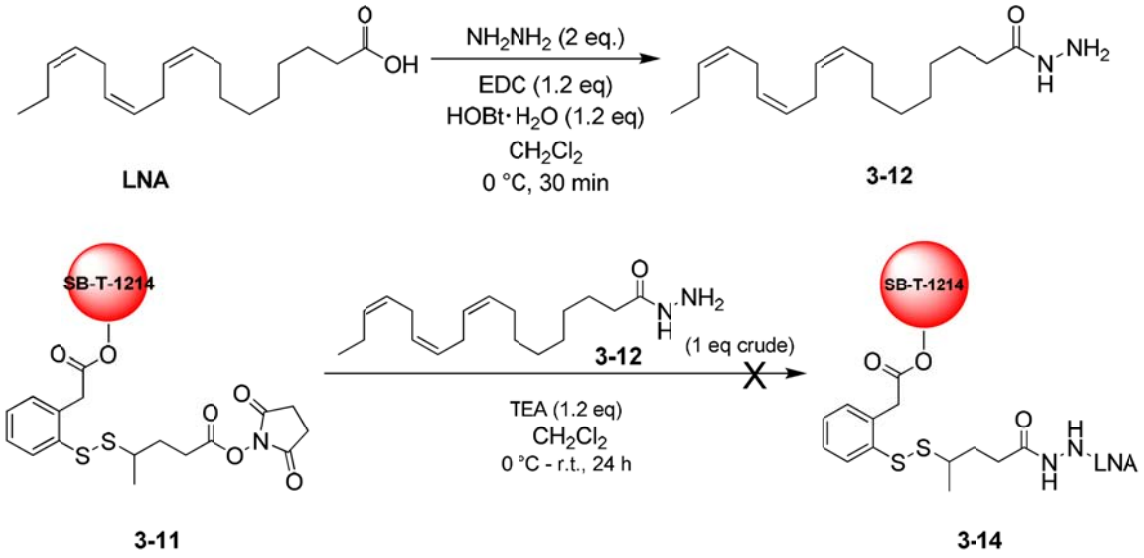

Scheme 4: The Synthesis towards the Drug Conjugate

After the completion of the coupling ready construct, **3-11**, the final steps toward the drug conjugate can be completed **(Scheme 4)**. LNA was converted to LNA hydrazide **(3-12)** in the presence of EDC coupling reagent and hydrazine. Compound **3-12** was then coupled to **3-11** to produce the SB-T-1214-Linker-LNA construct, **3-14**. However, no product was obtained on this intimal attempt. Spectroscopic data analysis showed no evidence of product formation. The use of EDC coupling reagent in the previous reaction could have caused the LNA hydrazide to be impure with the side product, di-isopropyl urea (DIU). DIU may have been detrimental in the final reaction. With this in mind, an alternative and more efficient route was taken to synthesize LNA-hydrazide without the use of and coupling reagents **(Scheme 5)**.

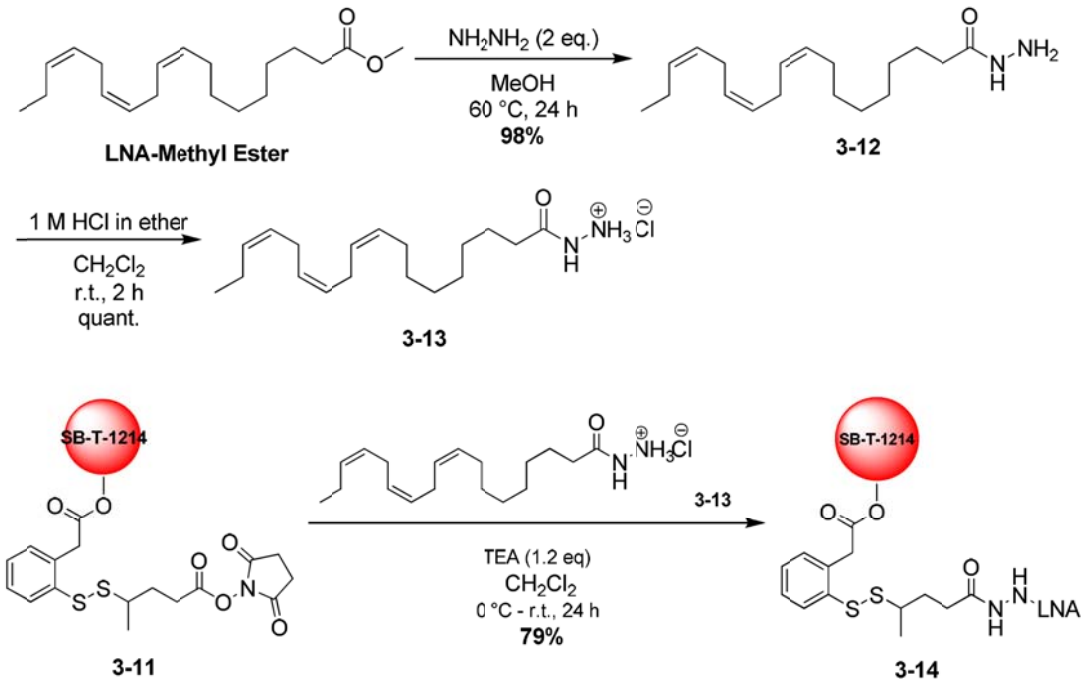

Scheme 5: Synthesis of Drug- Linker-Tumor-LNA Drug Conjugate

LNA methyl ester was refluxed with hydrazine in methanol for 24 hours to yield **3-12**. The use of the methyl ester derivative was cost effective because it was $63.20 for 5 g as opposed to the free carboxylic LNA for $87.60 for 100 mg. Also, refluxing in methanol reduced the need for purification and produced **3-12** in qualitative yields. Whereas the previous method reaction outlined in **scheme 4**, DIU was an undesirable side product. Also, the conversion of LNA-hydrazide to the hydrochloride salt (**3-13**) prolonged the stability and self-life of the material. Compound **3-13** was coupled to **3-11** in TEA and successfully produced the desired SB-T-1214-Linker-LNA construct, **3-14,** in good yields.

§2.5 Conclusions

PUFA-drug conjugates hold great promise in the future and severs as a model for targeted chemotherapy. Second and third generation taxanes can be incorporated into the PUFA-Drug conjugate model, making them more potent and active in MDR expressing cancer cell lines. Second generation taxane, SB-T-1214, and third generation taxane, SB-T-121602, were coupled to LNA via standard DIC coupling protocol, which afforded these conjugates in high yield. A self immolative methyl-branched disulfide linker was also incorporated in the tumor targeting drug conjugate drug approach. The synthesis of the methyl-branched disulfide linker and the SB-T-1214-Linker-OSu coupling ready construct were achieved in high yields. LNA was converted to the hydrazide derivative which was then coupled to the coupling ready construct to produce the desired tumor-targeting drug conjugate in good yields (76%). The LNA-Linker-Drug conjugate synthesized is novel. However, biological evaluation of theses conjugates as well as the linker is needed in order to fully understand the stability of the linker and conjugates in circulation and mechanism of action in cancer cells.

§2.6 Experimental

§ 2.6.1 General Methods and Materials

^{1}H and ^{13}C NMR spectra were measured on a Varian 300, 400 or 500 NMR spectrometer. Melting points were measured on a Thomas Hoover Capillary melting point apparatus and are uncorrected. Optical rotations were measured on a Perkin-Elmer Model 241 polarimeter. TLC was performed on Merck DC-alufolien with Kieselgel 60F-254 and column chromatography was carried out on silica gel 60 (Merck; 230-400 mesh ASTM). Mass to charge values were measured by flow injection analysis on an Agilent Technologies LC/MSD VL. In determining enantiopurity (% ee), a Chiracel OD-H chiral column was used, with an isocratic mixture of 85:15 Hexanes :IPA at a flow rate of 0.6 ml/min. In determining the purity of taxanes, a Phenomenex Jupiter 10 μ Proteo 9A column was used in reverse phase, with a mixture of 3:2 methanol: water at a flow rate of 0.4 mL/min.

The chemicals were purchased from Aldrich Co. and Sigma and purified before use by standard methods. Tetrahydrofuran was freshly distilled from sodium metal and benzophenone. Dichloromethane and methanol were also distilled immediately prior to use under nitrogen from calcium hydride. In addition, various dry solvents were degassed and dried using PureSolv™ solvent purification system (Innovative Technologies, Newburyport, MA).

§ 2.6.2 LNA-Taxane Conjugate [2-1]

LNA-SB-T-1214 (2-1)

A 41 mg (0.048 mmol) aliquot of **SB-T-1214,** 13 mg (0.048 mmol) of LNA, and 2 mg (0.014 mmol) of DMAP were dissolved in 1 mL of dicholoromethane and cooled to 0 °C under inert conditions. To this mixture, 0.008 mL (0.053 mmol) of DIC was added dropwise. The solution was allowed to warm to room temperature. The reaction was monitored TLC (3:2 hexane: ethyl acetate) and was completed in 30 min. Upon completion, the reaction was quenched with saturated NH_4Cl (10 mL) and extracted with dichloromethane (25 mL). The organic layer was washed three times with brine (35 mL), dried over anhydrous $MgSO_4$, and concentrated *in vacuo* to afford a clear oil. The resulting oil was purified by column chromatography on silica gel (2:1 hexanes: ethyl acetate) to yield **2-1** (43 mg, 81 %) as a white solid: m.p.=92-96 ^oC; $[\alpha]^{21}_D$ -60 (c 0.1, CH_2Cl_2; ^1H NMR (300 MHz, $CDCl_3$) δ 0.87 (m, 2 H) (H on *c*-propane), 0.97 (t, *J*= 3 Hz, 2H) (H on *c*-propane), 1.16 (s, 3 H), 1.26 (s, 3 H), 1.33 (s, 17 H) (8 H on saturated carbons of LNA and 9 H terminal methyl on *t*-boc), 1.75 (s, 8 H) (tertiary H), 1.92 (m, 5 H), 2.09 (s, 3 H), 2.45 (m, 4 H), 2.54 (m, 2 H), 2.80 (t, *J*= 3 Hz, 4 H) (allylic H on LNA), 3.82 (s, 1 H), 4.15 (d, *J* = 10 Hz, 1 H), 4.18 (s, 1 H), 4.30 (d, *J* = 9 Hz, 1 H), 4.90 (m, 2 H), 4.96 (d, *J* = 9 Hz, 1 H), 5.17 (s, 1 H), 5.36 (bs, 6H) (Vinyl H on LNA), 5.67 (d, *J* = 5 Hz, 1 H), 6.17 (t, *J* = 9 Hz, 1 H) (allylic H on SB-T-1214), 6.30 (s, 1 H) (C-10 H on SB-T-1214), 7.48 (t, *J* = 3 Hz, 2 H), 7.60 (t, *J* = 9 Hz, 1 H), 8.12 (d, *J* = 10 Hz, 2 H).). ^{13}C NMR (400 MHz, $CDCl_3$) δ 18.79, 22.52, 25.84, 28.34, 28.47, 35.71, 43.38, 45.82, 58.69, 75.65, 79.52, 80.08, 81.19, 129.49, 130.25, 130.47, 132.66, 155.08, 167.20, 168.57, 169.84, 173.13, 175.30, 204.29. LC/MS (positive mode) $[M^{+1}]$ 1114.4

m/z (major peak), [M^{+2}] 1115.4, [M^{+3}] 1116.4; Purity was determined to be 70 % by HPLC analysis on reverse phase with a Jupiter proteo column using methanol: water (2:3, 0.4 mL/min).

LNA-SB-T-121602 (2-2)

A 30 mg (0.048 mmol) aliquot of **SB-T-121602,** 10 mg (0.048 mmol) of LNA, and 2 mg (0.014 mmol) of DMAP were dissolved in 1 mL of dicholoromethane and cooled to 0 °C under inert conditions. To this mixture, 0.008 mL (0.053 mmol) of DIC was added dropwise. The solution was allowed to warm to room temperature. The reaction was monitored TLC (3:2 hexane: ethyl acetate) and was completed in 30 min. Upon completion, the reaction was quenched with saturated NH_4Cl (10 mL) and extracted with dichloromethane (25 mL). The organic layer was washed three times with brine (35 mL), dried over anhydrous $MgSO_4$, and concentrated *in vacuo* to afford a clear oil. The resulting oil was purified by column chromatography on silica gel (2:1 hexanes: ethyl acetate) to yield **2-2** (44 mg, 83 %) as a white solid: m.p.=78-82 ^oC; $[\alpha]^{21}_D$ -40 (c 0.1, CH_2Cl_2); ^1H NMR (500 MHz, $CDCl_3$) δ 0.99 (m, 2 H), 1.02 (m, 2H), 1.35 (s, 17 H) (8 H on saturated carbons of LNA and 9 H terminal methyl on *t*-boc), 1.16 (s, 3 H), 1.26 (s, 3 H), 1.33 (s, 9 H), 1.67 (s, 4 H), 1.76 (m, 6 H), 1.89 (m, 1 H), 2.04 (s, 3 H), 2.35 (m, 4 H), 2.54 (m, 2 H), 2.78 (t, *J*= 3 Hz, 4 H) (allylic H on LNA), 2.93 (s, 1 H), 3.06 (s, 1H), 3.82 (s, 1 H), 4.14 (d, *J* = 7.0 Hz, 1 H), 4.20 (m, 1 H), 4.30 (d, *J* = 9.0 Hz, 1 H), 4.44 (m, 1 H), 4.75 (s, 2 H), 4.96 (d, *J* = 7.5 Hz, 1 H), 5.24 (s, 1 H), 5.36 (bs, 6H) (Vinyl H on LNA), 5.67 (d, *J* = 10 Hz, 1 H), 6.09 (t, *J* = 8.0 Hz, 1 H), 6.41 (s, 1 H), 7.36 (m, 2 H), 7.92 (t, *J* = 9 Hz, 2 H) ^{13}C NMR (500 MHz, $CDCl_3$) δ 12, 17.62, 21.19, 23.96, 24.89, 24.99, 28.32, 29.52, 30.88, 38.09, 38.35, 38.66, 39.28, 45.88, 48.32, 54.26, 61.20, 7506, 75.12, 77.79, 78.91, 79.39, 79.65, 79.85, 79.90, 81.96, 82.54, 83.89, 87.30,

123.42, 129.95, 131.90, 133.45, 135.97, 137.02, 140.47, 140.97, 145.52, 158.05, 158.82, 169.74, 172.57, 208.28. LC/MS (positive mode) [M^{+1}] 1146.4 m/z (major peak), [M^{+2}] 1147.4, [M^{+3}] 1148.4; Purity was determined to be 81 % by HPLC analysis on reverse phase with a Jupiter proteo column using methanol: water (2:3, 0.4 mL/min).

§ 2.6.3 Disulfide linker

3*H*-Benzo[b]thiophen-2-one (3-1) [65,66]

A 5.0 g (28 mmol) aliquot of thianaphthene-2-boronic acid was dissolved in ethanol and 9.2 mL (100 mmol) of hydrogen peroxide was added to the mixture dropwise. The solution was stirred for 24 h at room temperature. The reaction was monitored by TLC (3:1 hexanes: ethyl acetate). After 24 h, the mixture was diluted with water and the organic layer was extracted with three allotments of $CHCl_3$ (35 mL). The organic layer was combined and dried over anhydrous $MgSO_4$. The solvent was removed and purification of the crude product was done using column chromatography on silica gel (3:1 hexanes:ethyl acetate) to yield **1-1** (3.2 g, 86%), as a off white solid: m.p.= 78-81 ^{o}C; ^{1}H NMR (300 MHz, $CDCl_3$) δ 3.85 (s, 2 H), 7.17 (d, 1 H), 7.21 (dd, 2 H), 7.24 (d, 1 H). All data are consistent with literature reported values.[65,66]

2-Sulfhydrylphenylacetic acid (3-2)[65,66]

A 2.0 g (13 mmol) aliquot of **3-1** was dissolved in 65 mL THF and warmed to 60 °C. A solution of 3.4 g (80 mmol) LiOH dissolved in 65 mL distilled water and added dropwise to the warmed solution containing **3-1**, producing a cloudy brown solution. The reaction mixture was stirred

overnight at 60 °C and monitored by TLC (3:1 hexanes: ethyl acetate). After 24 h, the mixture was removed from heat and cooled to room temperature. At room temperature, the mixture was diluted with water (15 mL) and diethyl ether (35 mL). The pH of the mixture was adjusted to pH 2 using 1 M HCl. The organic layer was extracted, washed with brine, dried over anhydrous Na_2SO_4, and concentrated *in vacuo*. Purification was done using column chromatography on silica gel (3:1 hexanes:ethyl acetate) to yield **3-2** (1.7 g, 80%): as an yellow solid ^{1}H NMR (300 MHz, $CDCl_3$) δ 3.49 (s, 1 H), 3.76 (s, 2 H), 7.16 (d, 2 H), 7.21 (dd, 1 H), 7.41 (dd, 1 H), 7.48 (d, 1 H). All data are consistent with literature reported values.[65,66]

1,2-di(pyridine-2-yl)disulfane (3-3)[67,68]

A 12.5 g (113 mmol) aliquot of pyridine-2(1H)-thione was dissolved in 225 mL dichloromethane. Subsequently, 53 g (337 mmol) of KMnO4 was added slowly over a period of 20 min and the solution was stirred vigorously producing a black solution. The reaction was monitored by TLC (1:1 hexanes:ethyl acetate). After 3.5 hours, the solution was filtered over celite and concentrated *in vacuo* to yield **3-3** (11.7 g, 95%) as a light-yellow solid without further purification: m.p. 55-56 °C (lit.[67] 58-60 ^{o}C); ^{1}H NMR (300 MHz, $CDCl_3$) δ 7.10 (dd, J = 7 Hz, 2 H), 7.61 (d, J = 7 Hz, 2 H), 7.62 (dd, J = 7 Hz, 2 H) 8.46 (d, J = 7 Hz, 2 H). In a second trial 7.35 g (66 mmol) pyridine-2(1H)-thione was used to obtain 3-III (7.5 g, 100% yield). All data are consistent with literature reported values.[67,68]

4-Sulfhydrylpentanoic acid (3-5)[69]

A 5.25 g (52.4 mmol) aliquot of γ-valerolactone was refluxed with 21.2 g (262 mmol) of HBr to 120 ^{o}C. After reflux was established, 20.0 g (262 mmol) of thiourea was added to the mixture

and solution was further refluxed for 24 h. After 24 h of reflux, the clear solution was diluted with ice-water (20 mL) and washed with three allotments dichloromethane (30 mL) and either (30 mL). The aqueous layer was then treated with 8 M NaOH to adjust the pH to 10. The mixture was refluxed for 24 h. After 24 h, the reaction mixture was allowed to cool to room temperature. The pH was adjusted to 1 with 1 M HCl. The aqueous layer was extracted with dichloromethane (30 mL). The combined organic layers were washed with brine (50 mL). The organic layer was dried over anhydrous $MgSO_4$ and concentrated *in vacuo* to yield **3-5** (4.79 g, 68%), as a yellow oil with strong stench: ^{1}H NMR (300 MHz, $CDCl_3$) δ 10.5 (s, 1 H), 2.904-2.950 (m, 1H), 2.461-2.501 (m, 2 H), 1.900-1.951 (m, 1H), 1.696-1.792 (m, 1 H), 1.417 (d, J = 3.5, 1 H), 1.323 (d, J = 3.5 Hz, 3 H). All data are consistent with literature reported values.[69]

4-(Pyridin-2-yldisulfanyl)pentanoic acid (3-6)[45]

A 0.67 g (5.00 mmol) aliquot of **3-3** was dissolved in 25 mL absolute ethanol. To the solution was added 6.61 g (30.0 mmol) of **3-5** dissolved in 150 mL ethanol. The reaction mixture was allowed to stir at room temperature and monitored by TLC (1:1 hexanes: ethyl acetate). After 16 h, the reaction solution was evaporated. The resulting yellow oil was dissolved in dichloromethane and purified via column chromatography on silica gel (3:2 hexane: ethyl acetate) to obtain unreacted **3-3** and desired **3-6**, and to obtain dimers and reaction side products. **3-6**(1 g, 82.4 %) was obtained as a yellow oil. ^{1}H NMR (300 MHz, $CDCl_3$) δ 1.311 (d, J = 3.3 Hz, 3 H), 1.875-2.003 (m, 2 H), 2.525 (t, J = 3.9 Hz, 2 H), 2.981-3.026 (m, 1H), 7.060-7.101 (m, 1 H), 7.604-7.661 (dt, 1 H), 7.721-7.748 (m, 1 H), 8.456 (m, 1 H). LC/MS (positive mode)-[M^{1+}] 244.0. All data are consistent with literature reported values.[45]

Triisopropylsilyl 4-(pyridin-2-yldisulfanyl)pentanoate (3-7)[45]

A 1.00 g (4.1 mmol) aliquot of **3-6** and 0.83 g (8.2 mmol) of TEA was dissolved in 20 mL of CH_2Cl_2 and cooled to 0 °C under inert conditions. To the mixture, 1.05 mL (5 mmol) of TIPSCl was added dropwise. The reaction mixture was stirred at room temperature and monitored by TLC (3:1 hexanes: ethyl acetate). The reaction was quenched with saturated NH_4Cl (20 mL) and extracted with dichloromethane (50 mL). The organic layer was dried over anhydrous $MgSO_4$ and concentrated *in vacuo*. Purification was done by column chromatography on silica gel (3:1 hexanes: ethyl acetate) to yield a light yellow oil, **3-7** (1.49 g , 91 %): ^{1}H NMR (300 MHz, $CDCl_3$) δ 8.421 – 8.396 (dq, 1 H), 7.721 – 7.688 (dt, 1 H), 7.621 – 7.563 (m, 1H), 7.619 (t, J = 7.6, 1 H), 7.058 (t, J = 5.2 Hz, 1 H), 3.011 – 2.960 (m, 1 H), 2.253 – 2.468 (m, 2 H), 2.004 – 1.866 (m, 2 H), 1.300 (m, 3 H), 1.007 (m, 21 H). All data are consistent with literature reported values.[45]

2-(2-5-Oxo-5-(triisopropylsilyloxy)pentan-2-yldisulfanylphenyl)acetic acid (3-8)[45]

A 280 mg (0.501 mmol) aliquot of **3-7** was dissolved in 0.63 mL of THF and cooled to -10 °C under inert conditions. To this mixture, 40 mg (0.501 mmol) of **3-2** previously dissolved in 0.63 mL of THF was added dropwise. The mixture was stirred at -10 °C for 30 min and was then warmed to room temperature for 60 min. The reaction was monitored by TLC (3:1 hexanes: ethyl acetate). The solvent was evaporated and the residual was purified by column chromatography on silica gel (5:1 hexanes: ethyl acetate) to yield **3-8** (279 mg, 88.2 %) as a light

yellow oil. ^{1}H NMR (400 MHz, $CDCl_3$) δ 7.803 – 7.784 (d, *J* = 7.6 Hz, 1 H), 7.297 – 7.267 (m, 1H), 7.211 – 7.178 (m, 1 H), 3.896 (s, 2 H), 2.918 – 2.884 (m, 1 H), 2.435 – 2.388 (m, 2 H), 1.954 – 1.917 (m, 1 H), 1.840 – 1.805 (m, 1 H), 1.310 – 1.235 (m, 3 H), 1.060 (m, 21 H). All data are consistent with literature reported values.[45]

§ 2.6.4 Coupling Ready Construct

SB-T- 1214-Linker-CO_2TIPS (3-9)[45]

A 130 mg (0.152 mmol) aliquot of **SB-T-1214** and 5.64 mg (0.046 mmol) of DMAP was dissolved in 1 mL of dichloromethane and cooled to 0 °C under inert conditions. To this mixture, 0.020 mL (0.182 mmol) of DIC was added dropwise, followed by the dropwise addition of 70 mg (0.154 mmol) of **3-8** dissolved in 0.5 mL of dichloromethane. The solution was stirred at 0 °C for 24 h and allowed to warm to room temperature. The reaction was monitored by TLC (1:1 hexanes:ethyl acetate). Upon completion, the mixture was filtered to remove excess impurities and washed with dichloromethane (35 mL). The organic layer was evaporated and the residual oil was purified by column chromatography on silica gel with (3:2 hexanes: ethyl acetate) to yield **3-9** (60 mg, 50%) as a white solid. ^{1}H NMR (500 MHz, $CDCl_3$) δ 8.110 – 8.094 (d, *J* = 6.4 Hz, 1 H), 7.822 – 7.784 (t, *J* = 11 Hz, 1 H), 7.616 – 7.587 (t, *J* = 5, 1 H), 7.298 (m, 1 H), 6.295 (d, *J* = 7 Hz, 1 H), 6.221 (m, 1 H), 5.678 (d, *J* = 7 Hz, 1 H), 5.142 (m, 1 H), 4.981 (m, 2 H), 4.407 (m, 1 H), 4.313 (m, 1 H), 4.183 (m, 1 H), 4.125 (s, 2 H), 3.784 (s, 1 H), 2.540 (m, 1 H), 2.380 (m, 4 H), 2.041 (s, 3 H), 1.903 (m, 2 H), 1.775 (m, 3 H), 1.717 (s, 2 H), 1.663 (s, 2 H),

1.358 (s, 6 H), 1.255 (m, 8 H), 1.147 (m, 3 H), 1.079 (m, 2 H), 0.988 (m, 2 H), 1.046 (m, 21 H). All data are consistent with literature reported values.[45]

SB-T- 1214-Linker-CO_2H (3-10)[45]

A 60 mg (0.046 mmol) aliquot of **3-9** was dissolved in 2.5 mL of a 1:1 mixture of acetonitrile: pyridine and cooled to 0 °C under inert conditions. To the mixture, 0.60 mL of HF/pyridine was added dropwise. The reaction was stirred at room temperature for 24 hours and monitored by TLC (1:1 hexanes: ethyl acetate). Upon completion, the reaction was quenched with saturated $NaHCO_3$ (15 mL) and extracted with ethyl acetate (50 mL). The organic layer was washed with $CuSO_4$ (3 X 30 mL), then with brine (3 X 30 mL), dried over anhydrous $MgSO_4$, and concentrated *in vacuo*. Purification was done by column chromatography on silica gel (1:1 hexanes:ethyl acetate) to yield **3-10** (48 mg, 93%) as an off white solid: ^{1}H NMR (500 MHz, $CDCl_3$) δ 8.110 – 8.094 (d, J = 6.4 Hz, 1 H), 7.822 – 7.784 (t, J = 11 Hz, 1 H), 7.616 – 7.587 (t, J = 5, 1 H), 7.298 (m, 1 H), 6.295 (d, J = 7 Hz, 1 H), 6.221 (m, 1 H), 5.678 (d, J = 7 Hz, 1 H), 5.142 (m, 1 H), 4.981 (m, 2 H), 4.407 (m, 1 H), 4.313 (m, 1 H), 4.183 (m, 1 H), 4.125 (s, 2 H), 3.784 (s, 1 H), 2.540 (m, 1 H), 2.380 (m, 4 H), 2.041 (s, 3 H), 1.903 (m, 2 H), 1.775 (m, 3 H), 1.717 (s, 2 H), 1.663 (s, 2 H), 1.358 (s, 6 H), 1.255 (m, 8 H), 1.147 (m, 3 H), 1.079 (m, 2 H), 0.988 (m, 2 H). All data are consistent with literature reported values.[45]

SB-T-1214-Linker-OSu Conjugate (3-11)[45]

A mixture of 50 mg (0.045 mmol) **3-10** and 10 mg (0.1 mmol) HOSu was dissolved in 1 mL pyridine. The reaction was stirred at room temperature and monitored by TLC (1:1 hexanes:

ethyl acetate). After 24 h, the reaction mixture was quenched with NH_4Cl (5 mL) and extracted with ethyl acetate (25 mL). The organic layer was washed with brine (3 x 25 mL), dried over anhydrous $MgSO_4$, and concentrated in *vacuo* resulting in a crude mixture. Purification was done using column chromatography on silica gel (3:2 hexane: ethyl acetate) to yield **3-11** (34 mg, 81%) as a yellow solid: ^{1}H NMR (500 MHz, $CDCl_3$) δ 8.115 – 8.097 (d, *J* = 9 Hz, 1 H), 8.015 (s, 1 H), 7.784 (m, 1 H), 7.594 (t, *J* = 5 Hz, 1 H), 7.316 (m, 1 H), 6.279 (s, 1 H), 6.221 (m, 1 H), 5.678 (m, 1 H), 4.974 (m, 2 H), 4.407 (m, 1 H), 4.287 (m, 1 H), 4.187 (m, 1 H), 4.083 (s, 2 H), 3.803 (m, 1 H), 2.957 (m, 11 H), 2.824 (s, 3 H), 2.656 (m, 1 H), 2.347 (m, 5 H), 2.076 (s, 5 H), 1.899 (s, 3 H), 1.725 (m, 7 H), 1.656 (s, 4 H), 1.358 (s, 6 H), 1.255 (m, 8 H), 1.147 (m, 3 H), 1.079 (m, 2 H), 0.988 (m, 2 H). All data are consistent with literature reported values.[45]

§ 2.6.5 Drug Conjugate with LNA as TTM

LNA Hydrazide (3-12)[45,70]

A 0.5 mL (1.5 mmol) aliquot of **LNA methyl ester** and 0.15 mL (3 mmol) of hydrazine were refluxed to 80 ^{o}C in 6 mL of methanol for 24 h. The mixture was concentrated in *vacuo* to yield **3-12** (430 mg, 98 %) as clear oil ^{1}H NMR (500 MHz, $CDCl_3$) 0.994 (t, *J*=8, 3 H), 1.364-1.270 (m, 11 H), 1.652 (m, 4 H), 2.111-2.048 (m, 4), 2.160 (t, *J*=8, 2 H), 2.823 (s, 4 H), 3.681 (s, 1 H), 3.914 (s, 1 H), 5.425-5.321 (m, 6 H), 6.747 (s, 1 H). This compound was used crude in the subsequent reaction. This All data are consistent with literature reported values.[45,70]

LNA Hydrazide Hydrochloride Salt (3-13)

A 400 mg (1.44 mmol) aliquot of **3-12** was dissolved in dichloromethane (2 mL). To this solution, 1 M HCl in either was added and the reaction mixture was stirred for 2 h at room temperature. After completion, the mixture concentrated in *vacuo* to yield **3-13** (420 mg, quantitive yield) as a white solid.

SB-T-1214- Linker-LNA (3-14) [45,70]

A 40 mg (0.033 mmol) aliquot of **3-11** was dissolved 2 mL of dichloromethane and cooled to 0 ^{o}C in inert conditions. A 10 mg (0.036 mmol) aliquot of pure **3-13** (derived from **LNA methyl ester**) previously dissolved in 1 mL of dichloromethane was added. To this mixture, 0.05 mL (0.04 mmol) of TEA was added dropwise to the solution. The reaction was mixed for 24 h at 0 ^{o}C and monitored by TLC (9: 1 dichloromethane: methanol). Upon completion the reaction was quenched with NH_4Cl (15 mL) and extracted with dichloromethane (35 mL). The organic layer was washed three times with brine (35 mL), dried over anhydrous $MgSO_4$, and concentrated in *vacuo* to yield a crude oil. Purification was done using column chromatography on silica gel (5:2 hexane: ethyl acetate) to yield **3-13** (37 mg, 79%) as a white-yellow solid: m.p.= 88-90 ^{o}C. ^{1}H NMR (500 MHz, $CDCl_3$) 0.976 (m, 4 H), 1.145 (m, 4 H), 1.335 (m, 16 H), 1.716 (m, 5 H), 1.946 (m, 10 H), 2.246 (s, 2 H), 2.368 (s, 1 H), 2.622 (s, 2 H), 2.808 (s, 4 H), 3.812 (s, 1 H), 4.072 (m, 1 H), 4.185 (m, 1 H), 4.226 (m, 1 H), 4.295 (m, 1 H), 4.307 (m, 1 H), 4.417 (m, 1 H), 4.972 (s, 1 H), 5.119 (s, 1 H), 5.363 (s, 6 H), 5.680 (s, 1 H), 6.313 (s, 1 H), 7.271 (m, 1 H), 7.467 (s, 1 H), 7.592 (m, 1 H), 8.109 (s, 1 H), 8.554 (s, 1 H). ^{13}C-NMR of this compound was done by William Burger in the Ojima group and the spectrum is shown in the appendix.[70] LC/MS (positive mode)

[M^{1+}] 1410.7, [M^{2+}] 1411.7, [M^{3+}] 1412.7; Purity was determined to be 84 % by HPLC analysis on reverse phase with a Jupiter proteo column using methanol: water (2:3, 0.4 mL/min). All data are consistent with literature reported values.[70]

§3 References

[1] Jemal, A.; Siegal, R.; Ward, E.; Murray, T.; Xu, J.; Smigal, C.; Thun, M. J. Cancer Statistics, 2006. *Ca-Cancer j. Clin.* **2006**, *56*, 106-130.

[2] Kung,H. Cancer Deaths: Finals Data 2005. *National Vital Statistics Reports*. **2008**, 56, 1-121.

[3] Goodman, J.; Walsh, V. *The Story of Taxol: Nature and Politics in the Pursuit of an Anti-Cancer Drug*. Cambridge University Press, **2001.**

[4] Suffness, M. *Taxol: Science and Applications*; CRC Press: New York, **1995.**

[5] Wall, M. E.; Wani, M. C. Camptothecin and Taxol: Discovery to Clinical-Thirteenth Bruce F. Cain Memorial Award Lecture. *Cancer Res.* **1995**, *55*, 753-760.

[6] Fuchs, D. A.; Johnson, R. K. Cytologic evidence that taxol, an antineoplastic agent from *Taxus brevifolia*, acts as a mitotic spindle poison. *Cancer Treatment Reports*. **1978**, *62*, 1219–1222.

[7] Schiff, P. B.; Fant, J.; Horwitz, S. B. Promotion of microtubule assembly *in vitro* by Taxol. *Nature*, **1979**, *277*, 655-667.

[8] Holmes, F. A.; Kudelka, A. P.; Kavanagh, J. J.; Huber, M. H.; Ajani, J. A.; Valero, V. Current Status of Clinical Trials with Paclitaxel and Docetaxel. Chapter 3, pp. 31-57. In, *Taxane Anticancer Agents: Basic Science and Current Status*, Editors: Georg, G. I.; Chen, T. T.; Ojima, I.; Vyas, D. M. American Chemical Society: Washington D.C., **1995**.

[9] Georg, G. I.; Chen, T. T.; Ojima, I.; Vyas, D. M. *Taxane Anticancer Agents: Basic Science and Current Status*. American Chemical Society: Washington D.C., **1995**.

[10] Schhiff, P. B.; Horwitz, S. B. Taxol stabilizes microtubules in mouse fibroblast cells. *Proc. Natl. Acad. Sci., U.S.A* **1980**, 77, 1561-1565.

[11] Wu, Xi. Design, synthesis and biological evaluation of tumor-targeting taxane-based anticancer agents and MDR modulators [Ph.D. dissertation]. United States -- New York: State University of New York at Stony Brook; **2003**. Available from: Dissertations & Theses @ SUNY Stony Brook. Publication Number: AAT 3106532.

[12] Blume, E. Government Moves To Increase Taxol Supply. *J. Natl. Cancer Inst.* **1991**, *83*, 1054-1056.

[13] Guéritte-Voegelein, F.; Sénilh, V.; David, B.; Guénard, D.; Potier, P. Chemical studies of 10-deacetyl baccatin III : Hemisynthesis of taxol derivatives. *Tetrahedron.* **1986**, *42*, 4451-4460.

[14] Ojima, I.; Habus, I.; Zhao, M. Efficient and Practical Asymmetric Synthesis of the Taxol C-13 Side Chain, N-Benzoyl-(2R,3S)-3-phenylisoserine and Its Analogues via Chiral 3-Hydroxy-4-

aryl-β-lactams through Chiral Ester Enolate-Imine Cyclocondensation. *J. Org.* Chem. **1991**, *56*, 1681-1683.

[15] Ojima, I.; Slater, J. C.; Kuduk, S. D.; Takeuchi, C. S.; Gimi, R. H.; Sun, C. M.; Park, Y. H.; Pera, P.; Veith, J. M.; Bernacki, R. J., Syntheses and Structure-Activity Relationships of Taxoids Derived from 14β-Hydroxy-10-deacetylbaccatin III. *J. Med. Chem.* **1997**, *40*, 267-278.

[16] Rowinsky, E. K. The Development and Clinical Utility of the Taxane Class of Antimicrotubule Chemotherapy Agents. *Annu. Rev. Med.* **1997**, *48*, 353-374.

[17] Pellegrini, F.; Budman, D.R. Review: Tubulin Function, Action of Antitubulin Drugs and New Drug Development. *Cancer Investigation*. **2005**, 23, 264-273.

[18] Croop, J. M. Evolutionary Relationships among ABC transporter. *Methods Enzymol.* **1998**, *292*, 101-116.

[19] Kingston, D. G. I. Recent Advances in the Chemistry of Taxol. *J. Nat. Prod.* **2000**, *63*, 726-734.

[20] Chen, S.; Farina, V.; Vyas, D. M.; Doyle, T. W.; Long, B. H.; Fairchild, C. Synthesis and Biological Evaluation of C-13 Amide-Linked Paclitaxel Analogs. *J. Org Chem.***1996**, *61*, 2065-2070

[21] Cabri, W.; Curini, M.; Marcotullio, M. C.; Rosati, O. A high yield semisynthetic approach to 2′-epi-Taxol. *Teterahedron Lett.* **1996**, *37*, 4785-4786.

[22] Guéritte-Voegelein, F.; Guénard, D.; Lavelle, F.; Le Goff, M. T.; Mangatal, L.; Potier, P. Relationships between the structure of taxol analogs and their antimitotic activity. *J. Med. Chem*. **1991**, *34*, 992-998.

[23] Ojima, I.; Lin, S.; Wang, T. Recent Advances in the Medicinal Chemistry of Taxoids with Novel β-Amino Acid Side Chain. *Curr. Med. Chem.***1999**, 6, 927-953.

[24] Ojima, I.; Slater, J. C.; Michaud, E.; Kuduk, S. D.; Bounaud, P. Y.; Vrignaud, P.; Bissery, M. C.; Veith, J. M.; Pera, P.; Bernacki, R. J., Syntheses and Structure-Activity Relationships of the Second-Generation Antitumor Taxoids: Exceptional Activity against Drug-Resistant Cancer Cells. *J. Med. Chem.* **1996**, *39*, 3889-3896.

[25] Spletstoser, J.T.; Turunen, B. J.; Desino, K.; Rice, A. Datta, A.; Dutta, D.; Huff, J. K.; Himes, R. H.; Audus, K. L.; Seelig, A.; Georg, G. I. Single-site Chemical Modification at C10 of the Baccatin Core of Palitaxel and Taxol C reduces P-glycoprotein interactions in bovine brain microvessel endothelial cells. *Bioorg. & Med. Chem. Lett.* **2006**, *16*, 495-498

[26] Chordia, M. D.; Kingston, D. G. I. Synthesis and Biological Evaluation of 2-*epi*-Paclitaxel. *J. Org. Chem.* **1996**, *64*, 799-801.

[27] Chen, S.; Farina, V.; Wei, J.; Long, B. H.; Fairchild, C.; Mamber, S. W.; Kadow, J. F.; Vyas, D. M.; Doyle, T. W. Structure-activity relationships of taxol®: synthesis and biological evaluation of C2 taxol analogs. *Bioorg. Med. Chem. Lett.*, **1994**, *4*, 479-482.

[28] Kingston, D. G. I.; Chaudhary, A. G.; Chordia, M. D.; Gharpure, M.; Gunatilaka, A. A. L.; Higgs, P. I.; Rimoldi, J. M.; Samala, L.; Jagtap, P. G.; Giannakakou, P.; Jiang, Y. Q.; Lin, C. M.; Hamel, E.; Long, B. H.; Fairchild, C. R.; Johnston, K. A. Synthesis and Biological Evaluation of 2-Acyl Analogues of Paclitaxel (Taxol). *J. Med. Chem.* **1998**, *41,* 3715-3726.

[29] Ojima, I.; Wang, T.; Miller, M. L.; Lin, S.; Borella, C. P.; Geng, X.; Pera, P.; Bernacki, R. J. Synthesis and structure-activity relationships of new second-generation toxoids. . *Bioorg. Med. Chem. Lett.*, **1999**, *9*, 3423-3428.

[30] Holten K. B.; Onusko, E. M. Appropriate prescribing of oral beta-lactam antibiotics. *American family physician.* **2000**, *62*, 611–620.

[31] Staudinger, H.; Justus, L. A. Zur Kenntniss der Ketene. Diphenylketen *Ann. Chem* **1907,** *356*, 51 – 123.

[32] Singh, G. S., Beta-lactams in the new millennium. Part-I: Monobactams and carbapenems. *Mini-Reviews in Medicinal Chemistry.* **2004**, *4*, 69-92.

[33] Lopez, R.; Sordo, T. L.; Sordo, J. A.; Gonzalez, J. Torquoelectronic effect in the control of the stereoselectivity of ketene-imine cycloaddition reactions. *J. Org. Chem*. **1993**, *58*, 7036-7037

[34] Brieva, R.; Crich, J. Z.; Sih, C. J. Chemoenzymic synthesis of the C-13 side chain of taxol: optically active 3-hydroxy-4-phenyl .beta.-lactam derivatives *J. Org. Chem.* **1993**, *58*, 1068-1075.

[35] Schwartz, A.; Madan, P.; Whitesell, J. K.; Lawrence, R. M. Lipase-Catalyzed Kinetic Resolution of Alcohols via Chloroacetate Esters: (-)-(1*R*, 2*S*)-*trans*-2-phenyl-cyclohexanol and (+)-(1*S*, 2*R*)-*trans*-2-phenyl-cyclohexanol. *Org. Synth. Coll.* **1990**, *69,* 1-9.

[36] Ojima, I.; Park, Y. H.; Sun, C. M.; Brigaud, T; Zhao, M. New and efficient routes to norstatine and its analogs with high enantiomeric purity by β-Lactam Synthon Method. *Tetrahedron Lett.* **1992***, 33,* 5737-5740.

[37] Ojima, I.; Habus, I.; Zhao, M.; Zucco, M; Park, Y. H.; Sun, C. M.; Brigaud, T. New and efficient approaches to the semisynthesis of taxol and its C-13 side chain analogs by means of β-lactam synthon method. *Tetrahedron*. **1992***, 48,* 6985-7012.

[38] Kolb, H. C.; van Nieuwenhze, M. S.; Sharpless, B. K., Catalytic Asymmetric Dihydroxylation *Chem. Rev.* **1994,** *94*, 2483 - 2547.

[39] DelMonte, A. J.; Haller, J.; Houk, K. N.; Sharpless, K. B.; Singleton, D. A.; Strassner, T.; Thomas, A. Experimental and Theoretical Kinetic Isotope Effects for Asymmetric Dihydroxylation. Evidence Supporting a Rate-Limiting "(3 + 2)" Cycloaddition. *J. Am. Chem. Soc.* **1997**, *119*, 9907-9908.

[40] Stayshich, R. M.; Meyer, T. Y., New Insights into Poly(lactic-*co*-glycolic acid) Microstructure: Using Repeating Sequence Copolymers To Decipher Complex NMR and Thermal Behavior *J. Am. Chem. Soc.* **2010,** *132*, 10920 - 10934.

[41] Ojima, I.; Chen, J.; Sun, L.; Borella, C. P.; Wang, T.; Miller, M. L.; Lin, S.; Geng, X.; Kuznetsova, L.; Qu, C.; Gallager, D.; Zhao, X.; Zanardi, I; Xia, S.; Horwitz, S. B.; Mallen-St. Clair, Jon; Guerriero, J. L.; Bar-Sagi, D.; Veith, L. M.; Pera, P.; Bernacki, R. J. Design, Synthesis, and Biological Evaluation of New Generation Taxoids. *J. Med Chem.* **2008,** *51,* 3203-3221.

[42] Kovár, J.; Ehrlichová, M.; Smejkalová, B.; Zanardi, I.; Ojima, I.; Gut, I. Comparison of cell death-inducing effect of novel taxane SB-T-1216 and paclitaxel in breast cancer cells. *Anticancer Res*. **2009**, *29*, 2951-2960.

[43] Jordan, M.A., Ojima, I.; Rosas, F.; Distefano, M.; Wilson, L.; Scambia, G.; Ferlini, C. Effects of novel taxanes SB-T-1213 and IDN5109 on tubulin polymerization and mitosis. *Chem. Biol.* **2002**, 9, 93-101.

[44] Appendino, G.; Belloro, E.; Del Grosso, E.; Minassi, A.; Bombardelli, E. Synthesis and Evaluation of 14-Nor-A-*seco*taxoids. *European Journal of Organic Chemistry*, **2002**, *2*, 277-283.

[45] Zuniga, E. Quarterly Reports 1-10. **2007-2009.** Stony Brook University.

[46] Wang, T. Applications of beta-lactam synthon method to the syntheses of peptidomimetics, amino/aza-sugar derivatives, and taxoid antitumor agents [Ph.D. dissertation]. United States -- New York: State University of New York at Stony Brook; **1999**. Available from: Dissertations & Theses @ SUNY Stony Brook. Publication Number: AAT 9942018.

[47] Burger, W. Quarterly Report: An efficient asymmetric Synthesis of (3*R*, 4*S*) di-methyl-vinyl-2-azetidinone. **2010.** Stony Brook University.

[48] Denis, J.-N.; Greene, A. E.; Gue´nard, D.; Gue´ritte-Voegelein, F.; Mangatal, L.; Potier, P. A Highly Efficient, Practical Approach to Natural Taxol. *J. Am. Chem. Soc.* **1988**, *110*, 5917-5919.

[49] Das M. Design, synthesis and biological evaluation of novel tumor-targeting taxane-based drug delivery systems [Ph.D. dissertation]. United States -- New York: State University of New

York at Stony Brook; **2010**. Available from: Dissertations & Theses @ SUNY Stony Brook. Publication Number: AAT 3422800.

[50] Seitz, J. D. Quarterly Reports: Taxane Synthesis. **2009**. Stony Brook University.
[51] Schindler, T.; Bornmann, W.; Pellicena, P.; Miller, W. T.; Clarkson, B.; Kuriyan, J. Structural Mechanism for STI-571 Inhibition of Abelson Tyrosine Kinase. *Science.* 2000, *15*, 1938-1942.

[52] Hanahan, D.; Weinberg. R. A.; The Hallmarks of Cancer. *Cell.* 2000, *100*, 57-70.

[53] Daley, G. Q. Gleevec Resistance: Lessons for Target-Directed Drug Development. 2003, *3*, 189-190.

[54] Ojima, I. Guided Molecular Missiles for Tumor-Targeting Chemotherapy—Case Studies Using the Second- Generation Taxoids as Warheads*Acc. Chem. Res.* 2008, *41*, 108-119.

[55] Wigmore, Ross, J. A.; Falconer, J. S.; Plester, C. E.; Tisdale, M. J.; Carter, D. C.; Ch Fearon, K. The effect of polyunsaturated fatty acids on the progress of cachexia in patients with pancreatic cancer. *Nutrition* **1996**, *12*, S27-S30.

[56] R. A. Hawkins, Kathryn Sangster and M. J. Arends. Apoptotic death of pancreatic cancer cells induced by polyunsaturated fatty acids varies with double bond number and involves an oxidative mechanism. *J. Pathol.* **1998**, *185*, 61-70.

[57] Ojima, I. Use of Fluorine in the Medicinal Chemistry and Chemical Biology of Bioactive Compounds-A Case Study on Fluorinated Taxane Anticancer Agents *ChemBioChem* **2004**, *5*, 628-635

[58] De Deckere, E.A. Possible beneficial effect of fish and fish *n*−3 polyunsaturated fatty acids in breast and colorectal cancer. *Eur J Cancer Prev.* **1999**, *8*, 213–221

[59]Augustsson, Katarina; *et al.* A prospective study of intake of fish and marine fatty acids and prostate cancer. *Cancer Epidemiology, Biomarkers & Prevention* **2003**, *12*, 64–67.

[60] Bradley, M. O.; Webb, N. L.; Anthony, F. H.; Devanesan, P.; Witman, P. A.; Hemamalini, S.; Chander, M. C.; Baker, S. D.; He, L. F.; Horwitz, S. B.; Swindell, C. S. Tumor Targeting by Covalent Conjugation of a Natural Fatty Acid to Paclitaxel *Clin. Cancer Res*. **2001**, *7*, 3229.

[61]Seitz, J. D.; Ojima, I. Drug Conjugates with Polyunsaturated Fatty Acids. (In press).

[62] Desai, N. Y., Z.; Trieu, V.; Soon-Shoing, P.; Dykes, D.; Noker, P. Evidence of greater tumor and red cell partitioning and superior antitumor activity of cremophor free nanoparticle paclitaxel (ABI-007) compared to taxol, *Breast Cancer Res. Treat.* **2003**, *82*, Abstract 348.

[63] Rowinsky, E. K. The Development and Clinical Utility of the Taxane Class of Antimicrotubule Chemotherapy Agents. *Annu. Rev. Med.* **1997**, *48*, 353-374.

[64] Jaracz, S.; Chen, J.; Kuznetsova, L. V.; Ojima, I. Recent advances in tumor-targeting anticancer drug conjugates. *Biorg. & Med. Chem*. **2005**, *13*, 5043–5054

[65] Dickinson, R. P., Iddon, B. *J. Chem. Soc.* **1970**, *14*, 1926-1928.

[66] Bordwell, F. G., Fried, H.E. *Journal of Organic Chemistry* **1991**, *56*, 4218-4223.

[67] Samukov, V. V. *Synthetic Communications* **1998**, *28*, 3213 - 3217.

[68] Shaabani, A.; Tavasoli-Rad, F.; Lee, D. G. *Synthetic Communications* **2005**, *35*, 571 - 580.

[69] Widdison, W. C.; Wilhelm, S. D.; Cavanagh, E. E.; Whiteman, K. R.; Leece, B. A.; Kovtun, Y.; Goldmacher, V. S.; Xie, H.; Steeves, R. M.; Lutz, R. J.; Zhao, R.; Wang, L.; Blattler, W. A.; Chari, R. V. J. *J. Med. Chem.* **2006**, *49*, 4392-4408.

[70] Burger, W. Quarterly reports. **2009**. Stony Brook University.

APPENDIX

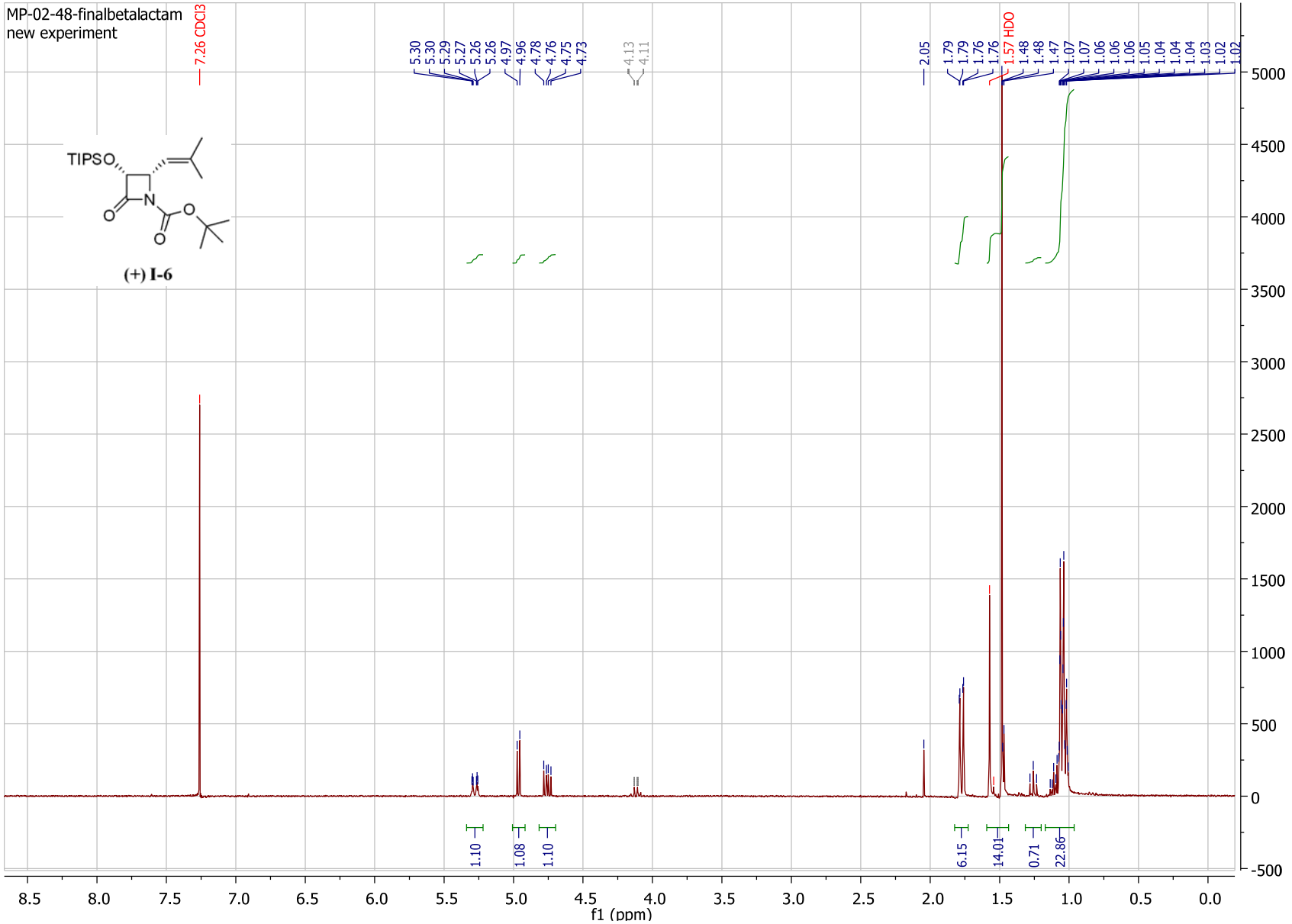
MP-02-48-finalbetalactam
new experiment
7.26 CDCl3
TIPSO
(+) I-6
5.30
5.30
5.29
5.27
5.26
5.26
4.97
4.96
4.78
4.76
4.75
4.73
4.13
4.11
2.05
1.79
1.79
1.76
1.76
1.57 HDO
1.48
1.47
1.07
1.07
1.06
1.06
1.06
1.05
1.04
1.04
1.03
1.02
1.02
1.10
1.08
1.10
6.15
14.01
0.71
22.86
f1 (ppm)

A

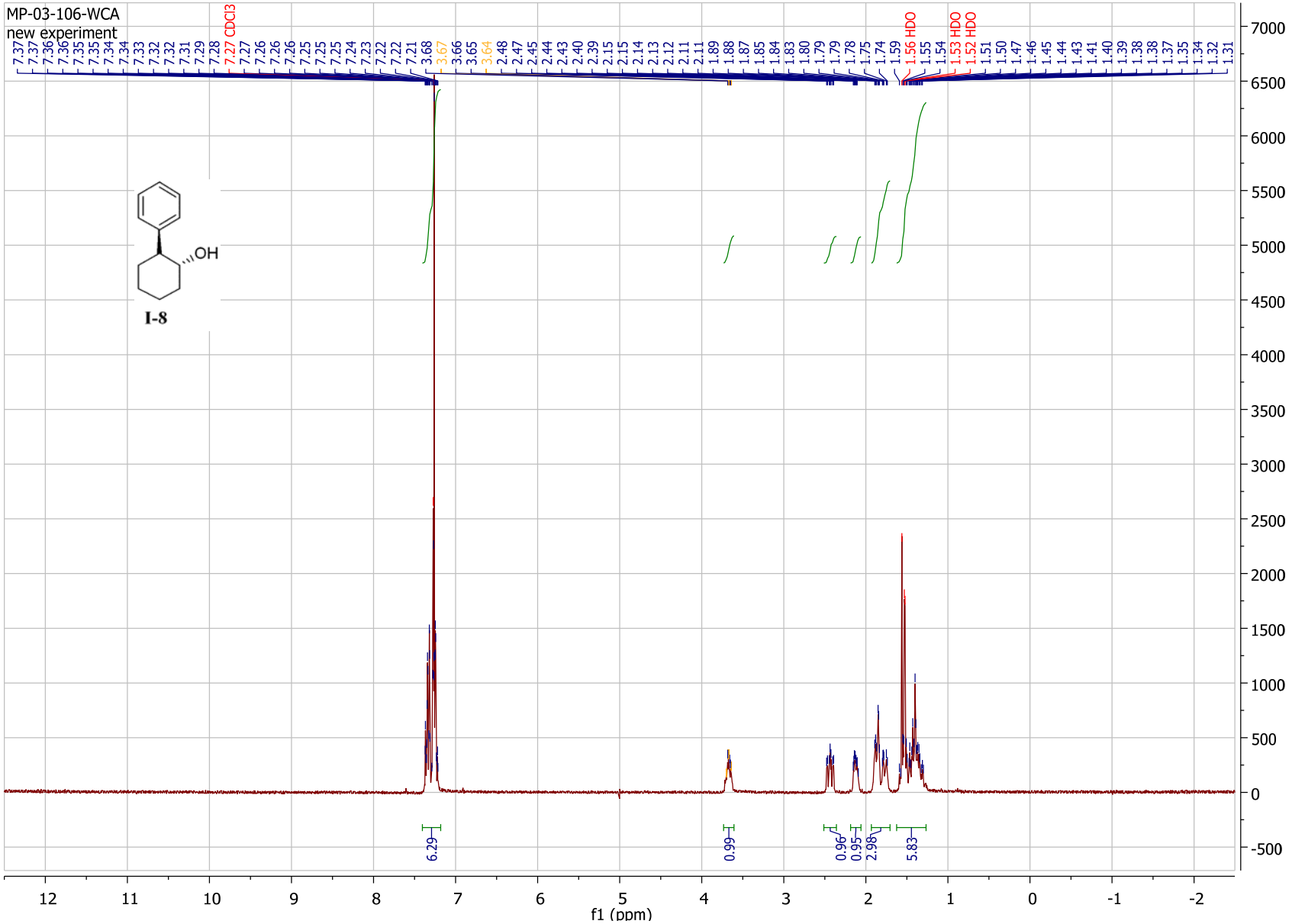

B

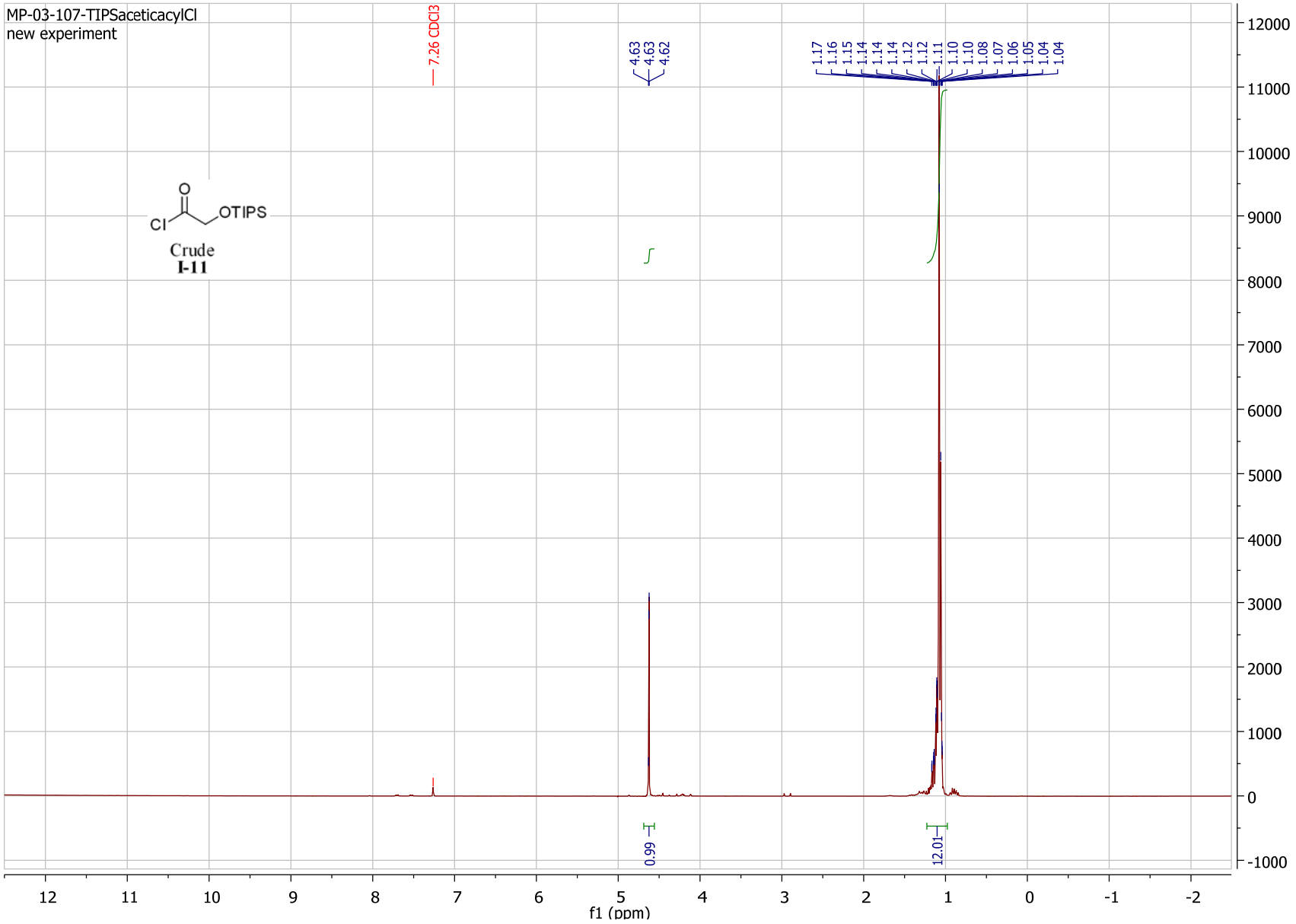
MP-03-107-TIPSaceticacylCl
new experiment
7.26 CDCl3
4.63
4.63
4.62
1.17
1.16
1.15
1.14
1.14
1.14
1.12
1.12
1.11
1.10
1.10
1.08
1.07
1.06
1.05
1.04
1.04
Cl
O
OTIPS
Crude
I-11
0.99
12.01
f1 (ppm)

C

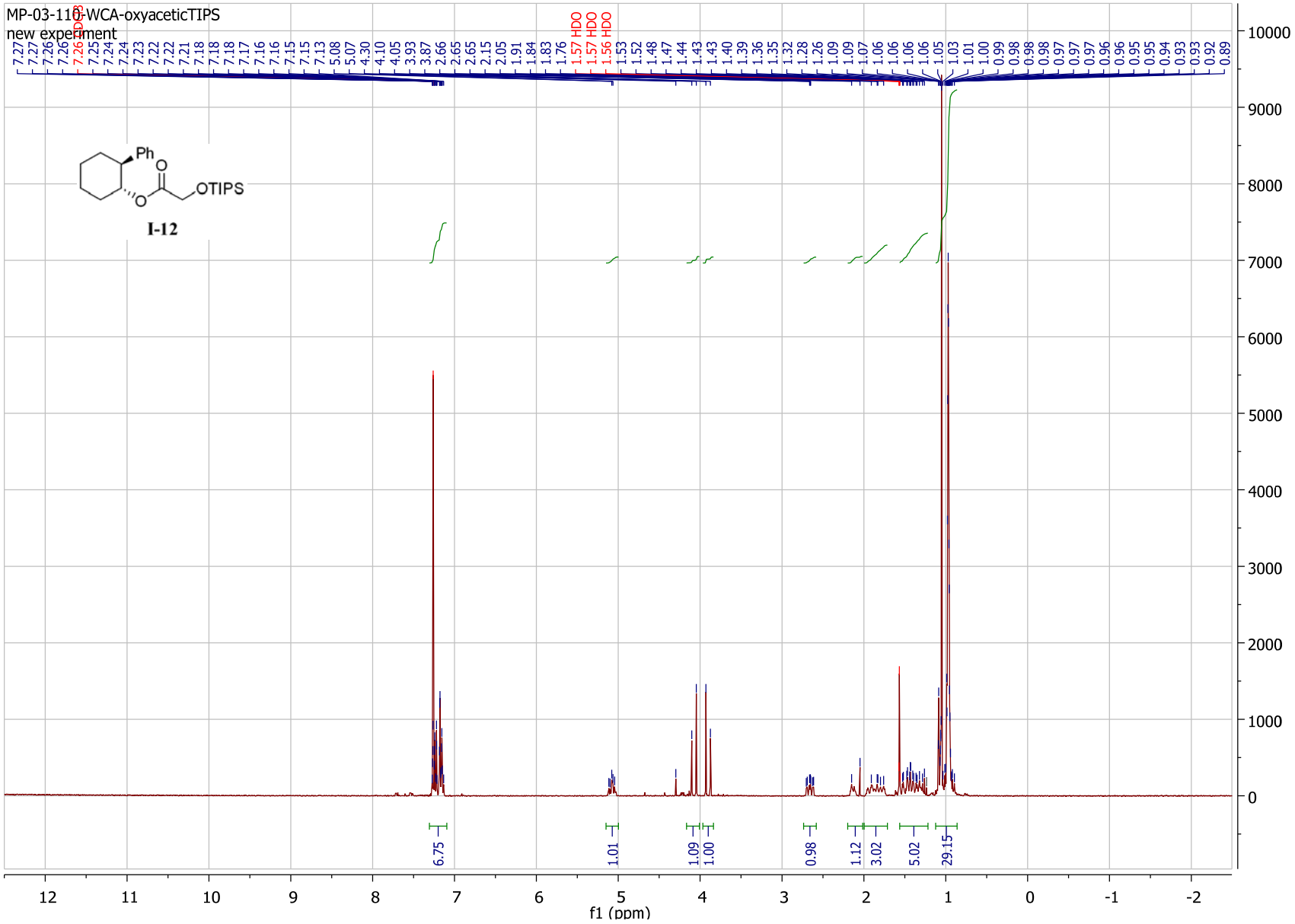
MP-03-110-WCA-oxyaceticTIPS
new experiment
Ph
O
O
OTIPS
I-12
HDO
HDO
HDO
HDO
6.75
1.01
1.09
1.00
0.98
1.12
3.02
5.02
29.15
f1 (ppm)

D

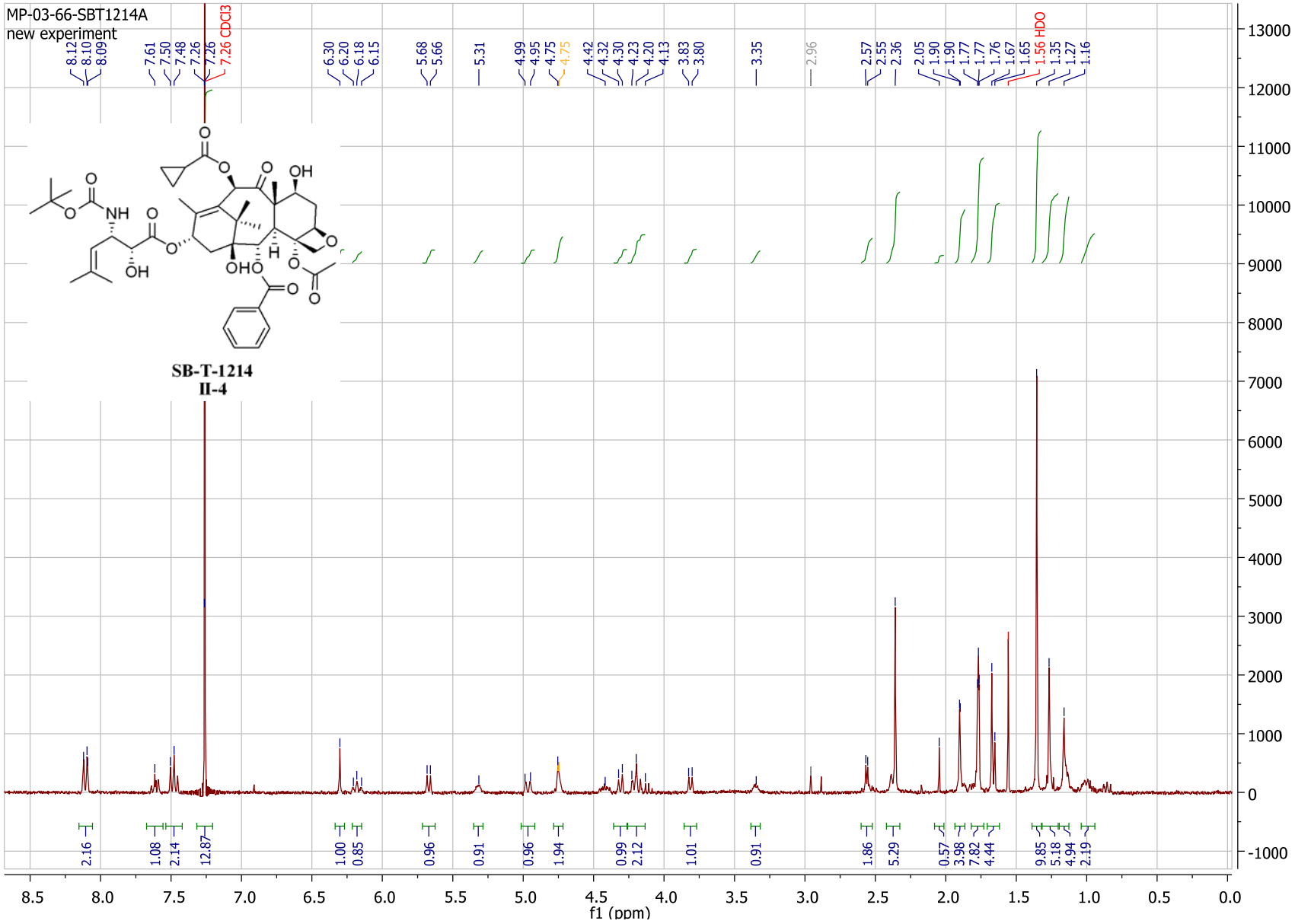

E

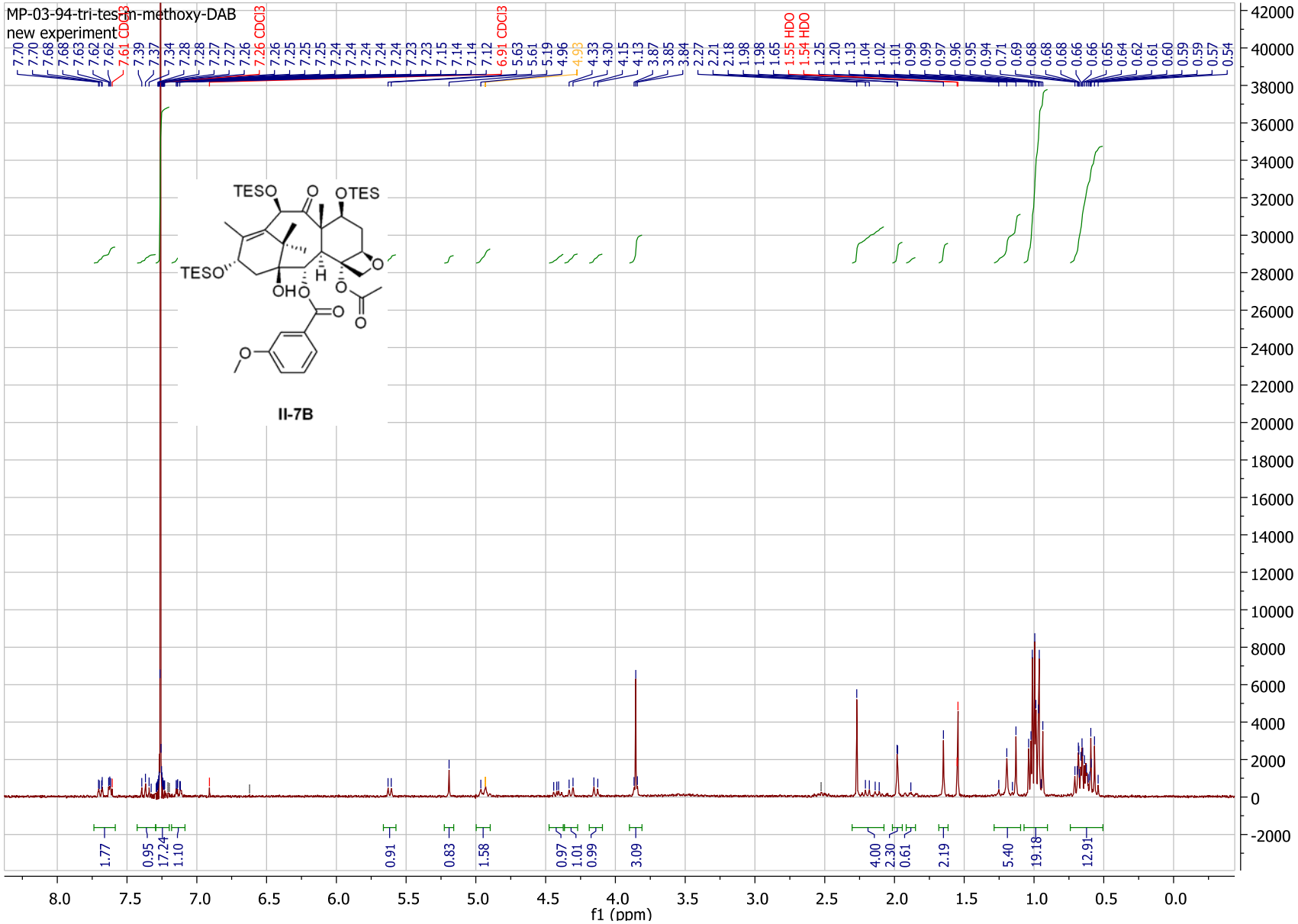
MP-03-94-tri-tes-m-methoxy-DAB
new experiment
TESO
OTES
TESO
OH
H
II-7B
f1 (ppm)

F

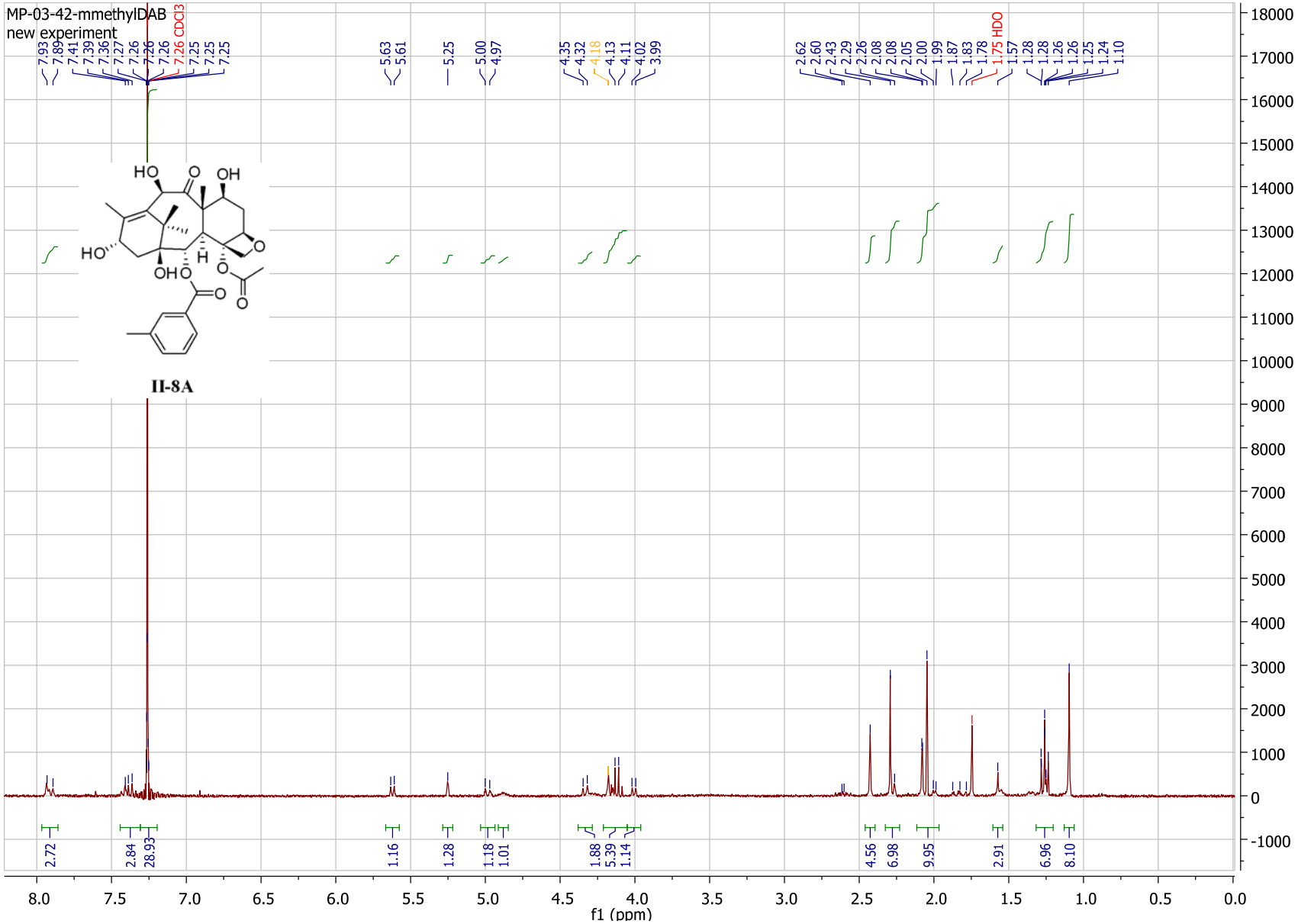
MP-03-42-mmethylDAB
new experiment
7.93 7.89 7.41 7.39 7.36 7.27 7.26 7.26 7.26 CDCl3 7.25 7.25 7.25
5.63 5.61 5.25 5.00 4.97 4.35 4.32 4.18 4.13 4.11 4.02 3.99
2.62 2.60 2.43 2.29 2.26 2.08 2.08 2.05 2.00 1.99 1.87 1.83 1.78 1.75 HDO 1.57 1.28 1.28 1.26 1.26 1.25 1.24 1.10
II-8A
2.72 2.84 28.93 1.16 1.28 1.18 1.01 1.88 5.39 1.14 4.56 6.98 9.95 2.91 6.96 8.10
f1 (ppm)

G

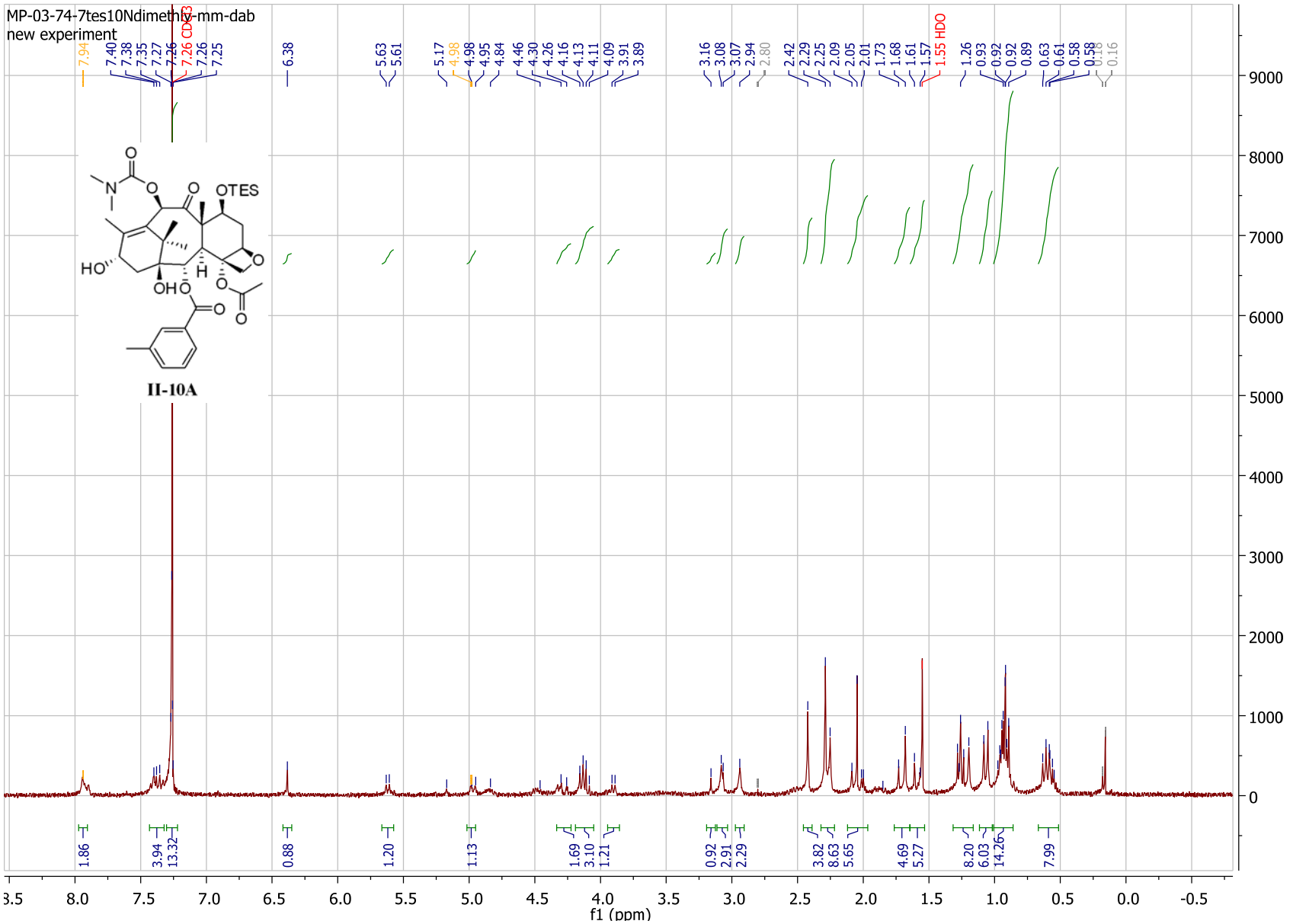

H

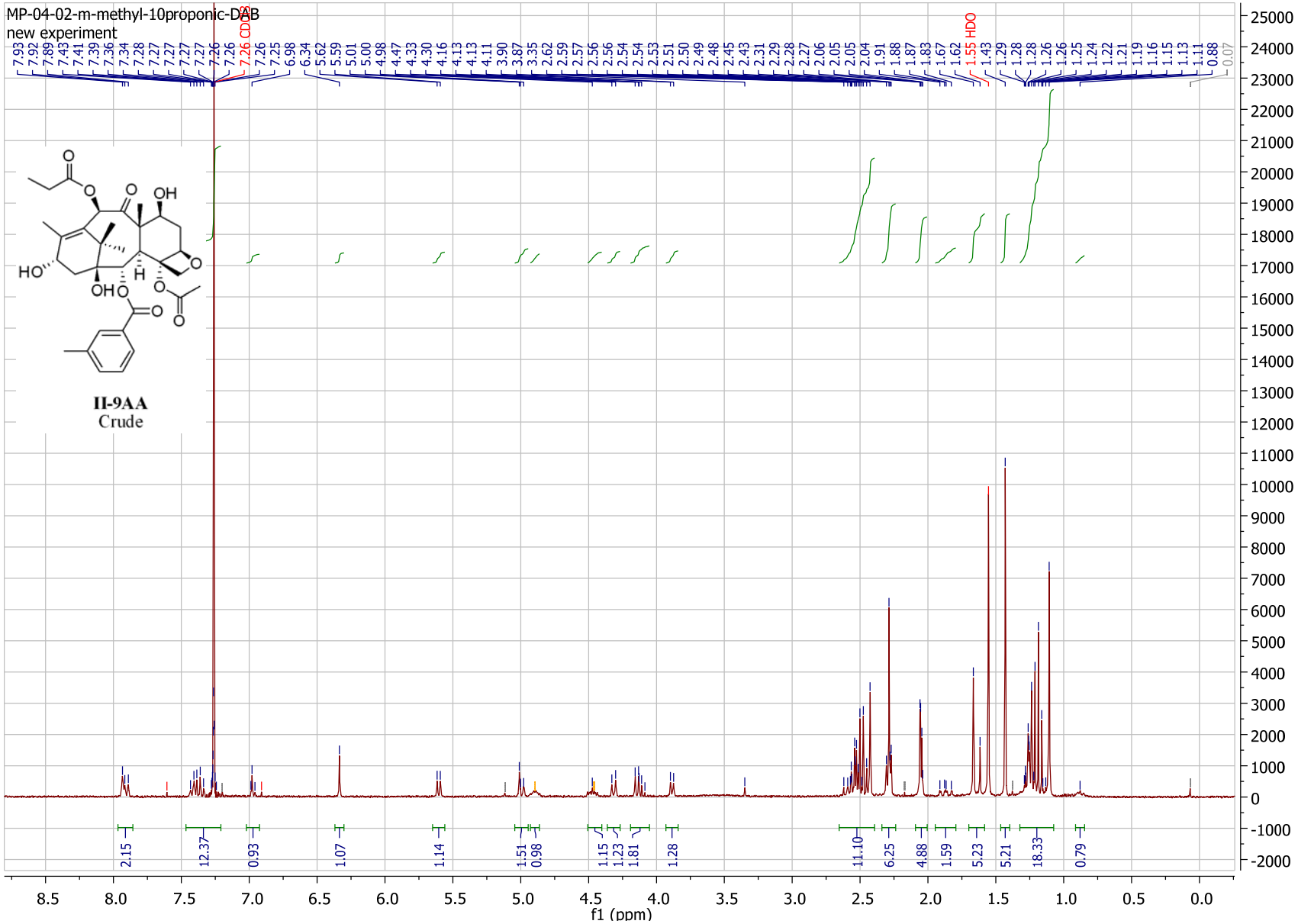
MP-04-02-m-methyl-10proponic-DAB
new experiment
II-9AA
Crude
f1 (ppm)

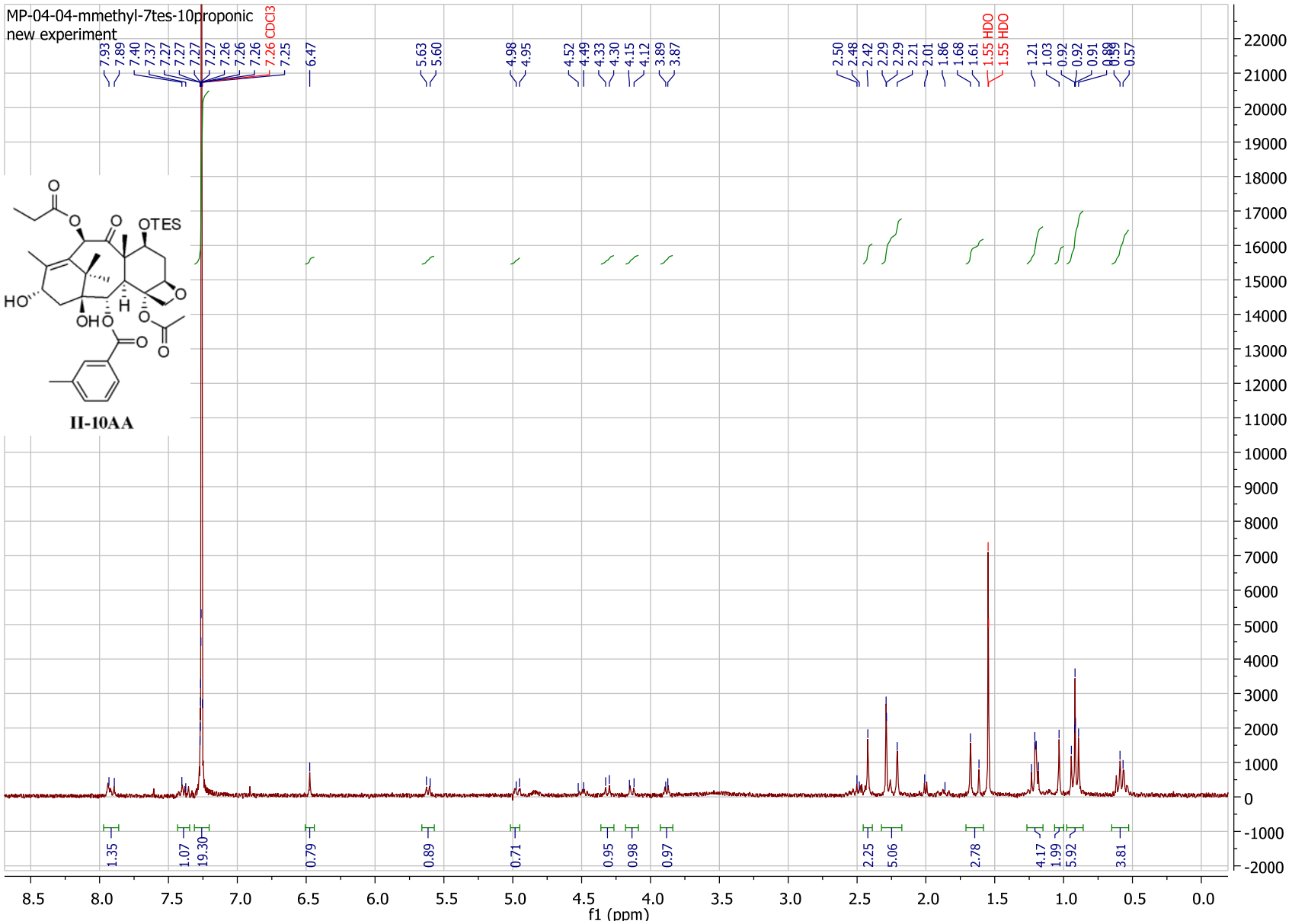
MP-04-04-mmethyl-7tes-10proponic
new experiment
II-10AA
f1 (ppm)

J

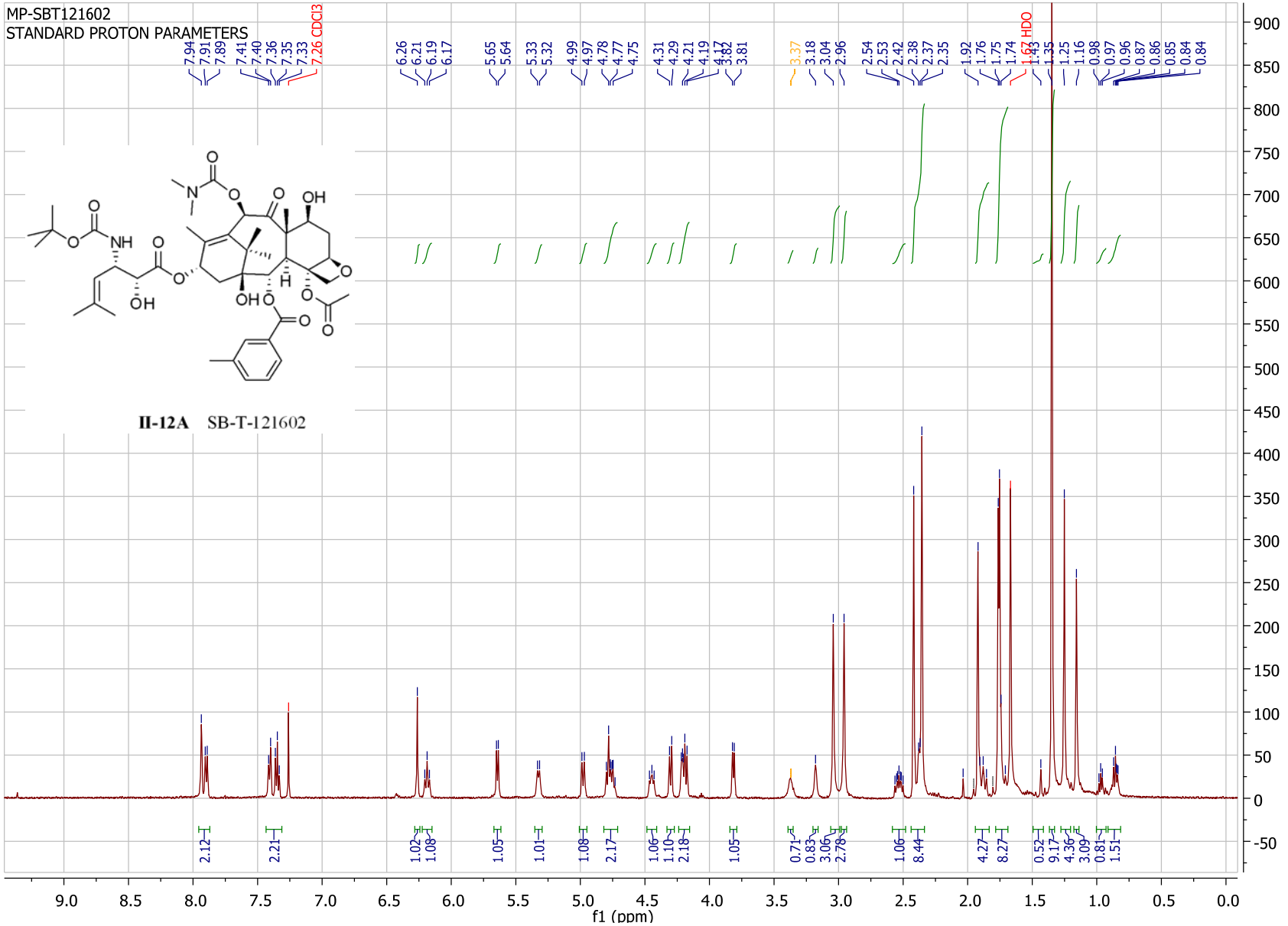
MP-SBT121602
STANDARD PROTON PARAMETERS
II-12A SB-T-121602
f1 (ppm)

K

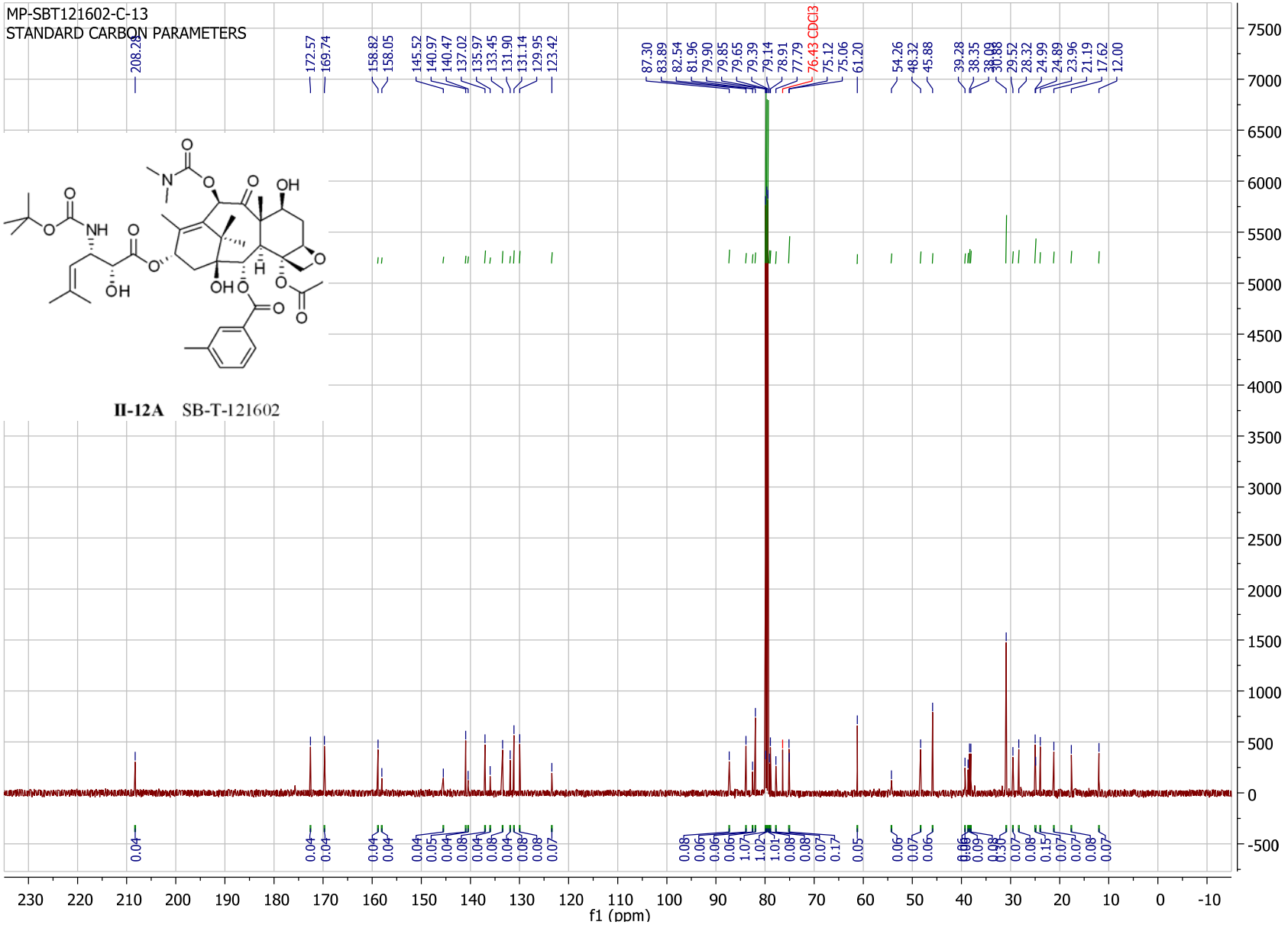
MP-SBT121602-C-13
STANDARD CARBON PARAMETERS
208.28
172.57
169.74
158.82
158.05
145.52
140.97
140.47
137.02
135.97
133.45
131.90
131.14
129.95
123.42
87.30
83.89
82.54
81.96
79.90
79.85
79.65
79.39
79.14
78.91
77.79
76.43 CDCl3
75.12
75.06
61.20
54.26
48.32
45.88
39.28
38.35
38.08
30.88
29.52
28.32
24.99
24.89
23.96
21.19
17.62
12.00
II-12A SB-T-121602
f1 (ppm)

L

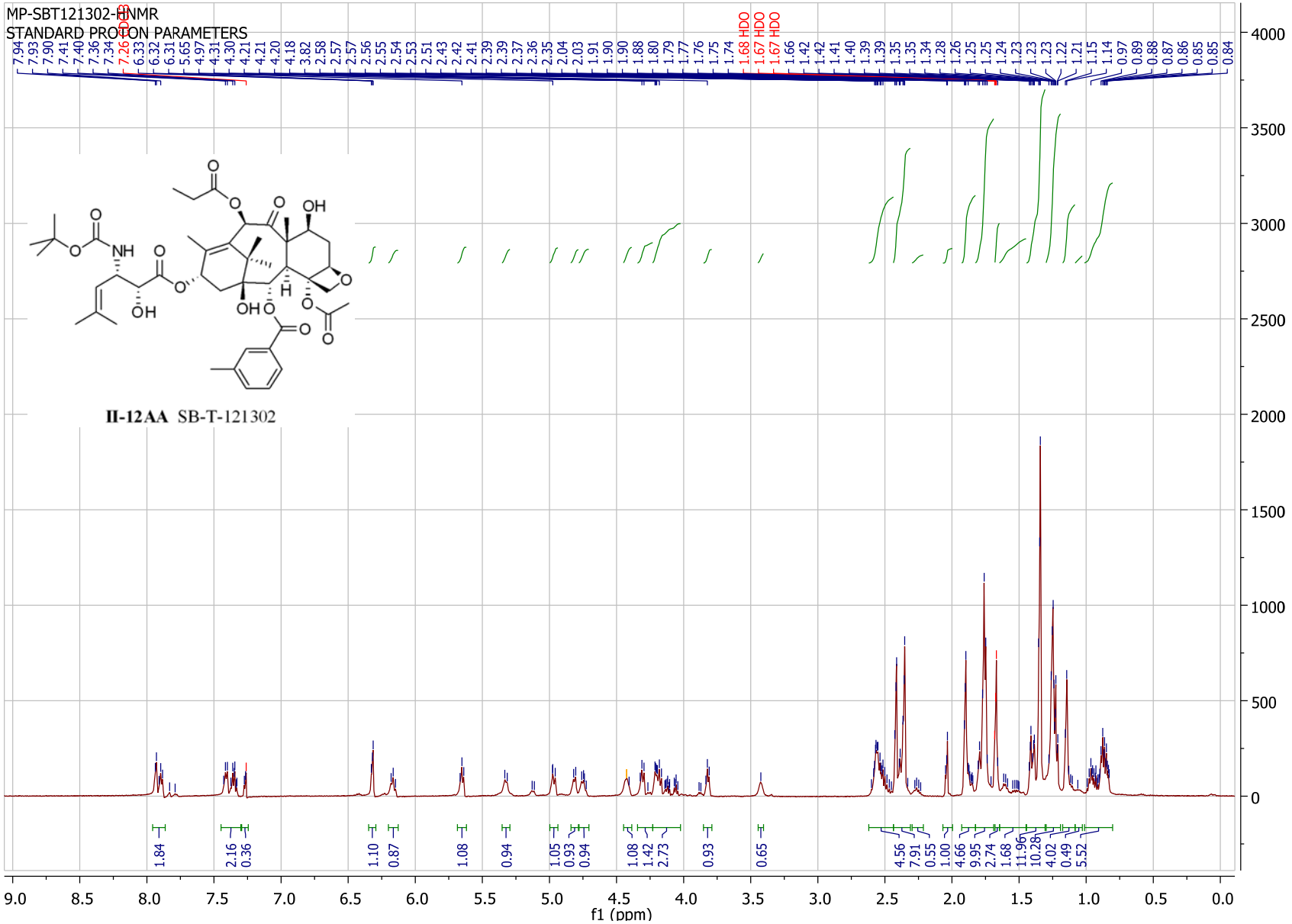
MP-SBT121302-HNMR
STANDARD PROTON PARAMETERS
II-12AA SB-T-121302
f1 (ppm)

M

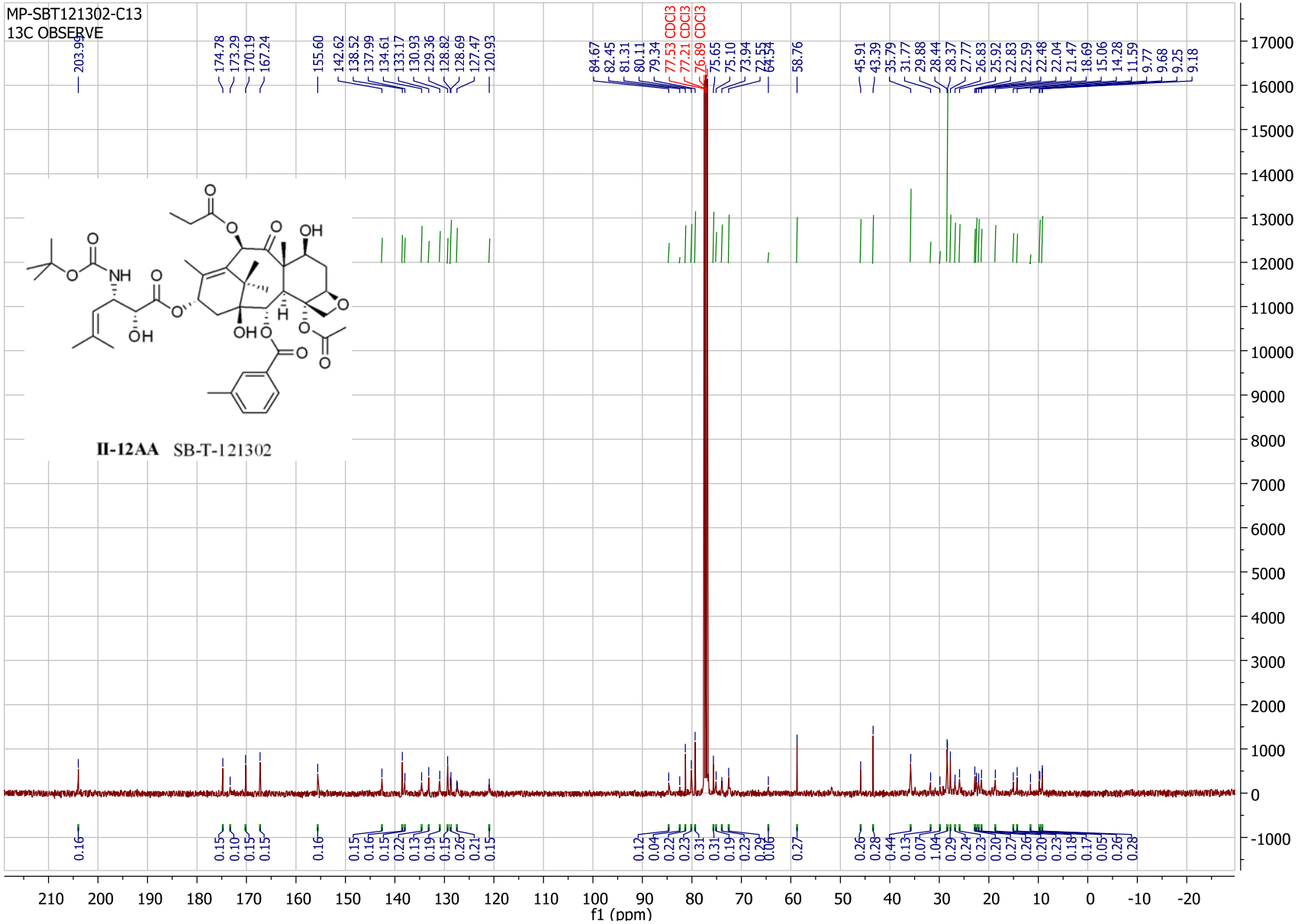
MP-SBT121302-C13
13C OBSERVE
II-12AA SB-T-121302
f1 (ppm)

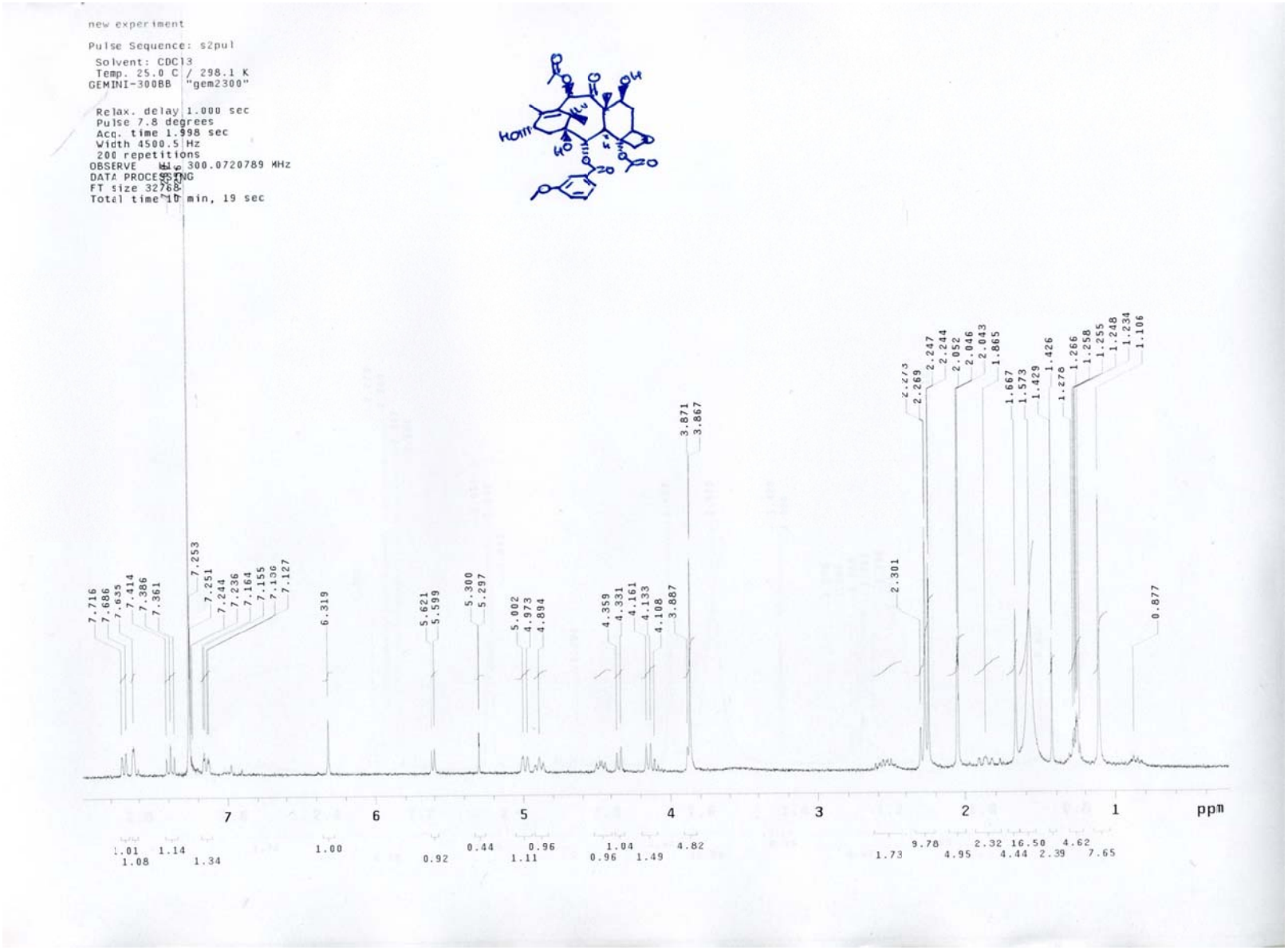
new experiment
Pulse Sequence: s2pul
Solvent: CDCl3
Temp. 25.0 C / 298.1 K
GEMINI-300BB "gem2300"
Relax. delay 1.000 sec
Pulse 7.8 degrees
Acq. time 1.998 sec
Width 4500.5 Hz
200 repetitions
OBSERVE H1, 300.0720789 MHz
DATA PROCESSING
FT size 32768
Total time 10 min, 19 sec
7.716
7.686
7.635
7.414
7.386
7.361
7.253
7.251
7.244
7.236
7.164
7.155
7.136
7.127
6.319
5.621
5.599
5.300
5.297
5.002
4.973
4.894
4.359
4.331
4.161
4.133
4.108
3.887
3.871
3.867
2.301
2.269
2.247
2.244
2.052
2.046
2.043
1.865
1.667
1.573
1.429
1.426
1.278
1.266
1.258
1.255
1.248
1.234
1.106
0.877
7
6
5
4
3
2
1
ppm
1.01
1.08
1.14
1.34
1.00
0.92
0.44
0.96
1.11
1.04
0.96
1.49
4.82
1.73
9.78
4.95
2.32
4.44
16.50
2.39
4.62
7.65

O

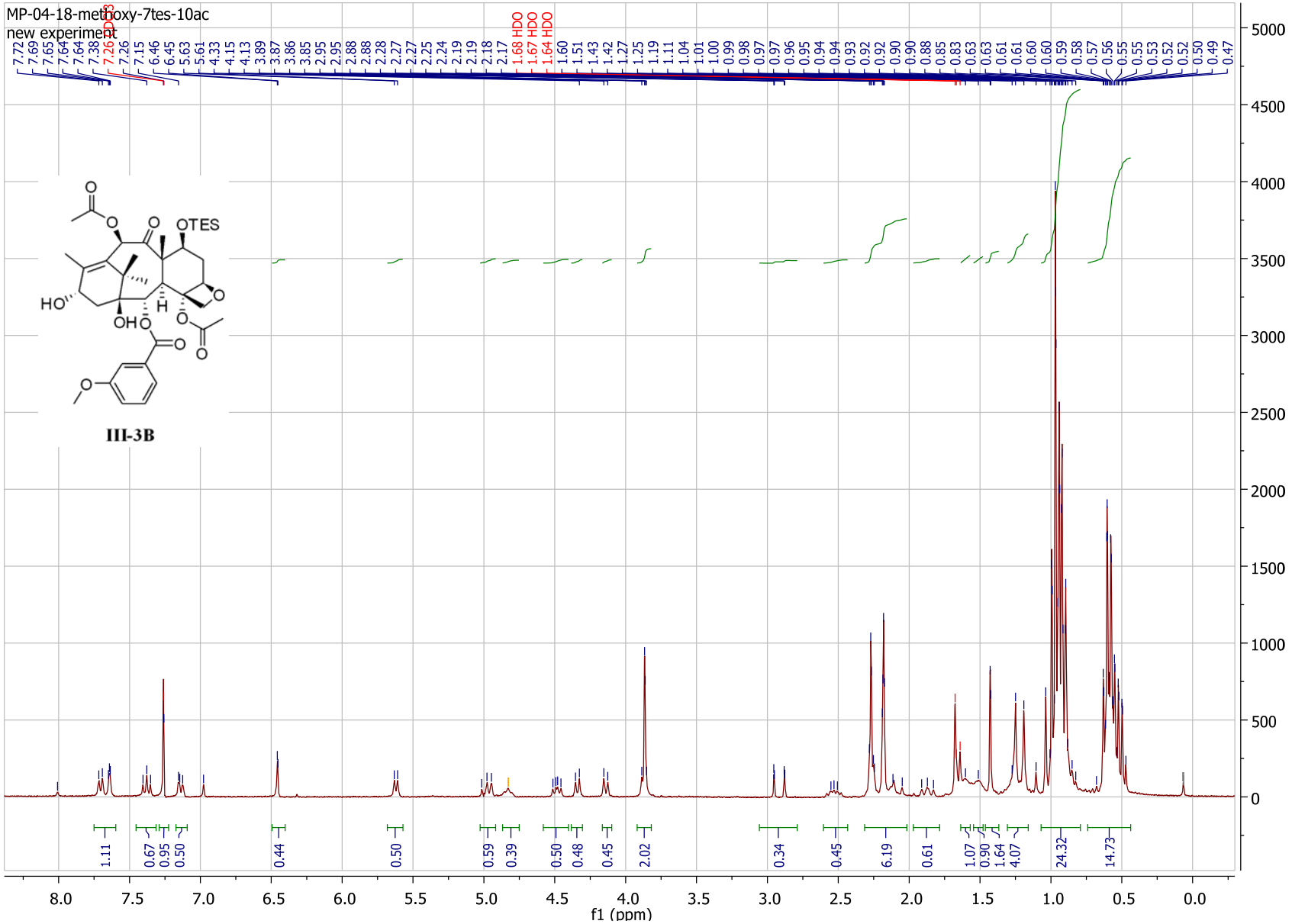
MP-04-18-methoxy-7tes-10ac
new experiment
III-3B
f1 (ppm)

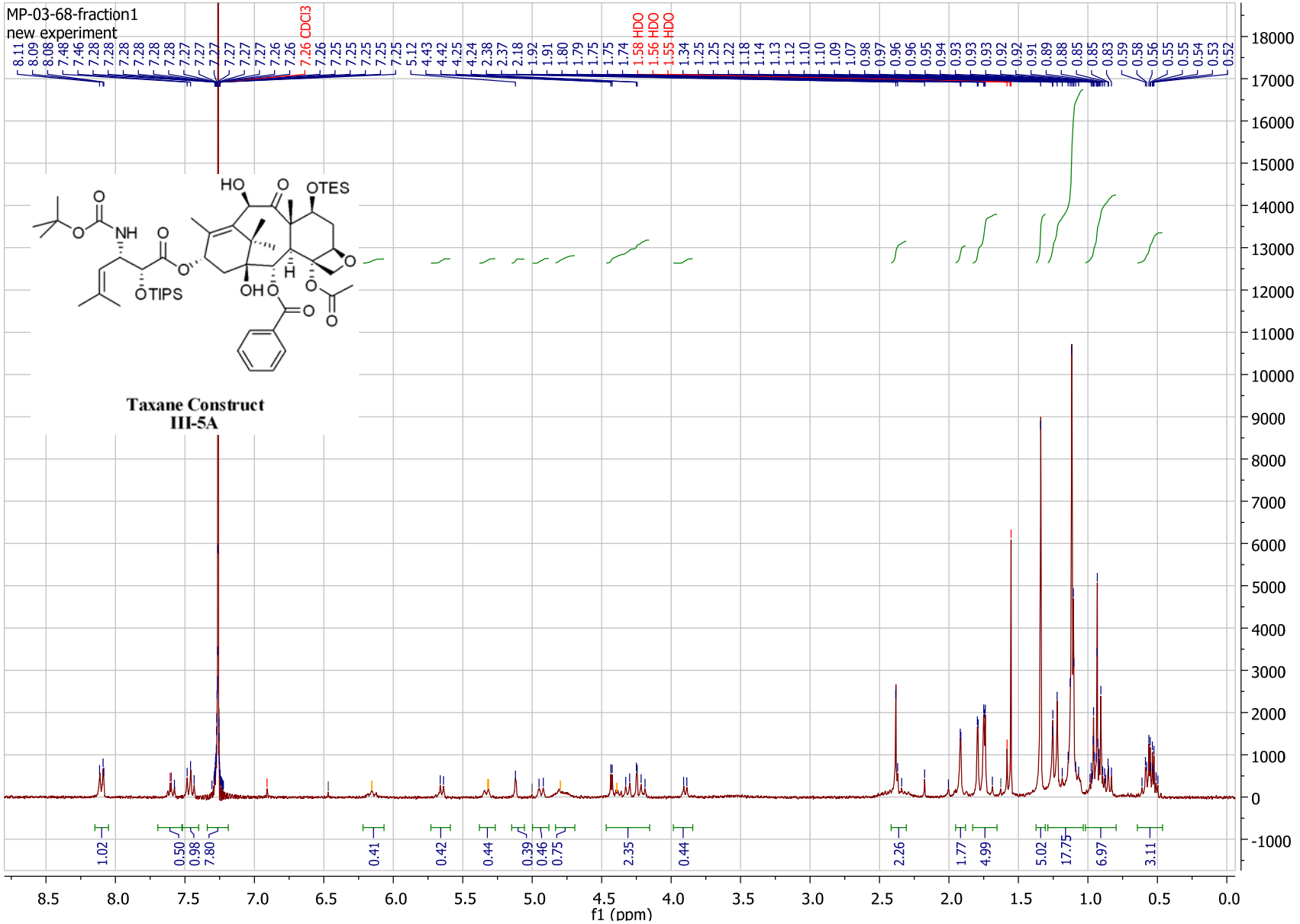
MP-03-68-fraction1
new experiment
Taxane Construct
III-5A
f1 (ppm)

Q

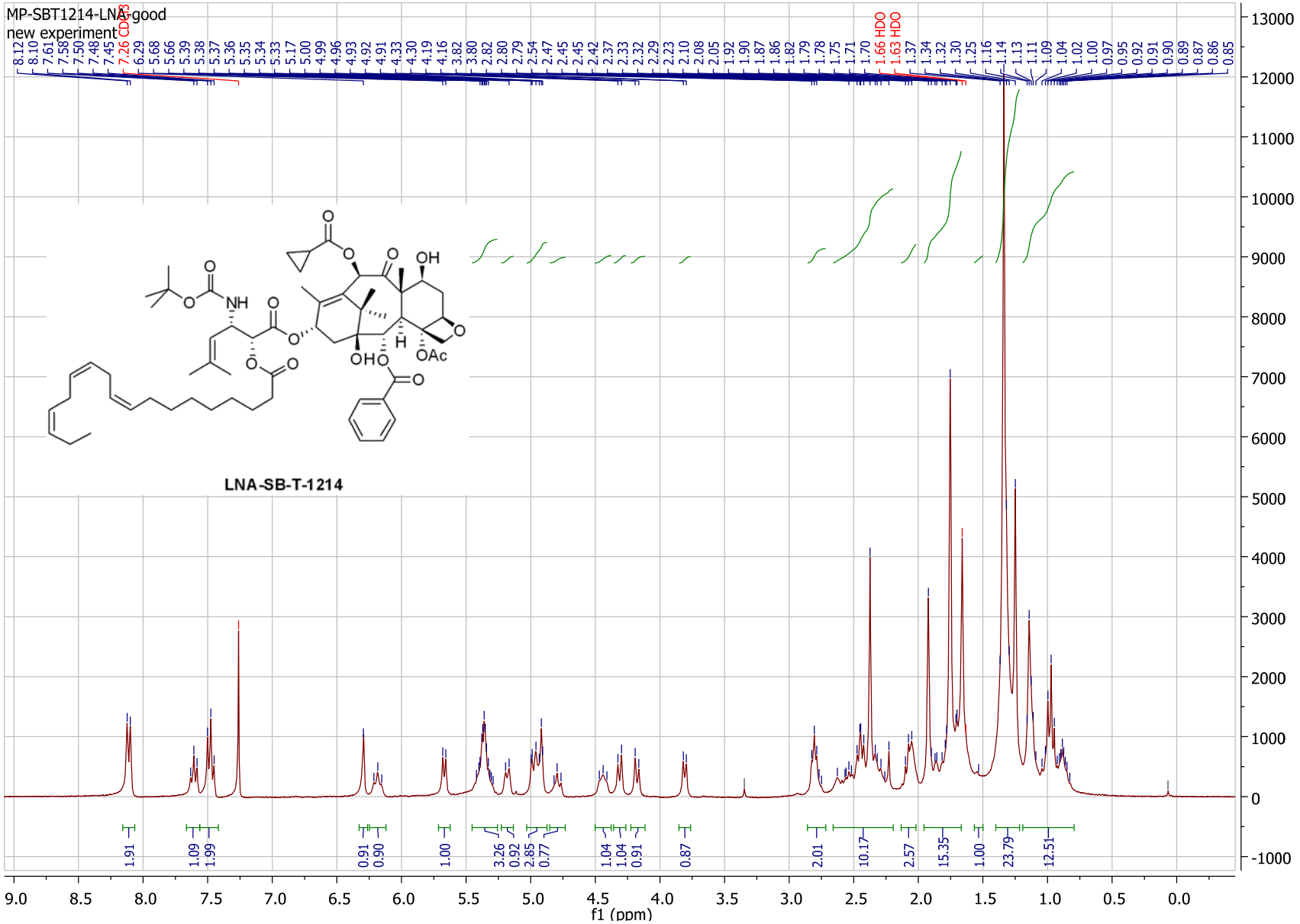

R

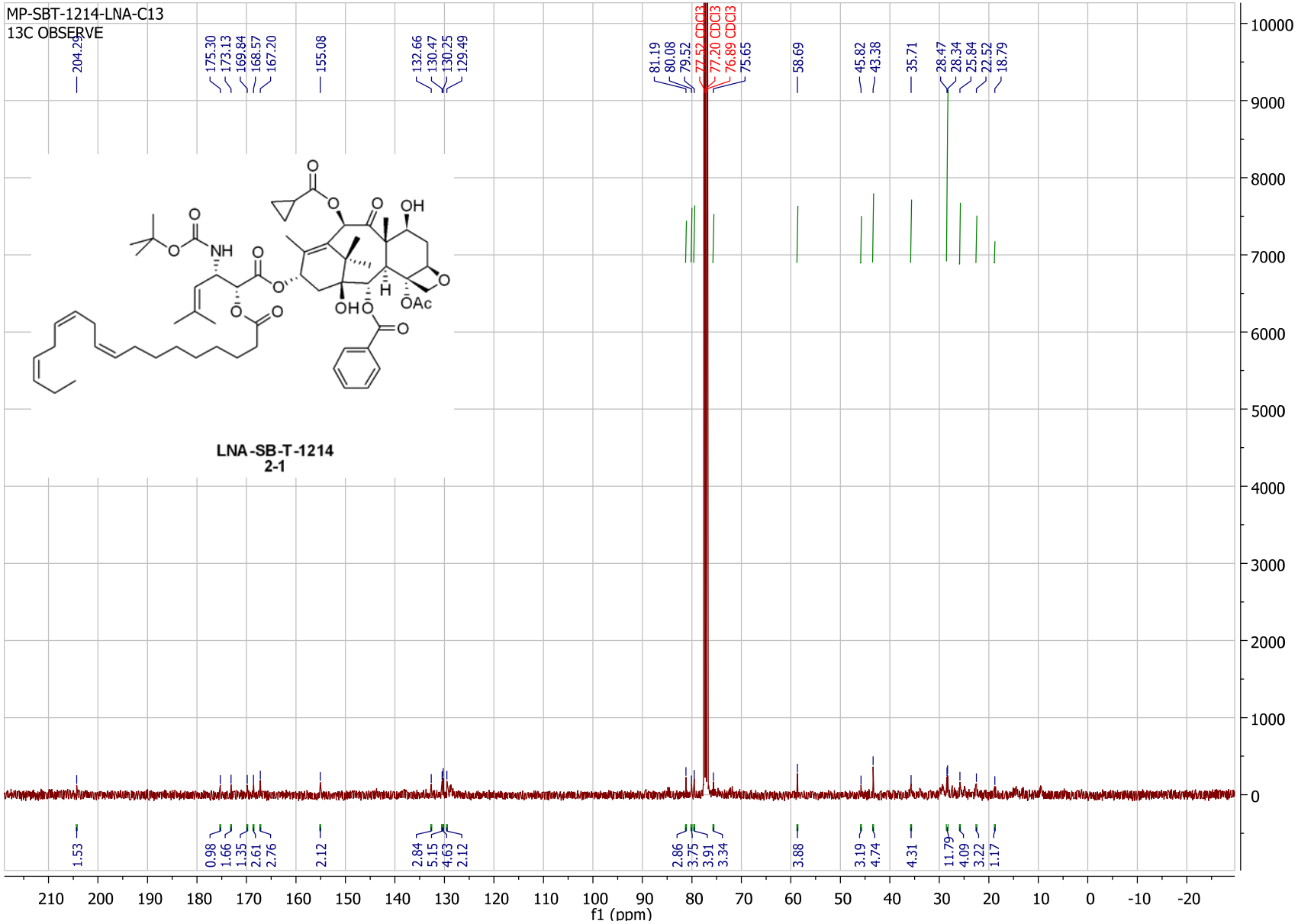
MP-SBT-1214-LNA-C13
13C OBSERVE
204.29
175.30
173.13
169.84
168.57
167.20
155.08
132.66
130.47
130.25
129.49
81.19
80.08
79.52
77.52 CDCl3
77.20 CDCl3
76.89 CDCl3
75.65
58.69
45.82
43.38
35.71
28.47
28.34
25.84
22.52
18.79
LNA-SB-T-1214
2-1
1.53
0.98
1.66
1.35
2.61
2.76
2.12
2.84
5.15
4.63
2.12
2.86
3.75
3.91
3.34
3.88
3.19
4.74
4.31
11.79
4.09
3.22
1.17
f1 (ppm)

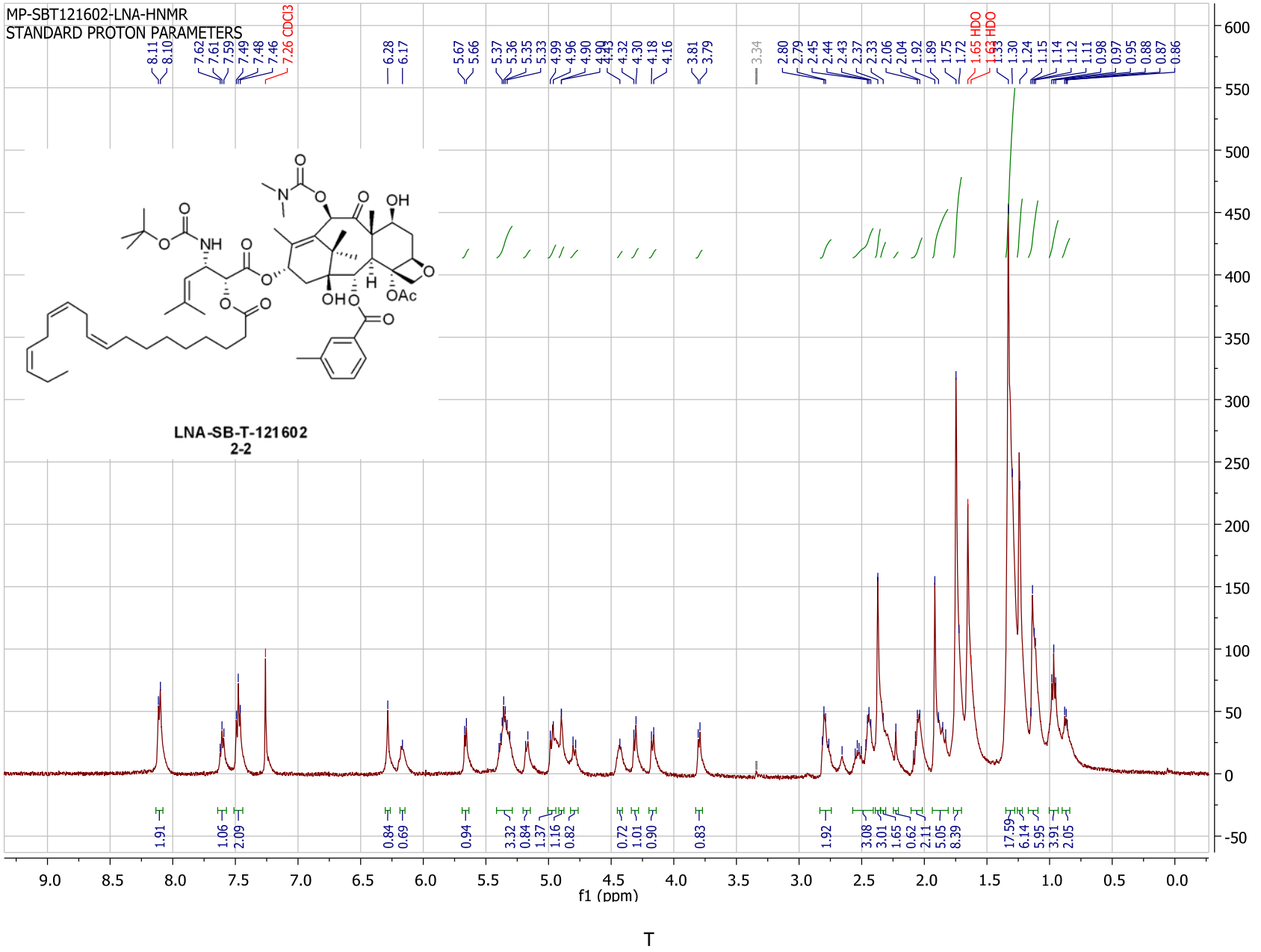
MP-SBT121602-LNA-HNMR
STANDARD PROTON PARAMETERS
LNA-SB-T-121602
2-2
f1 (ppm)
T

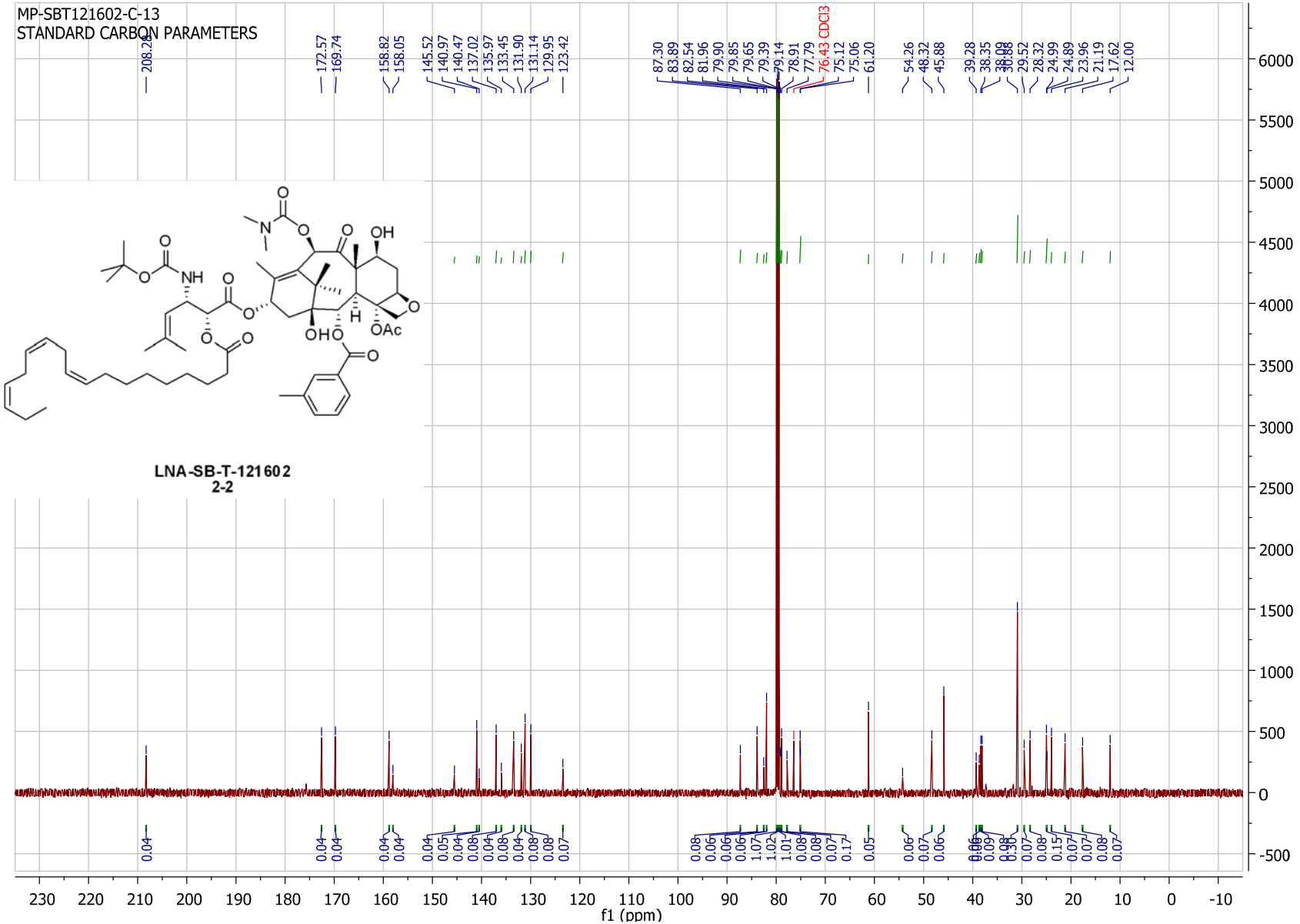
MP-SBT121602-C-13
STANDARD CARBON PARAMETERS
LNA-SB-T-121602
2-2
f1 (ppm)

U

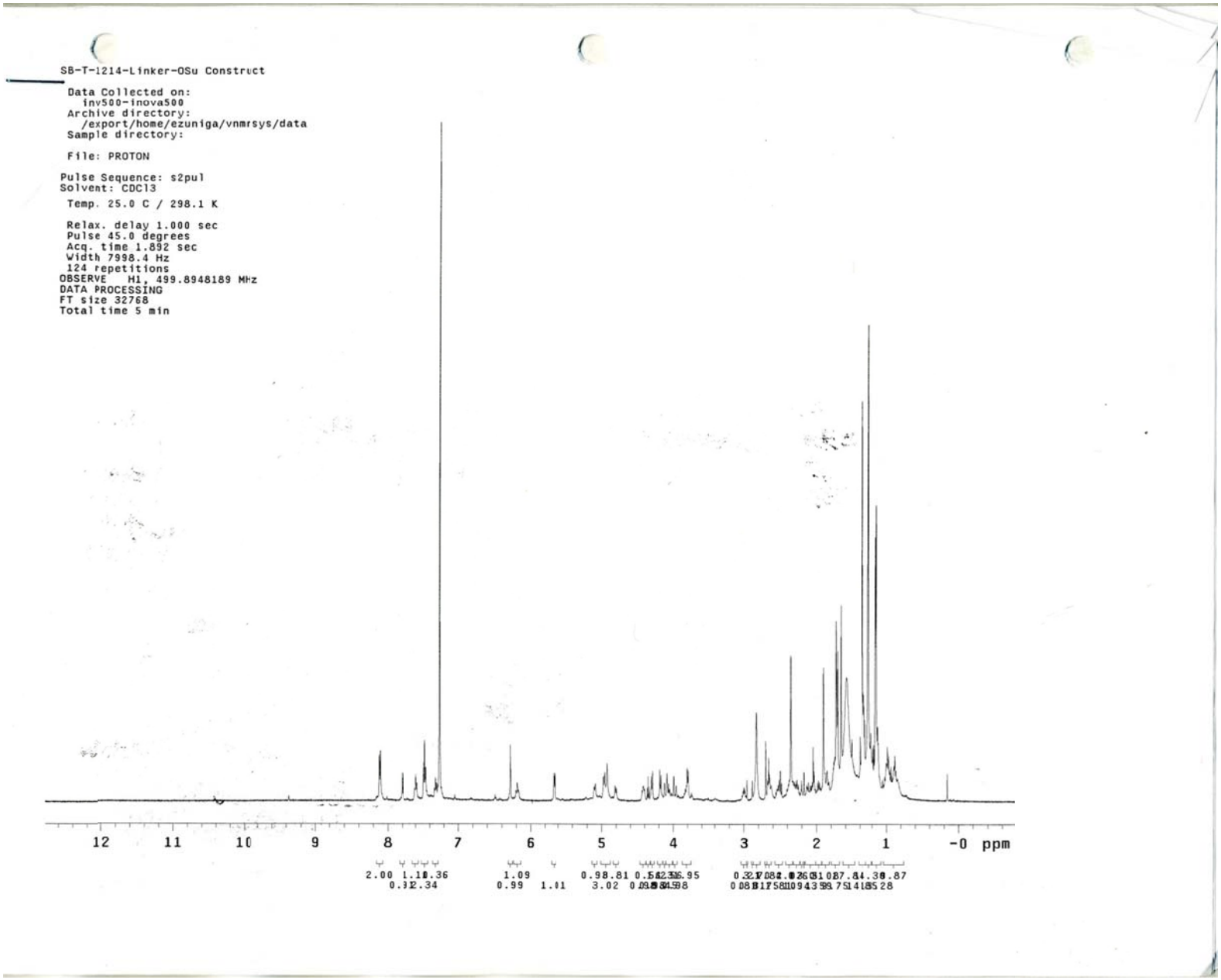
SB-T-1214-Linker-OSu Construct
Data Collected on:
inv500-inova500
Archive directory:
/export/home/ezuniga/vnmrsys/data
Sample directory:
File: PROTON
Pulse Sequence: s2pul
Solvent: CDCl3
Temp. 25.0 C / 298.1 K
Relax. delay 1.000 sec
Pulse 45.0 degrees
Acq. time 1.892 sec
Width 7998.4 Hz
124 repetitions
OBSERVE H1, 499.8948189 MHz
DATA PROCESSING
FT size 32768
Total time 5 min
12
11
10
9
8
7
6
5
4
3
2
1
-0 ppm

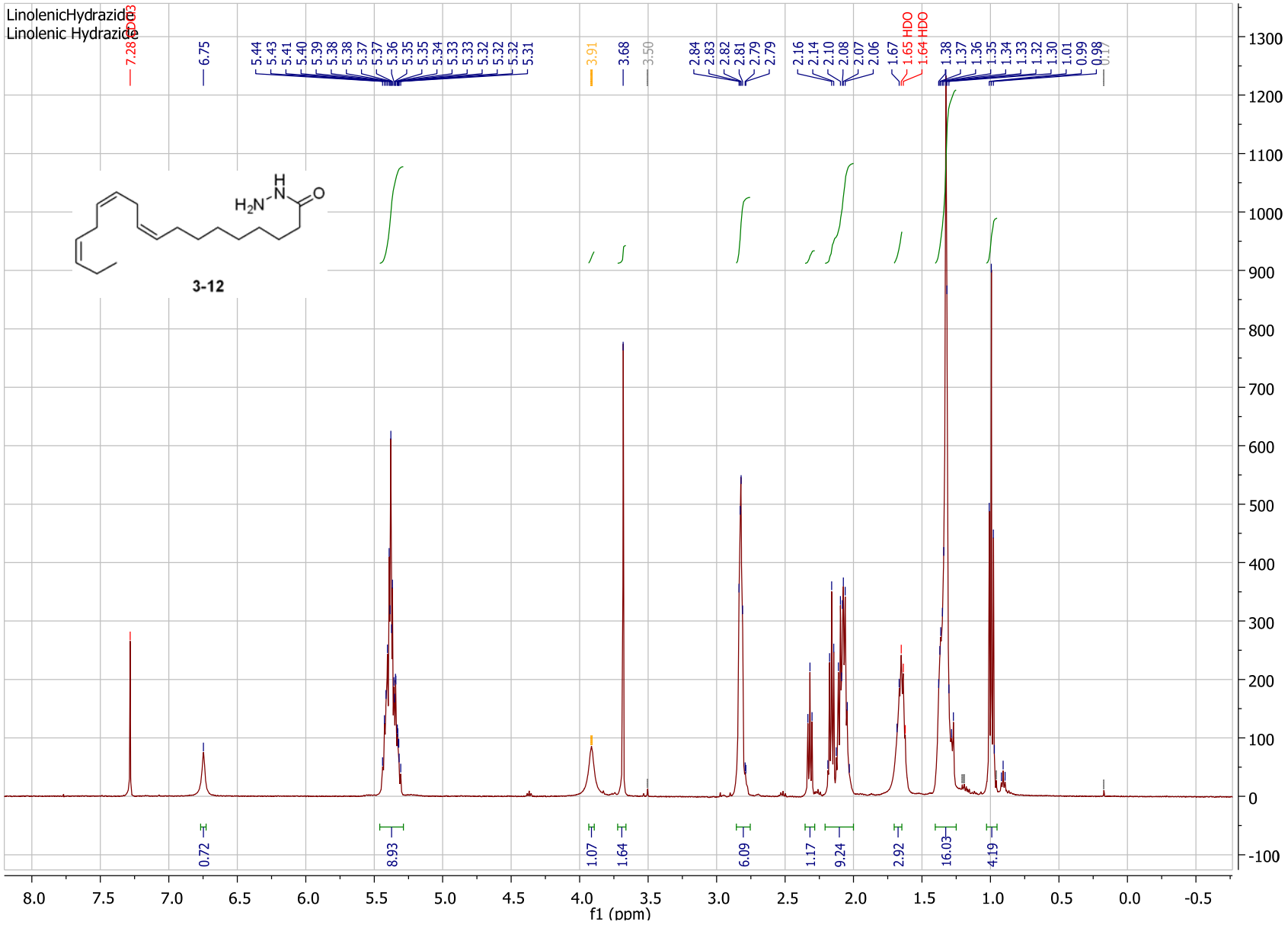

W

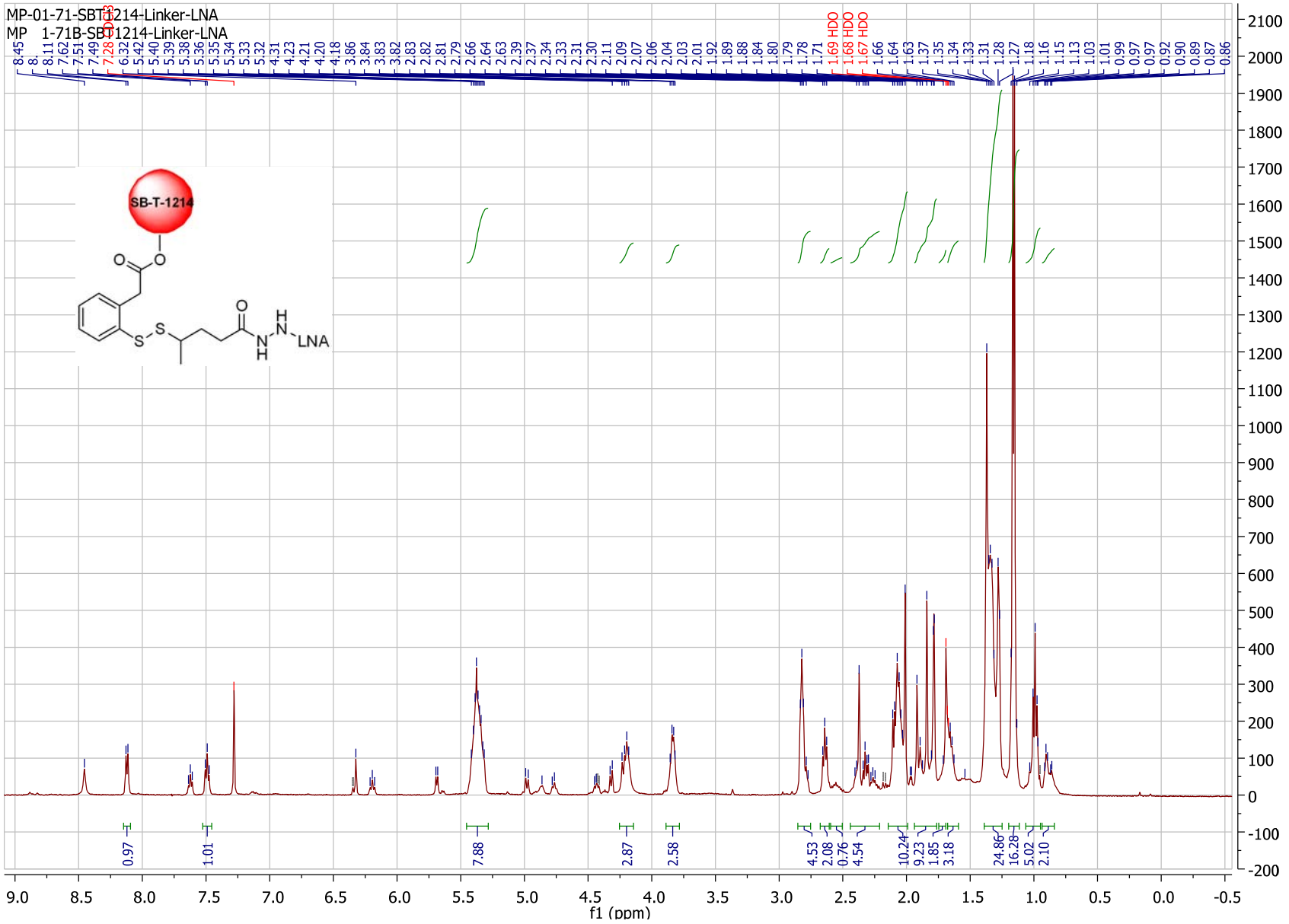
MP-01-71-SBT1214-Linker-LNA
MP 1-71B-SBT1214-Linker-LNA
SB-T-1214
LNA
HDO
f1 (ppm)

X

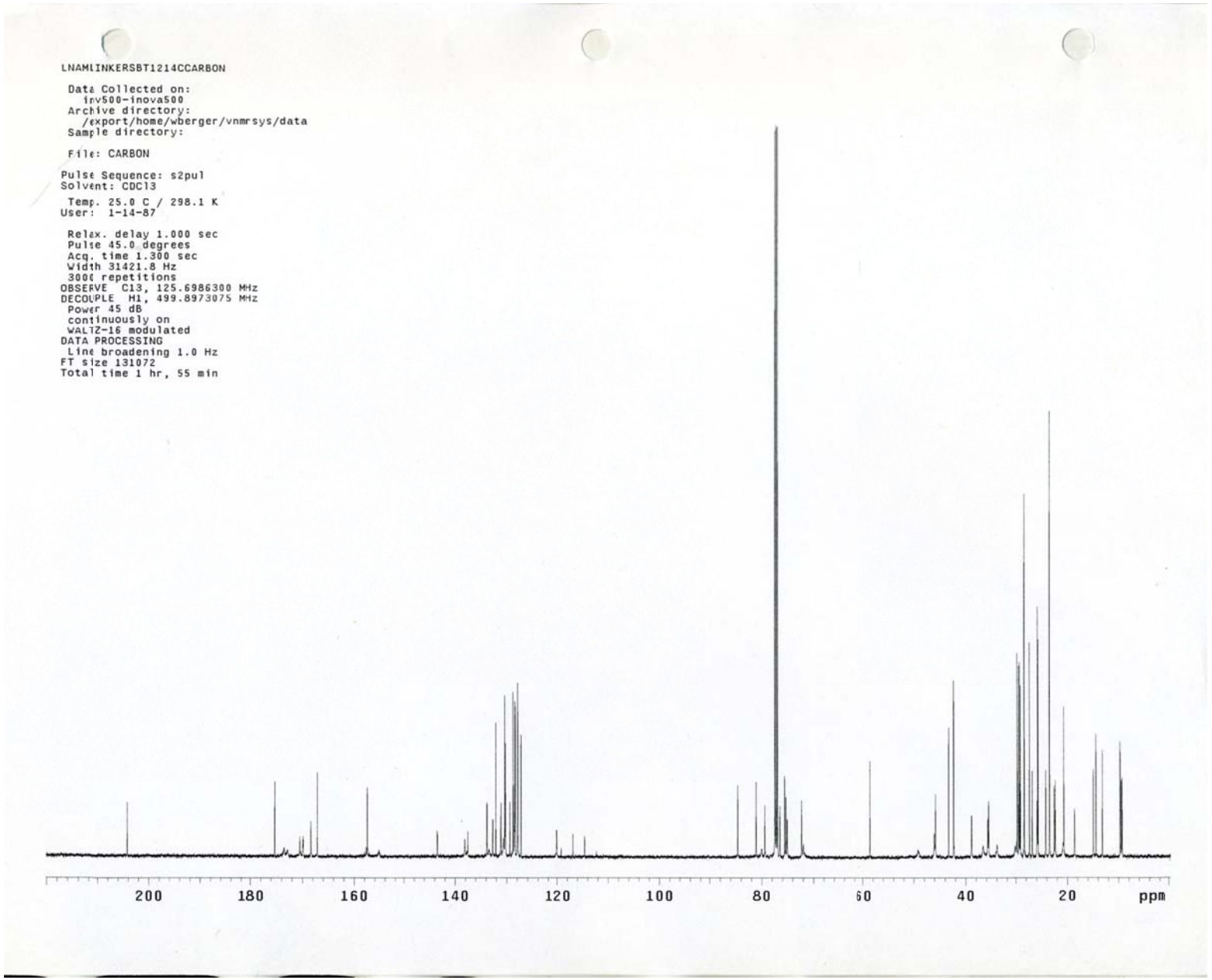
LNAMLINKERSBT1214CCARBON
Data Collected on:
inv500-inova500
Archive directory:
/export/home/wberger/vnmrsys/data
Sample directory:
File: CARBON
Pulse Sequence: s2pul
Solvent: CDCl3
Temp. 25.0 C / 298.1 K
User: 1-14-87
Relax. delay 1.000 sec
Pulse 45.0 degrees
Acq. time 1.300 sec
Width 31421.8 Hz
3006 repetitions
OBSERVE C13, 125.6986300 MHz
DECOUPLE H1, 499.8973075 MHz
Power 45 dB
continuously on
WALTZ-16 modulated
DATA PROCESSING
Line broadening 1.0 Hz
FT size 131072
Total time 1 hr, 55 min
200
180
160
140
120
100
80
60
40
20
ppm

Y

HPLC DATA

SB-T-1214

254 nm

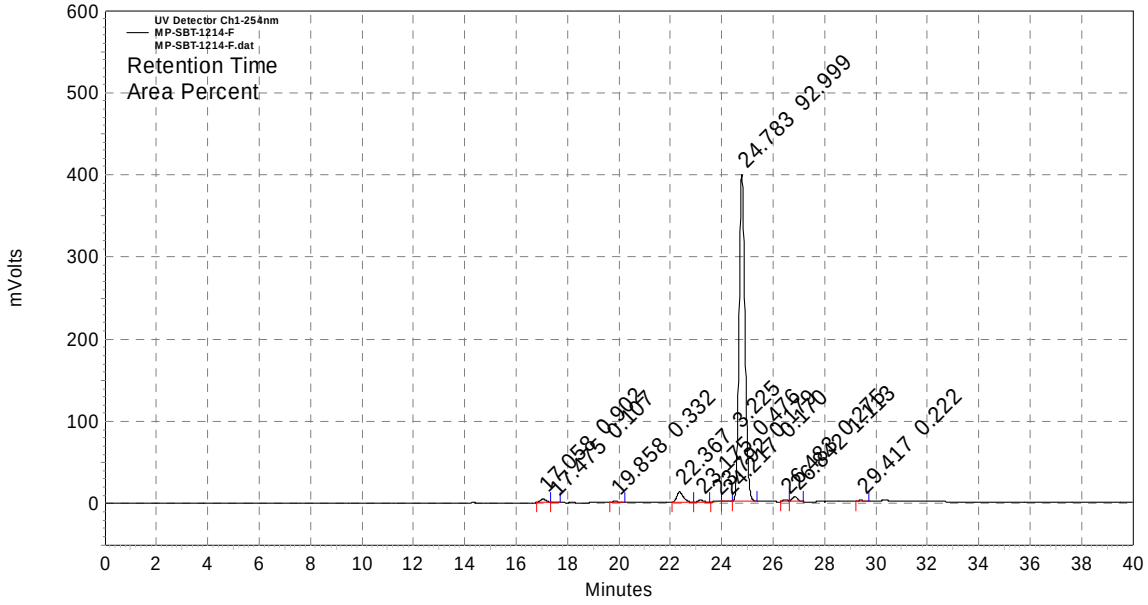

220 nm

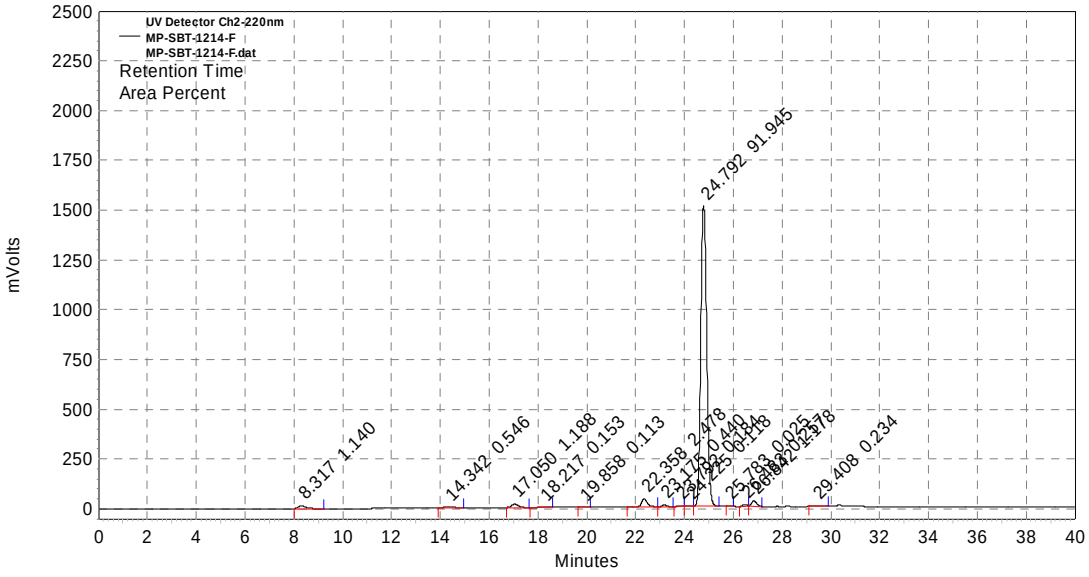

Z

SB-T-121602

254 nm

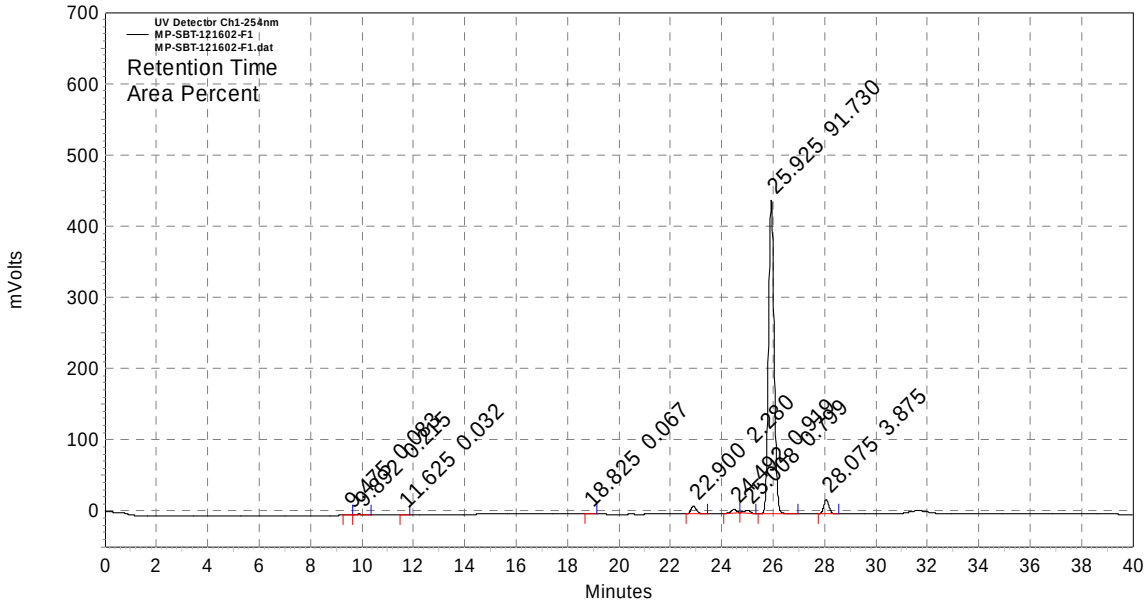

220 nm

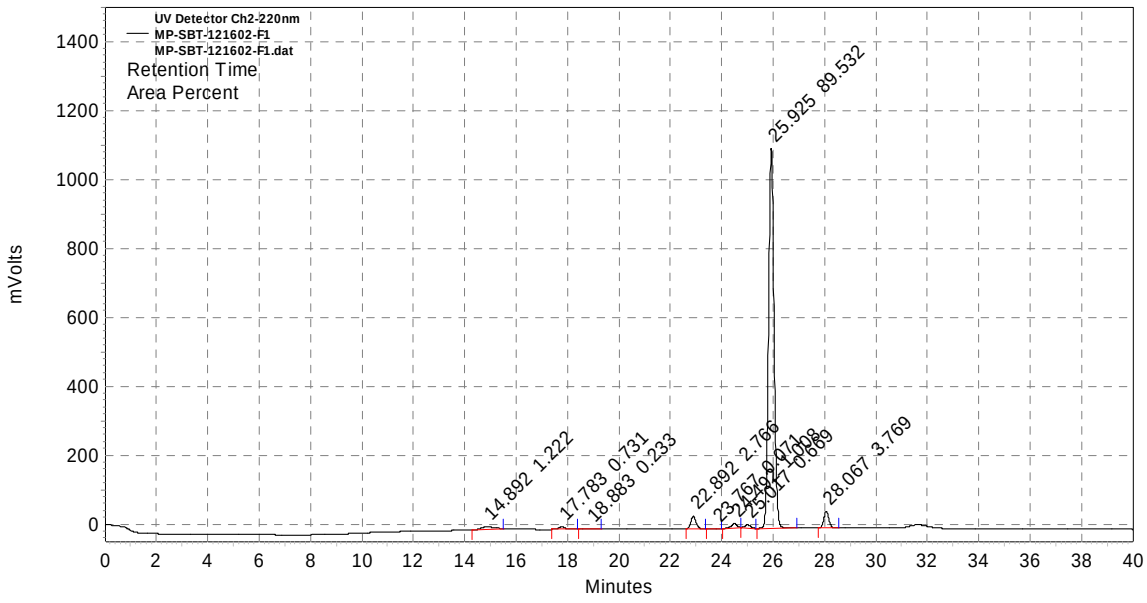

AA

SB-T-121302

254 nm

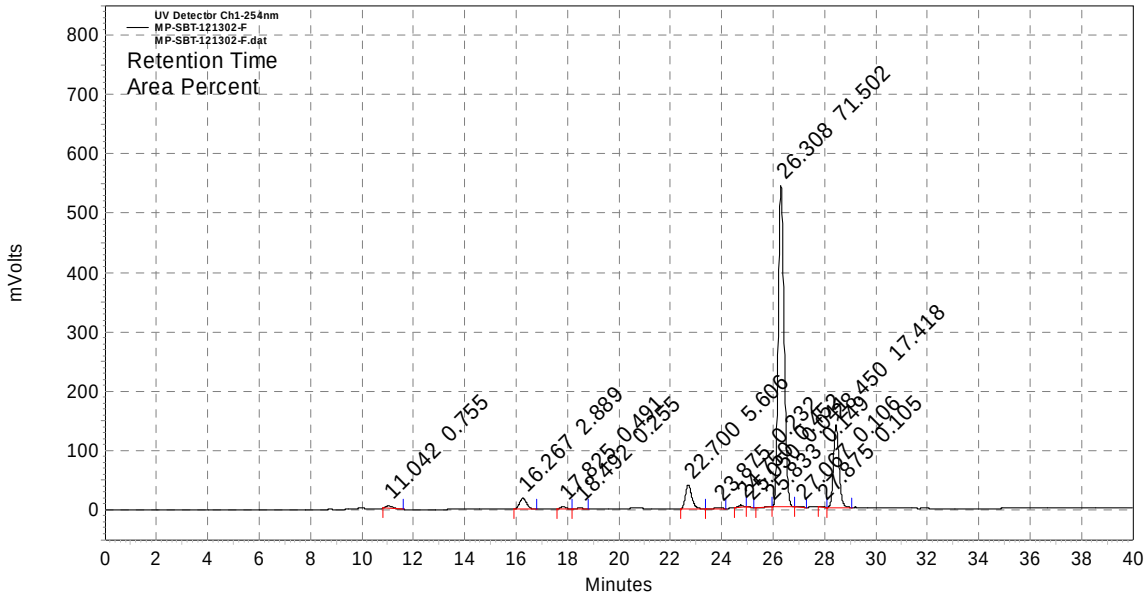

220 nm

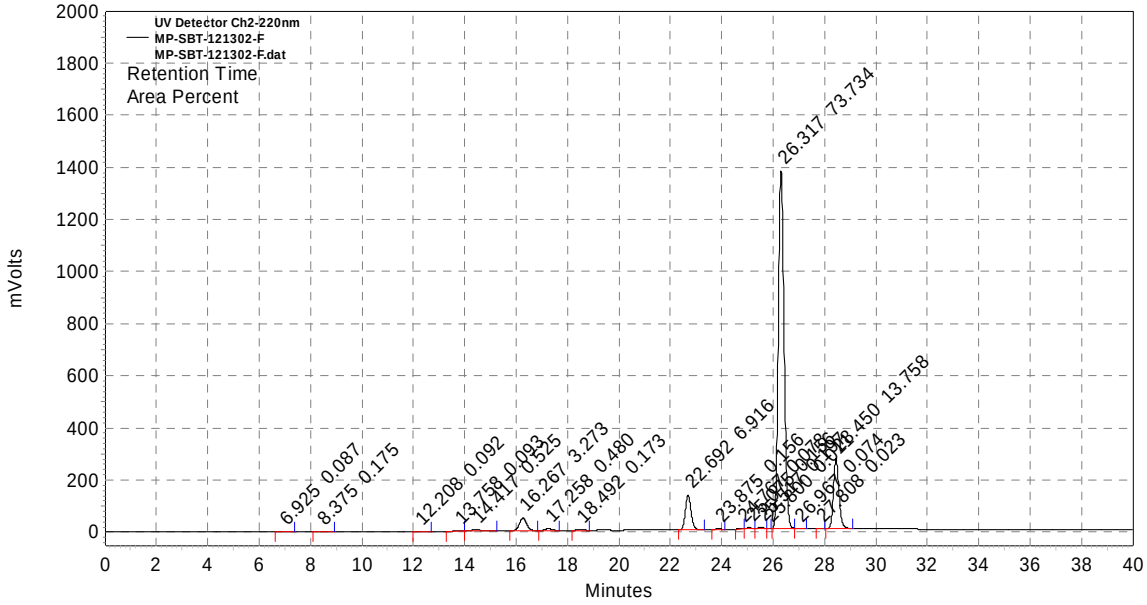

BB

LNA-Linker-SB-T-1214

254 nm

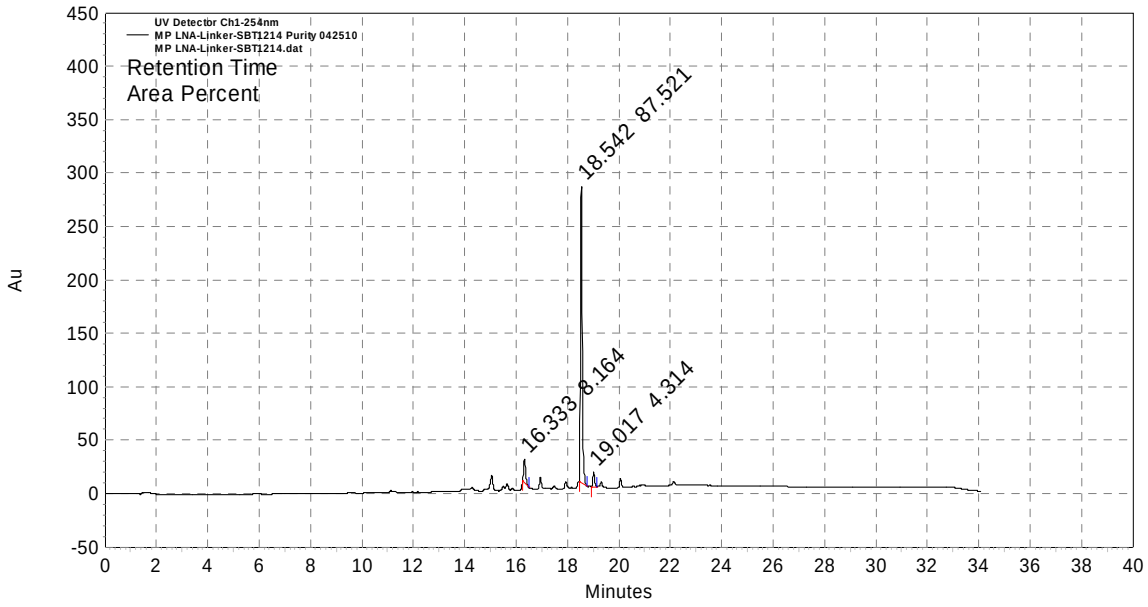

228 nm

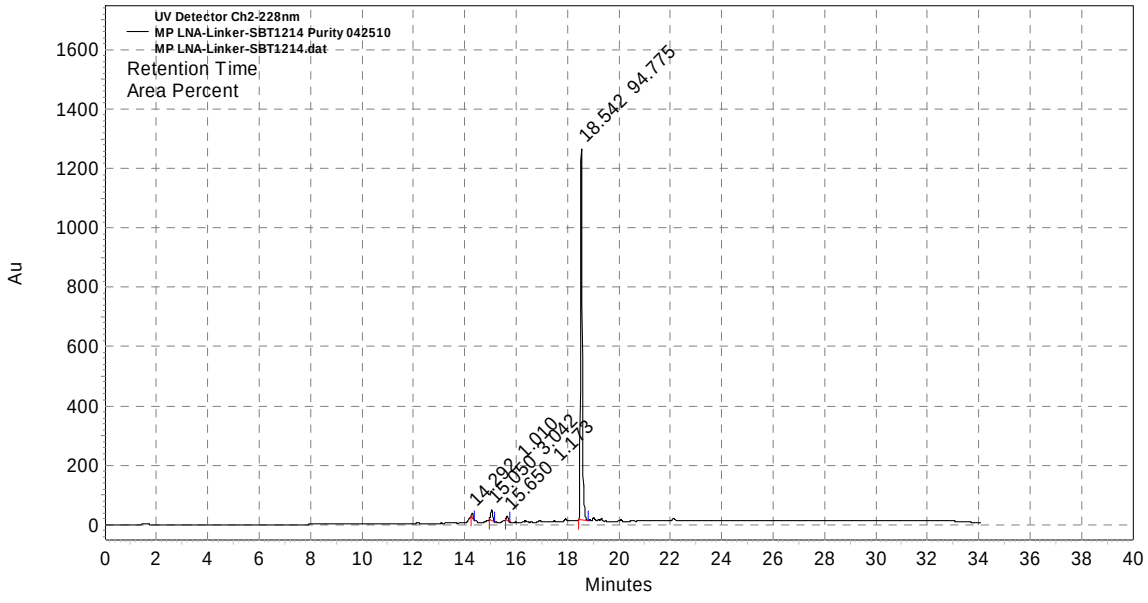

CC

SB-T-121602-LNA

254 nm

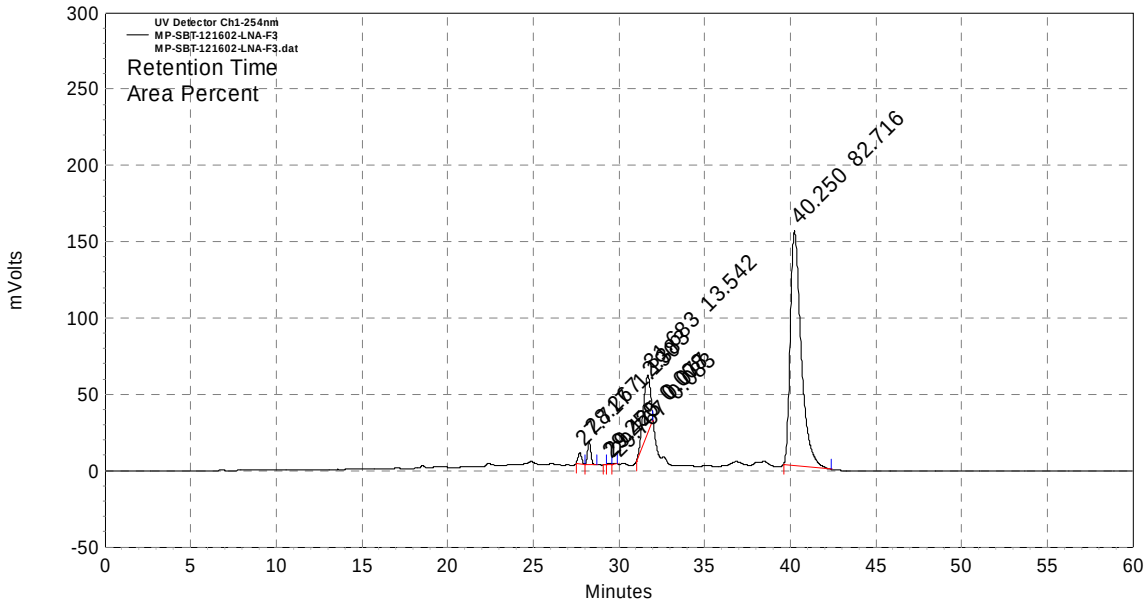

220 nm

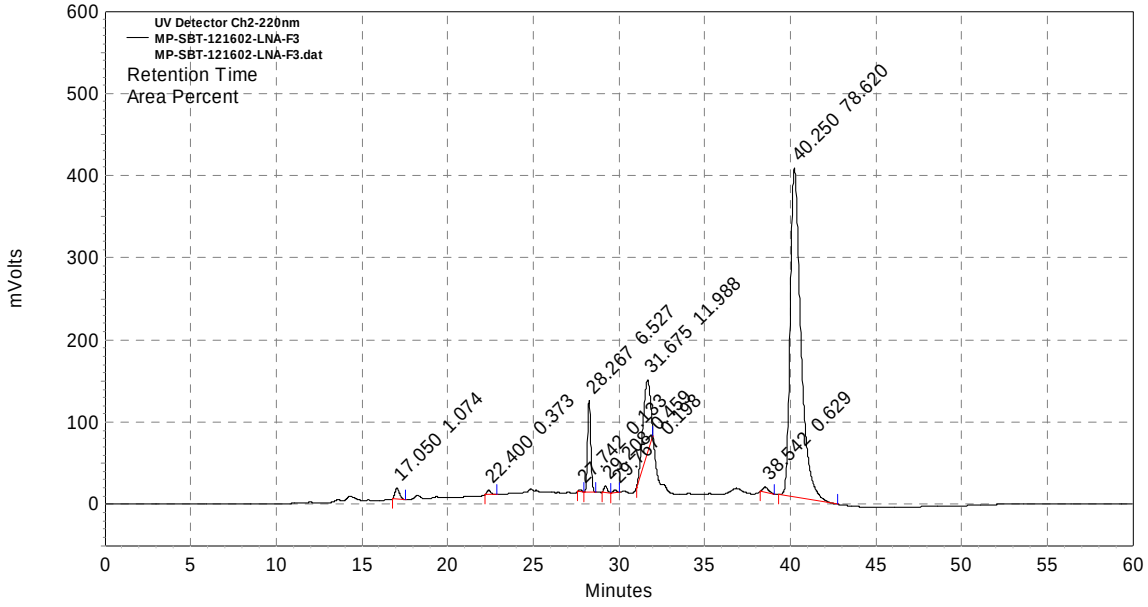

DD

SB-T-1214-LNA

254 nm

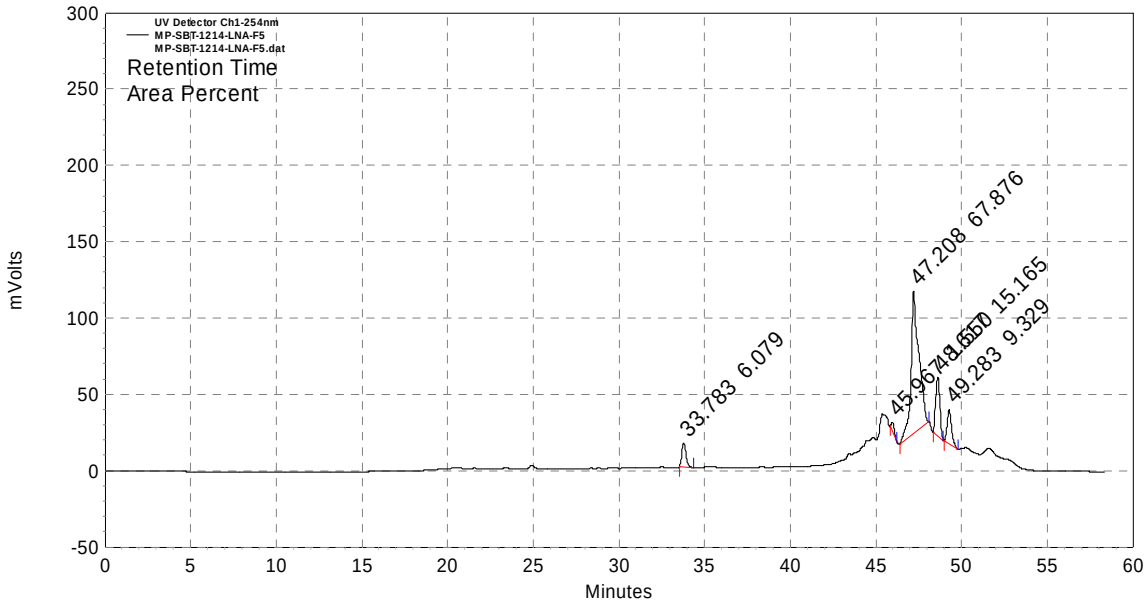

220 nm

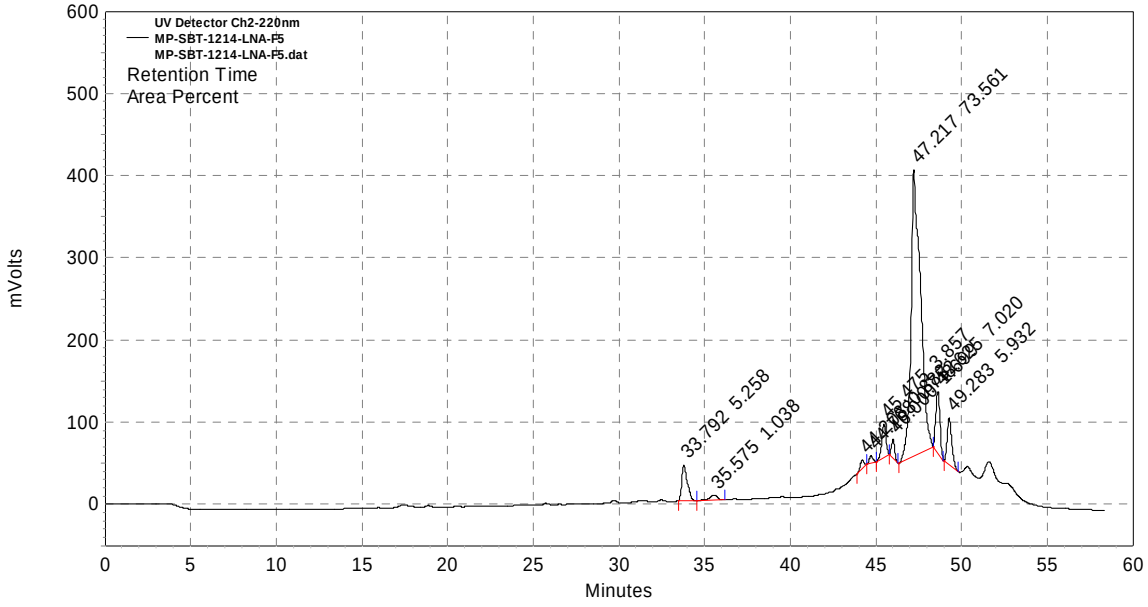

EE

A